2009

Cannabinoid Effects on NFkappaB Function in Microglial-Like Cells: Dual Mode of Action

LaToya Griffin-Thomas
Virginia Commonwealth University

CANNABINOID EFFECTS ON NFκB FUNCTION IN MICROGLIAL-LIKE CELLS: DUAL MODES OF ACTION

A dissertation submitted in partial fulfillment of the requirements for the degree of Doctor of Philosophy at Virginia Commonwealth University

By

LATOYA ANDREA GRIFFIN-THOMAS
B.S., Hampton University, 1998
M.S., Hampton University, 2002

Director: GUY A.CABRAL, Ph.D.
PROFESSOR, DEPARTMENT OF MICROBIOLOGY AND IMMUNOLOGY

Virginia Commonwealth University
Richmond, VA
April 2009

Acknowledgment

First and foremost I would like to give many thanks and glory to God for the many blessings that he continues to bestow upon me. I know that I tend to lose faith at times, but I do know that you will forever guide me to the path that you deem fit for me. Secondly, I would like to give a big thank you to two of my greatest blessings, my husband Anthony Thomas Jr. and my son Anthony (Tony) Thomas III. To my husband Anthony, thank you for your continued encouragement, support, friendship and love. You are my voice of reason and calm, and I would not have been able to complete this journey without you, I love you. To my son Tony, you are the greatest blessing that God could have ever given me. I never would have expected just how much joy and happiness you bring to my life. Your smile, laughter, hugs & kisses and singing brightens my gloomiest days. I am enjoying watching you learn new things and grow into a very independent, strong-willed and compassionate young fellow. I am truly proud to be your mommy, I love you. To my mother Alfreda Conaway, I never would be at this point in my life without your love, sacrifice and undying support, you are truly a remarkable woman, and I love you more than words will allow me to describe. I would also like to thank my other family members for their support and encouragement through the years: Calvin and April Conaway Sr. (brother and sister-in-law); Mildred Jones (aunt); Michael Griffin Jr. (brother); Gloria Conaway (grandmother); Bernard Conaway (cousin); Rachel Clark (grandmother-in-law); and Dalonte, Dionicio and Calvin (nephews). I would like to thank my fellow colleagues of the Cabral labs: Dr. Tammy Ferguson, Dr. Andrea Staab, Christina Hartman, Jenica Harrison, Dr. Erinn Raborn, Dr. Gabriela de Almeida Ferreira, Dr. Daniel Fraga, Dr. Rebecca McLean, Dr. Angela Fritzinger, Melissa Jameson, Alex Mensah and Dr. Bruno da Rocha Azevedo. I do not believe that I would have begun this program in 2002 without the help of Dr. Elaine Eatman (former Biology Department Chair, Hampton University) and Dr. Jan Chlebowski, thank you both for all of your help. I would also like to give a heartfelt thank you to Guy and Francine Cabral for their support, encouragement, understanding and compassion, I could not have asked for a better advisor and committee member, respectively, thank you.

Last and certainly not least, I would like to dedicate this dissertation to my late grandfather Ernest Conaway Jr. We shared an extraordinary bond from the time you delivered me into this world, and I continue to cherish it. Your love and the values you have instilled in me continue to steer me during all of my endeavors. I miss you and love you more than I probably have ever expressed to you. I look forward to the day that we meet again. I love you.

Table of Contents

List of Tables

List of Figures

Abbreviations

2-AG	=	2-arachidonoylglycerol
AD	=	Alzheimer's disease
AEA	=	arachidonoylethanolamide; anandamide
AIDS	=	Acquired Immune Deficiency Syndrome
ALS	=	Amyotropic Lateral Sclerosis
ARDS	=	adult respiratory distress syndrome
β-gal	=	beta-galactosidase
BBB	=	blood brain barrier
cAMP	=	cyclic adenosine monophosphate
CB_1	=	cannabinoid receptor 1
CB_2	=	cannabinoid receptor 2
CBD	=	cannabidiol
CBN	=	cannabinol
CD14	=	cluster of differentiation 14
cDNA	=	complementary DNA
cGMP	=	cyclic guanosine monophosphate
CINC	=	cytokine-induced neutrophil chemoattractant

CNS	=	central nervous system
CSF-1	=	colony stimulating factor-1
CSK II	=	casein kinase II
DAG	=	diacylglycerol
Δ^9-THC	=	delta-9-tetrahydrocannabinol
EST	=	expressed sequence tags
ERK	=	extracellular-signal-regulated kinase
GDP	=	guanosine diphosphate
GTP	=	guanosine triphosphate
GAE	=	granulomatous amoebic encephalitis
GCR	=	glucocorticoid receptor
HIVE	=	human immunodeficiency virus encephalitis
IFN-γ	=	interferon gamma
IL-1	=	interleukin-1
IL-6	=	interleukin-6
IL-8	=	interleukin-8
IκB	=	inhibitor of NFκB
IKK	=	IκB kinase
iNOS	=	inducible nitric oxide synthase
IP_3	=	inositol triphosphate
IPTG	=	isopropyl β-D-1-thiogalactopyranoside

LBP	=	LPS binding protein
LPS	=	lipopolysaccharide
Luc	=	luciferase gene
MAPK	=	mitogen activating protein kinase
MHC	=	major histocompatibility complex
MIP-1	=	macrophage inflammatory protein-1
MS	=	Multiple Sclerosis
NFκB	=	nuclear factor for kappa light chain in B cells
NFTs	=	neurofibrillary tangles
NK	=	natural killer
NLS	=	nuclear localization signal
NO	=	nitric oxide
PKA	=	cAMP-dependent protein kinase, protein kinase A
PLC	=	phospholipase C
RANTES	=	regulated on activation, normal T-cell expressed & secreted
RHD	=	Rel homology domain
ROI	=	reactive oxygen intermediates
ROS	=	reactive oxygen species
RT-PCR	=	reverse transcription-polymerase chain reaction
SDS-PAGE	=	sodium dodecyl sulfate-polyacrylamide gel electrophoresis
STAT	=	signal transducers and activator of transcription
SR1	=	SR141716A, CB_1 selective antagonist, SR141716A

SR2	=	SR144528, CB_2 selective antagonist
TAD	=	transactivation domain
TLR-4	=	toll-like receptor-4
TMEV	=	Theiler's murine encephalomyelitis virus
TNF-α	=	tumor necrosis factor-alpha
TRPV-1	=	transient receptor potential vanilloid-1

Abstract

CANNABINOID EFFECTS ON NFκB FUNCTION IN MICROGLIAL-LIKE CELLS:DUAL MODES OF ACTION

By LaToya Andrea Griffin-Thomas, Ph.D.

A Dissertation submitted in partial fulfillment of the requirements for the degree of Doctor of Philosophy at Virginia Commonwealth University

Virginia Commonwealth University, 2009

Major Director: Guy A. Cabral, Ph.D.
Professor, Department of Microbiology and Immunology

Cannabinoids have been shown to modulate the immune system *in vitro* and in animal models. A major area of interest is how cannabinoids impact the brain. A whole variety of neuropathies or brain disorders, such as AIDS dementia, Parkinson's disease, Multiple Sclerosis and Alzheimer's disease, are associated with a hyperinflammatory response within the brain. Microglia, the resident macrophages of the brain, are the major cell type responsible for the persistent elicitation of pro-inflammatory cytokines (IL-1α, IL-1β, IL-6, TNFα) and other mediators. *In vitro* experiments have demonstrated that the partial exogenous cannabinoid agonist delta-9-tetrahydrocannabinol (Δ^9-THC) and the potent synthetic exogenous cannabinoid agonist CP55940 down-regulate the robust production of pro-inflammatory cytokines elicited in

response to bacterial lipopolysaccharide (LPS) at the mRNA level. These observations suggest that cannabinoids, devoid of psychotropic properties, have the potential to betherapeutic agents. These highly lipophilic compounds can pass through the blood brain barrier and act through specific cannabinoid receptors, cannabinoid receptor 1 (CB_1) and cannabinoid receptor 2 (CB_2). CB_1 and CB_2 are expressed in the brain and the periphery, respectively, and may serve as molecular targets for ablating chronic brain inflammation. Electrophoretic mobility shift assays (EMSA) were used to assess the effects of Δ^9-THC and CP55940 on the LPS-induced binding interactions of the universal transcription factor NFκB to its cognate promoter binding site in BV-2 microglial-like cells. EMSA analyses demonstrated that the Δ^9-THC and CP55940 down-regulated LPS-induced NFκB binding in BV-2 cells in a biphasic manner. Furthermore, reporter activity assays determined that Δ^9-THC and CP55940 attenuated LPS-induced, NFκB transcriptional activity in the same biphasic manner. We then determined the specificity in which cannabinoids inhibit NFκB function. Real-Time RT-PCR analysis demonstrated that BV-2 cells did not express CB_1 mRNA, but they do express CB_2 mRNA when untreated and stimulated with IFN-γ or LPS. We performed specificity studies using CB_1 and CB_2 selective agonists and antagonists with our reporter activity assays. The CB_1-selective agonist ACEA did not affect NFκB transcriptional activity but the CB_2-selective agonist O-2137 exerted a significant decrease in activity. Furthermore, the CB_1 antagonist SR141716A could not reverse the inhibitory effects of CP55490 but those effects were blocked by the CB_2 antagonist SR144528. Lastly, we determined the site of action in which cannabinoids inhibit NFκB function by assessing the effects of Δ^9-

THC and CP55940 on NFκB's inhibitor protein IκBα. IκBα retains NFκB in the cytoplasm until stimulus-induced cell activation. Neither cannabinoid compound was able to inhibit the phosphorylation of IκBα, which initiates its degradation. However both cannabinoids inhibited the complete degradation of IκBα. Western immunoblot analysis also demonstrated that comparable levels of endogenous and phosphorylated p65, the transactivation subunit of the NFκB protein (p65/p50), were detected in the nucleus of LPS-stimulated BV-2 cells pre-treated with or without Δ^9-THC. These results suggest that, in addition to inhibiting the proteolytic degradation of IκBα, there is also a mechanism of action in the nucleus that prevents the proper binding and subsequent transcriptional activity of NFκB. Collectively, these results suggest that cannabinoids suppress pro-inflammatory cytokine gene expression at the transcriptional level, but it is likely that there is more than one signal transduction pathway involved in the cannabinoid-mediated inhibition of NFκB function.

Introduction

Cannabinoids

The marijuana plant *Cannabis sativa* has a multitude of constituents including the highly lipophilic, terpenoid-like compounds identified as cannabinoids, of which over 60 of these have been identified. Exogenous cannabinoids describe those compounds that have been isolated directly from the marijuana plant, such as delta-9-tetrahydrocannibanol (Δ^9-THC), cannabinol (CBN) and cannabidiol (CBD) or those that are chemically synthesized in the laboratory, such as the antagonists SR141716A, SR144528, and agonists WIN55212-2 and CP55490. WIN55212-2 and CP55940 are full receptor agonists, therefore eliciting maximum responses upon cannabinoid receptor interaction. Endogenous cannabinoids or endocannabinoids exist as part of a native endocannabinoid system that includes the endocannabinoids anandamide (AEA) and 2-arachidonoylglycerol (2-AG), cannabinoid receptors and the mediators responsible for endocannabinoid synthesis, transport/uptake and degradation. Endocannabinoids act as neurotransmitters and upon release, activate cannabinoid receptors locally or on nearby cells. But unlike other neurotransmitters that are synthesized in advance and stored in vesicles, endocannabinoids are produced "on demand". AEA was the first endocannabinoid to be identified and was isolated from porcine brain (Devane et al., 1992). The isolation of this cannabinoid was followed by the isolation and identification of 2-AG from canine gut (Mechoulam et al., 1995). Cannabinoids are the major contributors of the euphoric, sedative and cognitive effects experienced by marijuana

users, with Δ^9-THC being the most psychoactive compound. Medicinally, cannabinoids have been used to stimulate appetite, prevent nausea and diminish pain in patients suffering from a multitude of diseases and disorders. Additionally, cannabinoids inherently possess immune modulatory capabilities that may allow these compounds to serve as therapeutic agents, specifically in neuropathogenic diseases that are pathologically hallmarked by a chronic elicitation of pro-inflammatory mediators by cells of the central nervous system (CNS). Δ^9-THC is the major immunomodulatory component of marijuana, and has been shown to suppress immune function in a variety of immune cells within the periphery (Burnette-Curley and Cabral, 1995; Coffey et al., 1996; Klein et al., 1991; McCoy et al., 1999; Friedman et al., 1991; Klein and Friedman, 1990) and within the CNS (Puffenbarger et al., 2000; Facchinetti et al., 2003; Cabral et al., 2008; Cabral and Griffin-Thomas, 2008). Δ^9-THC by virtue of its lipophilic nature can exert direct effects on immune cells by perturbing cellular membranes (Cabral and Staab, 2005; Lawrence and Gill, 1975; Gill and Lawrence, 1976; Makriyannis et al., 1990) and penetrating the blood brain barrier (BBB) to access cognate cannabinoid receptors.

Cannabinoid Receptors

There are two known cannabinoid receptors, cannabinoid receptor 1 (CB_1) and cannabinoid receptor 2 (CB_2). CB_1 was identified in 1990 from a rat brain cDNA library (Matsuda et al., 1990) and is found primarily within the CNS and peripheral tissues such as the testis (Galiegue et al., 1995). CB_1 is a 473 amino acid long, seven-transmembrane,

$G_{(i/o)}$-protein coupled inhibitory receptor and is distributed throughout the various compartments of the brain, including the cerebellum, cerebral cortex, hippocampus, basal ganglia and spinal cord (Matsuda et al., 1990; Herkenham et al., 1990; Westlake et al., 1994). G_i-coupled proteins result in a decrease in adenylate cyclase production and intracellular calcium (Ca^{2+}) levels (Table 1). CB_1 has since been cloned from rat (Gerard et al., 1991) and mouse (Chakrabarti et al., 1995). Mouse CB_1 has been shown to share 99% and 97% amino acid identity to rat and human CB_1, respectively (Chakrabarti et al., 1995; Klein et al., 1998b).

The cloning and identification of CB_2 soon followed the discovery of CB_1. The CB_2 was cloned and identified from a human promyelocytic cell line (HL60) cDNA library (Munro et al., 1993). A distinct characteristic of this receptor is that it is predominantly distributed in cells and tissues of the peripheral immune system that include tonsils, thymus, B and T lymphocytes, monocytes, natural killer (NK) cells, polymorphonuclear cells, and macrophages (Galiegue et al., 1995; Schatz et al., 1997). After much debate and controversy in recent years, the CB_2 also has been identified in the CNS. The majority of CB_2 expression within the CNS is attributed to microglial cells (Carlisle et al., 2002), the resident macrophages of the brain, particulary during early states of inflammation (Nunez et al., 2004; Ramirez et al., 2005a; Cabral and Marciano-Cabral, 2005; Fernandez-Ruiz et al., 2007). CB_2 is a 360 amino acid long, seven-transmembrane, $G_{(i/o)}$-protein coupled inhibitory receptor, and like CB_1 is pertussis-toxin sensitive with an extracellular, glycosylated N-terminus and an intracellular C-terminus (Matsuda et al., 1990; Munro et al., 1993; Howlett et al., 1986). There is a great level of

amino acid identity of CB_2 between variant species, for example there is 81% amino acid identity between rat and human CB_2, and a 93% amino acid identity between rat and mouse species (Griffin et al., 2000).

Reports of the existence of additional cannabinoid receptors continue to amass, and are based on investigations utilizing CB_1 knockout or CB_1/CB_2 double-knockout mice that demonstrate that pharmacological responses of endogenous, exogenous and synthetic cannabinoids are exerted through mechanisms independent of CB_1 and CB_2 (Wiley and Martin, 2002; Breivogel et al., 2001; Di Marzo et al., 2000; Jarai et al., 1999). Several reports have implied that the GPR55 receptor and the transient receptor potential vanilloid 1 (TRPV1) may potentially be novel cannabinoid receptors. GPR55 is a $G_{s\alpha 12/13}$-protein coupled receptor first cloned and identified from an expressed sequence tags (ESTs) database, and like CB_1 and CB_2 has seven conserved transmembrane sequences (Sawzdargo et al., 1999; Baker et al., 2006; Pertwee, 2007). G_s-coupled proteins cause increases in adenylate cyclase production and intracellular Ca^{2+} levels (Table 1). Exogenous cannabinoids Δ^9-THC, CBD, HU-210 and CP55940, and the endogenous cannabinoids AEA, 2-AG and noladin ether have been shown to activate GPR55 (Ryberg et al., 2007), implicating GPR55 as a novel cannabinoid receptor. TRPV1, a ligand-gated cation channel, is a member of the transient receptor potential ion channel family and its natural ligands include capsaicin and vanilloids. The suggestion that TRVP1 may be a cannabinoid receptor arises from studies that demonstrated that the endogenous cannabinoid AEA, which is structurally similar to capsaicin, can interact with and activate this receptor (Smart et al., 2000; Ross, 2003). Although there is

accumulating evidence that additional cannabinoid receptor types exist, a novel cannabinoid receptor has yet to be identified that fulfills stringent characterization at both the pharmacological and functional levels.

Cannabinoid Receptor Signaling

CB_1 and CB_2 take part in signaling cascades involved in the activation and regulation of adenylate cyclase, cAMP and mitogen-activated protein (MAP) kinases, and intracellular calcium levels. Upon ligand interaction, the inactive G-protein coupled to both cannabinoid receptors is modified to an active state by switching the guanine nucleotide GDP to the active GTP. The heterotrimeric G-protein dissociates into the βγ subunit and the α subunit, which binds to adenylate cyclase, inhibits its enzymatic activity and prevents synthesis of cyclic AMP (cAMP). Signaling events that are cAMP-dependent, such as the activation of cAMP-dependent protein kinase (PKA) and further downstream phosphorylation events, are negatively affected by the lack of cAMP. These phosphorylation events control ion channel function, and regulation and activation of transcription factors. It is believed that the dimeric βγ subunit is involved in signaling pathways distinguishable from those involving the α subunit, such as the MAPK signaling cascade (Howlett and Mukhopadhyay, 2000). The lack of cAMP synthesis due to the inactivation of adenylate cyclase describes a mechanism by which CB_1 prevents neurotransmitter release and, thus maintains homeostasis within the CNS. Additionally, the activation of CB_2 and the subsequent linked signaling events represent a mode in which CB_2-mediated immunological homeostasis is regulated in the brain and periphery.

Microglia

Microglia, as resident macrophages in the CNS (Streit et al., 1988; Dickson et al., 1991; Ling and Wong, 1993), are involved in the remodeling and regeneration of cells within this compartment and also provide a first line of defense against infection and injury (Blasi et al., 1990; Aloisi, 2001; Facchinetti et al., 2003; Perry, 2004; Cabral and Marciano-Cabral, 2005). These parenchymal cells originate from the same monocyte lineage as other tissue macrophages (Facchinetti et al., 2003; Rock et al., 2004; Vilhardt, 2005), and perform some of the same functions including phagocytosis, antigen processing and presentation, and production of immune mediators (Giulian and Baker, 1986; Benveniste, 1997; Aloisi, 2001; Facchinetti et al., 2003). As a response to infection or injury, microglia transition from a resting state to a fully activated state that is characterized by a morphological remodeling from a ramified shape with long processes to an ameboid shaped with contracted processes (Ebert et al., 2005; Rock et al., 2004; Blasi et al., 1990). Microglia express antigens that are commonly expressed in macrophages, including CD11b, F4/80 and leukocyte common antigen (CD45). Resident microglia transition from a resting to a fully activated state in a multi-step process that can be replicated *in vitro*. Resting microglia become responsive phagocytes upon infection and/or injury, at which time they proliferate and migrate to the site of infection or injury. Other immune cells respond to the infection and/or injury, and secrete mediators such as interferon-gamma (IFN-γ) that prime microglia for antigen processing and presenting. Antigens such as bacterial lipopolysaccharide (LPS) can then drive these cells to a fully activated state, in which they secrete the pro-inflammatory cytokines

interleukin-1 alpha (IL-1α), interleukin-1 beta (IL-1β), interleukin-6 (IL-6) and tumor necrosis factor-alpha (TNF-α); chemokines such as interleukin-8 (IL-8/CXCL8), macrophage inflammatory protein-1 alpha (MIP-1α/CCL3) and beta (MIP-1β/CCL4)) and regulated on activation, normal T-cell expressed and secreted (RANTES/CCL5); reactive oxygen intermediates (ROI); and reactive nitrogen intermediates such as nitric oxide (NO) (Table 2) (Franciosi et al., 2005; Qin et al., 2005; Kremlev et al., 2004; Arimoto and Bing, 2003; Basu et al., 2002). In addition to morphological modifications during this multi-step activation process, Microglia also undergo differential gene expression of a host of surface receptors including Fc receptors (Fcγ-RI, RII and RII); CD14 receptors; Toll-like receptors (TLR); chemokine receptors (CCR2, CCR3, CCR5, CXCR4, CX3CRI); interferon-gamma receptors (IFN-α, β, γ); tumor necrosis factor-alpha (TNF-α) receptors (TNFRI, TNFRII); and transforming growth factor-beta (TGF-β) receptors (TGFβ-RI, RII and RII) (63, 65) (Qin et al., 2005; Rock et al., 2004).

Microglial Cell Lines

The EOC-20 cells are adherent, immortalized cells derived from the brains of normal 10 day old C3H/HeJ mice, and are dependent on colony stimulating factor 1 (CSF-1) (Walker, 1994). Comparable to brain macrophages, EOC-20 cells display phagocytic activity, IFN-γ-inducible expression of major histocompatibility complex (MHC) II (Walker et al., 1995), and can be used as an *in vitro* cell model to investigate

the role of microglia or "brain macrophages" within the CNS, specifically their immune responses upon activation.

BV-2 cells were generated by immortalizing primary mouse microglia through infection with the v-raf/v-myc oncogene carrying J2 retrovirus (Blasi et al., 1990). These cells possess functional and phenotypic properties common to primary microglial, including phagocytic ability, secretion of pro-inflammatory cytokines and expression of surface receptors and antigens. These cells have been used extensively as *in vitro* models to study microglial function, immune responses and the role of microglia in neurodegenerative diseases. BV-2 cells have been shown to become activated upon exposure to IFN-γ (Han et al., 2002; Hwang et al., 2004) and LPS (Blasi et al., 1990; Kim et al., 2004; Kremlev et al., 2004, Lau et al., 2007). BV-2 cells have been employed to study the effects of anti-inflammatory agents on pro-inflammatory cytokine and iNOS gene expression (Kim et al., 2004; Lau et al., 2007), and to study the expression profiles of chemokines and chemokine receptors upon microglial activation (Kremlev et al., 2004).

Neuroinflammation

The blood brain barrier affords the brain protection from the peripheral environment, and microglial maintain immunological homeostasis within the brain through production and elicitation of neurotropic factors that promote neuronal survival. However, activated microglia have been associated as a direct cause of, or a contributor to, exacerbation of a multitude of chronic neurodegenerative diseases that are

characterized pathologically by an atypical production of pro-inflammatory factors. Elicitation of pro-inflammatory and other neurotroxic factors from other cells in the CNS, such as astrocytes and perivascular macrophages, and from peripheral immune cells that have penetrated the BBB, contributes to the pathology of neurodegenerative and neuroinflammatory diseases (Perry, 2004; Gonzalez-Scarano and Baltuch, 1999). These chronic diseases include Alzheimer's disease (AD), multiple sclerosis (MS) and human immunodeficiency virus encephalitis (HIVE) (Cabral and Marciano-Cabral, 2005; Ramirez et al., 2005a; Arevalo-Martin et al., 2003; Arimoto and Bing, 2003; Facchinetti et al., 2003; McGreer and McGreer, 2003) (Table 3). AD is a very common neurodegenerative disorder that leads to senile dementia. The pathological hallmark of this disease is the presence of extracellular neuritic amyloid plagues and intracellular neurofibrillary tangles (NFTs) that are accompanied by activated microglial and astrocytes. MS is a chronic inflammatory disease that is characterized by T-cell-mediated demyelination of axonal myelin sheaths that protect axons. MS patients suffer from cognitive impairment, muscle weakness, and impaired coordination, balance, speech and sight. HIVE, also referred to as Acquired Immune Deficiency Syndrome (AIDS)-dementia complex, is a neuroinflammatory disorder caused by the production of pro-inflammatory cytokines and neurotoxins, such as glutamate and reaction oxygen species (ROS), elicited by HIV-infected monocytes and microglia. In the neuroinflammatory diseases described above, there is a failure in maintaining the immunological and overall homeostatic balance within the brain, and activated microglia play a critical role in this imbalance.

Cannabinoid-Mediated Immune Modulation

The immune modulatory effects of endocannabinoids and exogenous cannabinoids such as Δ^9-THC have been well documented. In the 1970s, a few studies suggested that marijuana use was associated with an increased incidence of viral infection and implied that cannabinoids suppressed immune resistance to such microbes as Friend leukemia virus, herpes simplex viruses (HSV), *Acanthamoeba*, *Listeria monocytogenes*, *Staphylococcus albus*, *Treponema pallidum* and *Legionella pneumophila* (Cabral and Staab, 2005; Morahan et al., 1979; Juel-Jensen, 1972; Cabral and Dove-Pettit, 1998; Arata et al., 1991; Arata et al., 1991; Marciano-Cabral et al., 2001, Newton et al., 1994; Klein et al., 1998b). Exogenous cannabinoids have been shown to suppress both cell-mediated and humoral immune responses in a wide array of immune cells. Δ^9-THC suppressed the antibody response of B-cells (Carayon et al., 1998; Friedman et al., 1991; Kaminski et al., 1994), and diminished B and T cell proliferation in response to cell-specific mitogens (Carayon et al., 1998; Derocq et al., 1995). Both Δ^9-THC and CP55940 prevented macrophage cell-contact dependent cytolysis of tumor cells (Burnette-Curley et al., 1993; Burnette-Curley and Cabral, 1995), while Δ^9-THC lessened the cell-killing activity of NK cells (Massi et al., 2000). In addition, Δ^9-THC and CP55940 have been shown to affect chemotaxis to sites of infection and/or injury (Raborn et al., 2008; Sacerdote et al., 2000), and this modulatory affect was demonstrated in a mouse model of granulomatous amoebic encephalitis (GAE), where migration to the

site of infection was decreased in Δ^9-THC-exposed macrophages and macrophage-like cells (Marciano-Cabral et al., 2001; Cabral and Marciano-Cabral, 2004).

Through their interactions with cannabinoid receptors, the immune modulatory effects of cannabinoids are down-stream consequences of the inhibition of adenylate cyclase activity (Howlett and Fleming, 1984; Howlett, 1985; Howlett et al., 1986; Kaminski et al., 1994). A significant downstream effect of cannabinoid signaling is the modulation of gene expression of pro-inflammatory mediators. In LPS- stimulated microglia, Δ^9-THC has been shown to inhibit pro-inflammatory cytokine (IL-1α, IL-1β, IL-6 and TNF-α) mRNA expression, as well as ablate TNF-α release (Puffenbarger et al., 2000; Facchinetti et al., 2003). In astrocytes and other immune cells such as macrophages, Δ^9-THC, WIN55,212-2 and CP55940 have been shown to inhibit production of nitric oxide (NO) (Coffey et al., 1996; Jeon et al., 1996; Waksman et al., 1999; Molina-Holgado et al., 2002, Ross et al., 2000). Because cannabinoids can inhibit expression of pro-inflammatory mediators, they have therapeutic potential for neuropathies characterized by chronic elicitation of these factors. The therapeutic benefits of cannabinoids have been demonstrated both in *in vitro* and *in vivo* models of MS and AD. Treatment with the synthetic cannabinoid agonist WIN55,212-2 and HU-210 improved motor function in Theiler's murine encephalomyelitis virus (TMEV)-infected mice (Croxford and Miller, 2003; Arevalo-Martin et al., 2003), a model of chronic demyelinating disease that resembles MS. These same cannabinoid agonists were shown to prevent microglial activation and cognitive impairment in AD based on examination of brain samples and primary microglial (Ramirez et al., 2005a). Thus,

using cannabinoid receptors as molecular targets, one may be able to ablate the various neuropathological processes associated with improper management of chronic brain inflammation.

Nuclear Factor for Kappa Light Chain in B cells (NFκB)

NFκB is a universal transcription factor involved in a plethora of host regulatory immune and inflammatory responses that involve the induction of cytokines, growth factors, adhesion molecules, immunoreceptors and acute-phase proteins (Sancho et al., 2003; Ghosh and Karin, 2002; Vermeulen et al., 2002; Lawrence et al., 2001; Herring and Kaminski, 1999; Ghosh et al., 1998; Tzen et al., 1994; Blackwell and Christman, 1997). NFκB, first identified in 1986 (Sen and Baltimore, 1986), belongs to the Rel family of proteins, and in mammals can be composed of homo- and hetero- dimmers of the subunits p65 (Rel A), Rel B, c-Rel, p50/p105 (NFκB1) and p52/p100 (NFκB2). The classical NFκB protein is the p65/p50 hetereodimer which plays a critical role in acute inflammatory responses by up-regulating the transcription of pro-inflammatory cytokine and chemokine genes, including IL-1α, IL-1β, IL-6, TNF-α, IL-8 and macrophage inflammatory protein-1 (MIP-1) and RANTES (Blackwell and Christman, 1997; Lawrence et al., 2001; Ye and Johnson, 2001). As members of the Rel family, NFκB proteins have an N-terminal Rel homology domain (RHD) that is involved in DNA binding, dimerization, IκB inhibitor interaction and nuclear translocation. The p65, Rel B and c-Rel subunits have a C-terminal activation domain that is involved in transcriptional activation, and this domain interacts directly with the cellular basal transcription

apparatus (Blackwell and Christman, 1997; Schmitz and Baeuerle, 1991) (Figure 1). The p105 and p100 precursor subunits have C-terminal ankyrin repeat motifs that can be cleaved by the ubiquitin-proteasome system to generate the p50 and p52 subunits, respectively (Orian et al., 1995) (Figure 1).

Activation of NFκB is stringently regulated both intracellularly and extracellularly. In unstimulated cells, NFκB is retained in the cytoplasm by the masking of its nuclear localization signal (NLS) by the IκB family of inhibitor proteins. This family of proteins consists of IκBα, IκBβ, IκBε, IκBγ/p100, IκBζ/p105, and Bcl3. These proteins are tissue-specific, and have variable affinities for the different NFκB dimers (Gilmore, 2006). IκB proteins consist of ankyrin repeat motifs with two N-terminal serine residues (Figure 1), and these structural features allow IκB proteins to bind to NFκB, and to be phosphorylated and degraded upon stimulus-induced cell activation. The major inhibitor of the p65/p50 NFκB heterodimer is the IκBα protein (Tergaonkar, 2006; Li and Stark, 2002; Karin and Neriah, 2000). Homodimers of p105 or p100 subunits can act as inhibitors through direct interaction with the RelA subunit. There are various activators of the classical form of NFκB signaling including the pro-inflammatory cytokines IL-1 and TNF-α, growth factors, viruses, and most notably the bacterial antigen LPS. LPS binds to the serum protein LPS-binding protein (LBP), which facilitates binding to CD14, a cell surface receptor found on monocytes and neutrophils (Wright et al., 1990). LPS/LBP complexes bind CD14, which acts in concert with Toll-like receptors (TLR) such as TLR-4 and TLR-2 to activate cells and activate NFκB

(Ghosh et al., 1998, Ghosh and Karin, 2002; Pomerantz and Baltimore, 2002; Yamamoto and Gaynor, 2004). Upon cell activation, IκBα is phosphorylated at serine residues Ser32 and Ser36 by several kinases including cAMP-dependent protein kinase (PKA) and the IκB kinases (IKK), and the phosphorylated protein serves as a recognition marker for the β-TrCP-containing SCF ubiquitin ligase complex (Li and Stark, 2002). The ubiquitinated protein is then recognized by the 26S proteasome that degrades IκBα. IκBα makes multiple contacts with NFκB and its degradation not only allows for NFκB translocation into the nucleus, but also allows for kinase-specific phosphorylation of the p65 subunit at serine residues Ser276, Ser529 and Ser539 (Sasaki et al., 2005; Wang and Baldwin, 1998; Wang et al., 2000; Sakurai et al., 2003; Sakurai et al., 1999; Sizemore et al., 2002; Yang et al., 2003). Serine residues 529 and 536, located in the transactivation domain of p65, are phosphorylated by casein kinase (CSK) II and IKK, respectively. Serine 276 is located in the Rel homology domain and is phosphorylated by PKA. Serine residues 536 and 276 are phosphorylated upon TNF-α or LPS stimulation. The events that lead to the degradation of IκBα, and the termination of NFκB sequestration act in concert to allow nuclear translocation and recognition and binding to the DNA consensus sequence **5'-GGGACTTTCC-'3** located in the promoter regions of pro-inflammatory cytokine and chemokine genes.

Although its activation is tightly regulated, improper regulation of NFκB has been linked to inflammatory and autoimmune diseases such as asthma, rheumatoid arthritis, and Alzheimer's disease (Yamamoto and Gaynor, 2004). Alveolar macrophages of patients suffering from adult respiratory distress syndrome (ARDS) have been shown to

have increased levels NFκB, that were linked to an increase in the production of IL-8 and TNF-α (Miller et al., 1992; Hyers et al., 1991). In another study, rats were subjected to intraperitoneal injections (IP) of endotoxin, which caused an increase in NFκB levels in alveolar macrophages and lung tissue (Blackwell et al., 1994; Blackwell, 1996). This increase in NFκB correlated to an increase of mRNA expression for cytokine-induced neutrophil chemoattractant (CINC); however, blocking endotoxin induction of NFκB led to a decrease in CINC mRNA expression and lung inflammation (Blackwell et al., 1994; Blackwell et al., 1996). In a rat model of autoimmune encephalomyelitis, an animal model widely used to investigate MS, microglial cells isolated from these animals were shown to have elevated levels of NFκB activation (Kaltschmidt et al., 1994).

There are several inhibitors of NFκB activation, including antioxidants, protease and proteasome inhibitors and glucocorticoids and corticosteroids (Epinant and Gilmore, 1999), whose mechanisms of action include suppressing phosphorylation of IκB proteins (Cho et al., 1998; Schreck et al., 1992b), inhibiting degradation of IκB proteins (Grisham et al., 1999; Jobin et al., 1998a; Palombella et al., 1994) and preventing the transactivation of NFκB (Auphan et al., 1995; Brostjan et al., 1996; Ray and Prefontaine, 1994; Scheinman et al., 1995), respectively.

Cannabinoids are believed to behave as anti-inflammatory agents due to their inhibitory effects on mRNA expression of pro-inflammatory cytokines. The critical question that we wish to answer in these studies is, can appropriately engineered cannabinoids, devoid of any psychotropic properties, have the potential to be therapeutic agents for neuroinflammatory diseases that are pathologically hallmarked by a chronic

elicitation of pro-inflammatory mediators? This task may be feasible when considering that highly lipophilic cannabinoids can readily pass through the BBB, and act through specific receptors. While cannabinoids have been shown to down-regulate the inducible gene expression of pro-inflammatory mediators, the exact mechanism(s) of this down-regulation have yet to be fully elucidated, specifically in microglial. The overall goal of this investigation was to define the mechanism(s) in which cannabinoids down-regulate the gene expression of pro-inflammatory mediators in microglia. It was postulated that cannabinoid-mediated down-regulation of cytokine gene expression may take place at the promoter and/or transcriptional level by modulating the activity of transcription factors, such as NFκB**,** that play a critical role in inducing the inflammatory immune response. Three specific aims were established in order to test this hypothesis. The first specific aim was to define the effects of Δ^9-THC and CP55940 on the binding of NFκB to its cognate consensus sequence and its transcriptional activity. The second specific aim is to define the specificity of action in which Δ^9-THC and CP55940 modulates NFκB activity. With this aim, we asked whether effects are mediated through the CB_1, the CB_2 or another mechanism that is not specific for either cannabinoid receptor (Non CB_1/ CB_2). Lastly, the third specific aim was to define the site of action in which Δ^9-THC and CP55940 modulate NFκB activity. We assessed the effects of both exogenous cannabinoids on critical regulatory steps of NFκB activation in both the cytoplasm and nucleus.

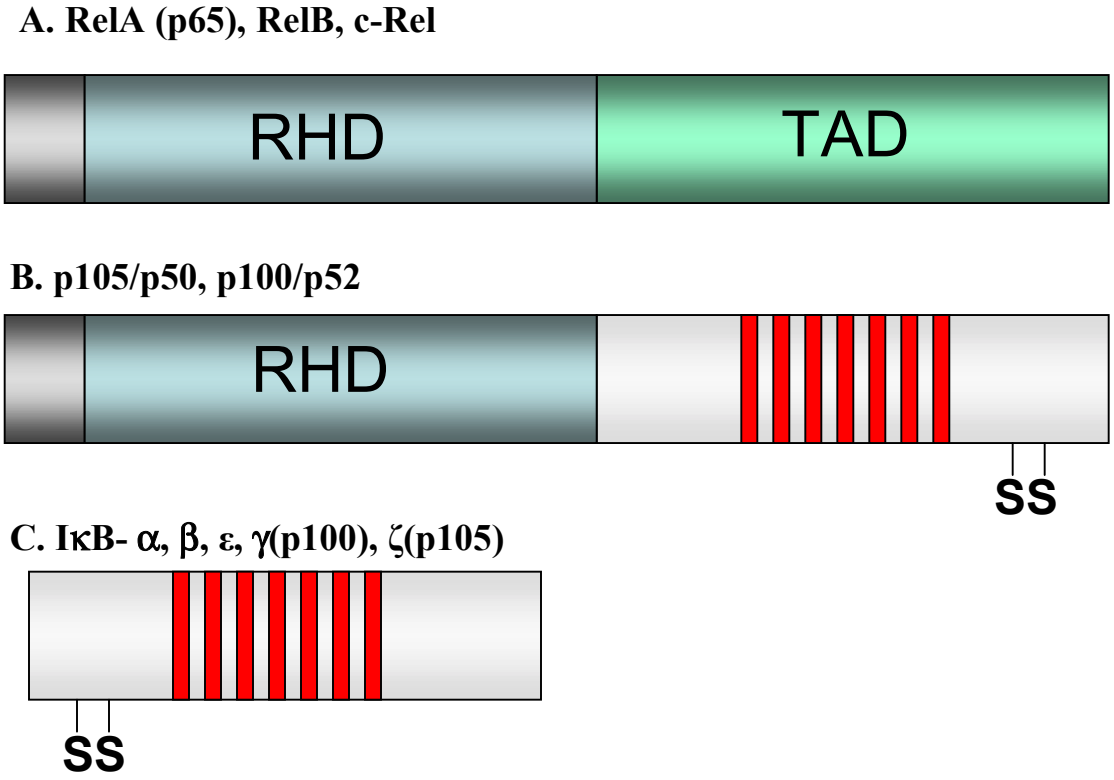

Figure 1. Structure of NFκB and IκB Proteins. (A), The Rel subfamily- RelA(p65), RelB and c-Rel. The N-terminal domain has the Rel homology domain (RHD) that aids in dimerization, DNA and IκB binding, and nuclear translocation. The C-terminal domain contains the transactivation domain (TAD) that interacts directly with the cellular transcription apparatus. (B), The NFκB subfamily- p105/p50 and p100/p52 proteins. The N-terminus also has a RHD, but its C-terminal domain has ankyrin repeat motifs that are recognized by the ubiquitin-proteasome system. The degradation of the ankyrin motifs generates the p50 and p52 subunits, respectively. The C-terminus also has two serine residues that can be phosphorylated by serine kinases. (C), The IκB family of proteins, IκB- α, β, ε, γ, and ζ. IκB proteins are mainly ankyrin repeat motifs with two serine residues that are required for proteolytic degradation and phosphorylation, respectively.
Abbreviations: RHD = Rel homology domain; TAD = transactivation domain; SS = serine residues; solid stripes = ankyrin repeats.

Adapted from Gilmore, T.D., 2006

Table 1- Receptor-linked G Proteins

G-protein Subtype	Signaling Effects	Second Messenger
G_s	↑ adenylate cyclase (AC)	cAMP
	↑ Ca^{2+} channel	Ca^{2+}
	↓ Na^{2+} channel	Δ in membrane potential
G_i	↓ adenylate cylcase (AC)	cAMP
	↑ K^+ channel	Δ in membrane potential
	↓ Ca^{2+} channel	Ca^{2+}
G_q	↑ phospholipase C (PLC)	IP_3, DAG
G_o	↑ phospholipase C (PLC)	IP_3, DAG
	↓ Ca^{2+} channel	Ca^{2+}
G_t	↑ cGMP phosphodiesterase	cGMP
$G_{\beta\gamma}$	↑ phospholipase (PLC)	IP_3, DAG
	↓ adenylate cyclase (AC)	cAMP

Abbreviations: Δ = change; AC = adenylate cyclase; cAMP = cyclic adenosine monophosphate; cGMP = cyclic guanosine monophosphate; DAG = diacylglycerol; Ca^{2+} = calcium ion; IP_3 = inositol triphosphate; K^+= potassium ion; Na^{2+} = sodium ion; PLC = phospholipase C.

Table 2- Pro-Inflammatory Mediators

Cytokine/Chemokine	Description
Interleukin-1 alpha/beta (IL-1α/β)	Inflammatory cytokines – produced by macrophages, monocytes and dendritic cells.
	Induces NFκB activation.
	Increases expression of adhesion molecules.
	Endogenous pyrogen – induces fever during infection.
Interleukin-6 (IL-6)	Inflammatory cytokine.
	Produced by T-cells and macrophages.
	Mediator of fever during the acute phase response.
Tumor Necrosis Factor-alpha (TNF-α)	Inflammatory cytokine – plays critical role in sepsis. Stimulates the acute phase response.
	Produced by macrophages and a host of other cell types.
	Induces apoptosis and inhibits tumorigenesis.
	Associated with inflammatory disorders.
Nitric Oxide (NO)	Chemical messenger molecule – synthesized by iNOS.
	Produced by macrophages, monocytes and neutrophils.
	Induces production of pro-inflammatory cytokines.
	Associated with various inflammatory diseases.
Macrophage Inflammatory Protein-1 (MIP-1)	Inflammatory chemokine – 2 subtypes, alpha (CCL3) and beta (CCL4).
	Produced by endotoxin-induced macrophages.
	Activates neutrophils, basophils and eosinophils.
	Associated with neutrophilic inflammation.
	Induces production of pro-inflammatory cytokines.

Abbreviations: iNOS = inducible nitric oxide synthase.

Table 3- Neuroinflammatory Disorders

Disease	Symptoms/Pathology	Cannabinoid Effects
AD	Neurodegenerative disorder; Causes senile dementia; Extracellular amyloid plaques; Intracellular neurofibrillary tangles.	Inhibits microglial activation; Prevents/rescues blood lymphocytes from apoptosis.
MS	Chronic demyelinating disease; T-cell mediated degeneration of axonal myelin sheaths; Causes motor deficits and/or paralysis.	Improves neurological deficits; Reduces microglial activation and T-cell infiltration.
ALS	Progressive degeneration of cortical motor neurons; Causes musle wasting, weakness and spasticity; complete paralysis.	Delays onset of symptoms and disease progression.
HIVE	Chronic brain inflammation; Causes impaired memory, intellect and motor function; Neuronal loss; Persistent microglial activation.	Inhibits activation of the HIV co-receptor CCR5; CB_2 activation inhibits transendothelial T-cell migration.

Abbreviations: AD = Alzheimer's Disease; MS = Multiple Sclerosis; ALS = Amyotropic Lateral Sclerosis; HIVE = Human Immunodeficiency Virus Encephalitis.

Materials and Methods

Drugs and Reagents

The studies performed for this project included the use of plantonic and synthetic exogenous cannabinoid agonists and antagonists (Table 4). The partial CB_1/CB_2 receptor agonist delta-9-tetrahydrocannabinol (Δ^9-THC; CB_1 Ki = 40.7 nM; CB_2 Ki = 36.4 nM) was obtained from the National Institute on Drug Abuse (NIDA) (Rockville, MD). The CB_1/CB_2 receptor full agonist CP55940 (CB_1 and CB_2 Ki = 1.4 nM) and CB_2 selective agonist O-2137-2 (CB_1 K_i = 2700 nM, CB_2 K_i = 11 nM) were provided by Dr. Billy R. Martin (Department of Pharmacology and Toxicology, Virginia Commonwealth University). CP55940 was also purchased from Tocris Cookson (Ballwin, MO). The CB_1 selective agonist ACEA (arachidonyl-2-chloroethylamide) (CB_1 K_i = 1.4 nM, CB_2 K_i = > 2000 nM) was purchased from Tocris Crookson in addition to CP55940. The CB_1 selective antagonist SR141716A (CB_1 K_i = 2 nM, CB_2 K_i > 1000 nM) and the CB_2 selective antagonist SR144528 (CB_1 Ki = 437 nM, CB_2 K_i = 0.6 nM) were obtained from Sanofi Recherche (Montpellier, France). Stock solutions of cannabinoids at 10^{-2}M were prepared in 100% ethanol and stored at -20°C. Stock solutions were diluted in complete growth medium to generate working concentrations used in experimental studies with a

Table 4- Selected Cannabinoid Receptor Ligands

Ligands	Receptor Selectivity	Dissociation Constant (K_i)	
		CB_1 K_i	**CB_2 K_i**
Δ^9-THC	CB_1/CB_2 partial agonist	40.7 nM	36.4 nM
CP55940	CB_1/CB_2 full agonist	1.37 nM	1.37 nM
ACEA	CB_1 selective agonist	1.4 nM	>2000 nM
O-2137	CB_2 selective ligand	2700 nM	11 nM
SR141716A (SR1)	CB_1 selective antagonist	11.8 nM	13200 nM
SR144528 (SR2)	CB_2 selective antagonist	437 nM	0.6 nM
O-2095	Non CB_1/CB_2 selective agonist	8700 nM	8800 nM

Abbreviations: Δ^9-THC = delta-9-tetrahydrocannabinol; CP55940 = ((-)-cis-3-(2-Hydroxy-4-(1,1-dimethylheptyl)phenyl)-trans-4-(3-hydroxypropyl) cyclohexanol); ACEA = (*N*-(2-Chloroethyl)-5Z,8Z,11Z,14Z- eicosatetraenamide); O-2137 = ((1R,3R)-1-(4-(1,1-Dimethylheptyl)- 2,6-dimethoxyphenyl)-3-methylcyclohexanol); SR141716A = (5-(4-Chlorophenyl)-1-(2,4-dichlorophenyl)-4-methyl-*N*-(1-piperidyl)pyrazole-3-carboxamide); SR144528 = ((1S-endo)-5-(4-Chloro-3-methyl-phenyl)-1-((4methylphenyl)methyl)-*N*-(1,3,3-trimethylbicyclo(2.2.1)hept-2-yl)-1H-pyrazole-3-carboxamide); O-2095 = 1-Norarachidonyl-3-(2'-hydroxyethyl)urea.

Adapted from Howlett *et al*., 2002; Ng *et al*., 1999

final ethanol concentration of 0.01%. The vehicle control consisted of 0.01% ethanol in complete growth medium.

For cell activation, we utilized bacterial lipopolysaccharide (LPS) from *Escherichia coli* strain 0127:B8, purchased from Sigma Aldrich (St. Louis, MO). A stock solution of 1mg/ml was made in complete growth medium and stored at -20°C. Working solutions of 0.1μg/ml were made from dilution of the stock solution for all experiments.

Cell Culture

The EOC-20 cells were purchased from American Type Tissue Culture (ATCC) (Manassas, VA). Cell cultures were maintained at 37°C with 5% CO_2 in ventilated T-175 flasks in complete Dulbecco's Modified Eagle's Medium (DMEM) (Mediatech, Herndon, VA) supplemented with 1% each of L-glutamine, non-essential amino acids, and MEM vitamins, 0.01M HEPES buffer, penicillin (100 IU/ml)/streptomycin (100 μg/ml)/ amphotericin B (0.25 μg/ml), 20% LADMAC-conditioned media and 10% heat-inactivated fetal bovine serum (HI-FBS). The complete growth medium was supplemented with LADMAC-conditioned media for a source of colony stimulating factor-1 (CSF-1), which EOC-20 cells require for proper growth. Confluent monolayers of EOC-20 cells were scraped from the culture flasks using rubber cell scrapers.

LADMAC cells, transformed cells derived from mouse bone marrow cells that constitutively secrete the CSF-1 growth factor, were maintained in complete Eagle's Minimal EssentialMedium (EMEM) at 37°C with 5% CO_2 in ventilated T-175 flasks. To

harvest LADMAC-conditioned media, confluent cell suspensions were centrifuged, and the supernatants were collected and sterile filtered. The conditioned media then were stored at -20°C until used in experiments.

The BV-2 cell line (obtained from Dr. Michael McKinley, Mayo Clinic, Jacksonville, FL) is an immortalized murine primary microglia line generated through infection with a v-raf/v-myc oncogene carrying J2 retrovirus (Blasi et al., 1990). Cell cultures were maintained at 37°C with 5% CO_2 in ventilated T-175 flasks in complete Dulbecco's Modified Eagle's Medium (DMEM) (Mediatech, Herndon, VA) supplemented with 1% each of L-glutamine, non-essential amino acids, and MEM vitamins, 0.01M HEPES buffer, penicillin (100 IU/ml)/streptomycin (100 μg/ml)/ amphotericin B (0.25 μg/ml) and 10% heat-inactivated fetal bovine serum (HI-FBS). For use in *in vitro* experiments, confluent BV-2 cells were detached from culture flasks with Cellstripper (Mediatech, Herndon, VA), a non-enzymatic detachment buffer.

Isolation of Primary Microglia

Primary microglia cultures were prepared using neonatal Sprague-Dawley 1-2 day-old rat pups (Zivik-Miller Laboratory, Zeleinople, PA). The rat pups were sacrificed, and the cerebral cortices were isolated and dissected in dissection saline (2.8% (v/v) stock dissection HEPES (352 mM HEPES); 5% (v/v) stock dissection saline (137 mM NaCl, 5.3 mM KCl, 0.17 mM Na_2PO_4-$7H_2O$, 0.22 mM KH_2PO_4, and 0.0012 g/L Phenol red); 5% (v/v) stock glucose/sucrose solution (6 g/L glucose, 15 g/L sucrose); and penicillin/streptomycin (100 U/ml)). The meninges surrounding the cortices were

removed, and the tissues were trypsinized and manually homogenized in porcine pancreas-derived trypsin (Sigma) for 10 min. The trypsinization was terminated upon the addition of complete DMEM, and the homogenized tissue was filtered through a 70 μm BD Falcon nylon cell strainer (BD Biosciences, San Jose, CA). The filtered cell suspension was centrifuged at 212 x g for 30 min. at 4°C. The mixed glial culture consisting of astrocytes and microglial were seeded in T175 cm^2 culture flasks (Greiner, Monroe, NC), and incubated at 37°C with 5% CO_2. The complete DMEM was dumped the following day, and fresh complete DMEM was added to the flasks, at which time the cultures were allowed to grow for 14-21 days. To isolate primary microglia, the astrocyte-microglia cultures were shaken at 180 rpm on an orbital shaker for 2 h at room temperature.

Cell Treatment

Detached EOC-20 and BV-2 cells were collected in sterile 50 ml conical tubes, centrifuged (170 x g; 1000 rpm) for 8 min., resuspended, and seeded in complete DMEM at 1 x 10^6cells/ml and 7 x 10^5cells/ml, respectively. The seeded cells were incubated overnight to allow for attachment. The following day, cells were pre-incubated for 3 h with Δ^9-THC or CP55940 (10^{-5}M to 10^{-10}M) and stimulated with 100 ng/ml LPS for specified times. For experiments with cannabinoid receptor-specific antagonists, cells were treated for 1 h with SR141716A or SR144528 (10^{-6}M), treated for 3 h with CP55940 or Δ^9-THC (10^{-7}M) , and then stimulated with 100 ng/ml LPS for specified times. In additional experiments, cells were stimulated with various concentrations of

TNF-α (10 ng/ml – 100 ng/ml) or IFN-γ (50 U/ml or 100 U/ml) for various time periods. Each experiment included vehicle (0.01% ethanol) and LPS/vehicle control groups. At the conclusion of experiments, the treatment medium was discarded and replaced with ice cold 1X phosphate buffer saline (PBS) containing 0.5X phosphatase inhibitor. Cell suspensions were centrifuged (170 x g) for 5 min. at 4°C in 1.5 ml conical tubes. Cell pellets were subjected to whole protein or cytoplasmic and nuclear protein extraction or stored at -80°C until needed.

Isolation of Plasmid Contructs

CB_1 and CB_2 DNA served as the positive controls in all Real-Time RT-PCR assays, and was isolated from expression vectors containing the DNA sequence for each cannabinoid receptor. The CB_1 plasmid pCD-rSKR6 was a gift from Dr. L. Matsuda (Medical University of South Carolina, Matsuda *et al*., 1990), and the CB_2 plasmid pUC18-mCB2 was a gift from Dr. T. Bonner (NIMH, Bethesda, MD). DH5α *E. coli* cells transformed with the pCD-rSKR6 vector were cultured in 10 ml of Luria Bertani (LB) broth (10 g Bacto-tryptone; 5 g yeast extract; 10 g NaCl per liter) containing 100 μg/ml ampicillin (amp), and the isolated plasmid was prepared using the Midi Prep Kit (Qiagen, Valencia, CA). Similar methods were applied to isolate and prepare the pUC18-mCB_2 plasmid using Qiagen's Midi Prep Kit. Both vectors were digested with BamHI and EcoRI restriction enzymes to release 2.4 kb and 1.3 kb DNA fragments for CB_1 and CB_2, respectively (Figure 2). The DNA fragments were gel extracted from a 1.5%

agaraose gel using the QIAquick Gel Extraction Kit (Qiagen), and stored at -20°C in DNase-free dH_2O.

Real-Time Reverse Transcriptase-PCR (RT-PCR)

Real-Time Reverse Transcriptase-Polymerase Chain Reaction (RT-PCR) was carried out to assess for the presence of CB_1 and CB_2 mRNA. Constitutive mRNA expression of glyceraldehyde-3-phosphate dehydrogenase (GAPDH) was assayed as the housekeeping control. Total RNA was prepared from BV-2 cells using TRIzol reagent (Invitrogen) according to manufacturer's instructions. Chloroform/isopropanol extraction was used to isolate the RNA which then was resuspended in 50 µl of PCR grade water. Residual genomic DNA was removed from the isolated RNA by RNase-free DNase I Amplification grade (Invitrogen) treatment. The initial step in the reverse transcription of isolated RNA into cDNA was carried out in a 13 µl reaction volume according to the Superscript III RT kit instructions (Invitrogen), using 1 µg of DNase-treated RNA, 50 ng/µl of random hexamers and 10 mM of dNTP mix. The reaction mixture was heated to 65°C (5 min.) and cooled to 4°C in a Biorad MyCycler (Biorad, Richmond, CA). The cDNA synthesis was performed in a 23 µl reaction mixture containing the RNA/random hexamer/dNTP mixture, 1X RT-PCR buffer, 10 mM $MgCl_2$, 20 mM DTT, 40 U of RNaseOUT (Invitrogen) and 200 U of Superscript III reverse transcriptase. DNA synthesis was carried out under the following conditions: (25°C, 10 min.; 50°C, 50 min.; 85°C, 5 min.; and 4°C, 1 min.). Real-Time PCR was performed in a Cepheid (Sunnyvale, CA) Smart Cycler using a SYBR green PCR mix (SuperArray). The

fluorescent stainSYBR green binds nucleic acid and displays a greater binding affinity for double-stranded DNA which heightens the fluorescent signal. Amplification was performed in a 25 µl reaction mixture consisting of 12.5 µl of Syber green mix, 1 µl of primer mix for the murine CB_1 gene (*Cnr1*: PPM04603A), 2 µl of cDNA and 9.5 µl of PCR grade water. A similar approach was applied to assess for CB_2 mRNA, using a primer mix for the mouse CB_2 gene (*Cnr2*: PPM04826A). Reaction mixtures were pipetted into Smart Cycler PCR tubes, and subjected to amplification under the following conditions: initial denaturation at 95°C, 15 min.; and 40 cycles of additional denaturation at 95°C, 30 sec; annealing at 55°C, 30 sec, and extension at 72°C, 30 sec. A crossover threshold (Ct) of 30 fluorescence units was used as the reference point to measure DNA amplification. A separate reaction mixture using primers for the GAPDH gene (*GAPDH*: PPM02946A) was included as the internal standard. PCR products were resolved on a 4% OmniPur agarose (VWR, West Chester, PA) gel. Using this methodology, the 167 bp and 207 bp products of CB_1 and CB_2, respectively, were amplified.

Cytoplasmic and Nuclear Protein Extraction

Cytoplasmic and nuclear protein fractions were extracted from EOC-20 or BV-2 cells using a Nuclear Extract Kit (Active Motif, Carlsbad, CA), according to the manufacturer's protocol. Briefly, cell pellets were resuspended in 150 µl of 1X hypotonic buffer and incubated on ice for 15 min. Detergent then was added and the tubes were briefly vortexed and centrifuged (14,000 X g) for 1 min. The supernatant containing the cytoplasmic protein fraction was collected in pre-chilled microfuge tubes and stored at -

80°C until used in experiments. The pellet containing nuclei was resuspended in complete lysis buffer (1 mM DTT, lysis buffer AM1, protease inhibitor cocktail) and incubated on ice for 30 min. Resuspended nuclei were vortexed briefly and centrifuged (14,000 X g) for 10 min. and nuclear protein fractions were collected in pre-chilled microfuge tubes and stored at -80°C until used in experiments. Protein concentrations of cytoplasmic and nuclear fractions were determined by Bradford assay (M. M. Bradford, 1976).

TransAM NFκB ELISA

The TransAM NFκB ELISA (Active Motif, Carlsbad, CA) was employed to assess for NFκB activation by way of measuring levels of the p65 protein in EOC-20 cells. EOC-20 cells were either treated overnight with various concentrations of TNF-α (10 ng/ml – 100 ng/ml) or treated with 50 U/ml of IFN-γ for various times (0.25 h to 24 h). A standard curve was prepared by performing serial dilutions of recombinant p65 protein (Active Motif). The stock solution (100 ng/µl) of recombinant p65 was diluted to a working solution of 0.5 ng/µl, which was serially diluted to generate 0.5 ng/µl, 0.25 ng/µl, 0.125 ng/µl, 0.0625 ng/µl, 0.0312 ng/µl, 0.0156 ng/µl and 0.008 ng/µl standards. Aliquots of 20 µl for each standard were assayed and correspond to the following quantities of p65 per well: 10 ng, 5 ng, 2.5 ng, 1.25 ng, 0.625 ng, 0.312 ng, 0.156 ng and 0 ng (Figure 5). Complete lysis buffer served as the negative control (0 ng/well).

Experimental samples, and positive, negative, competitor and non-competitor control samples were prepared according to the manufacturer's instructions. The experimental samples consisted of 10 μg of EOC-20 nuclear protein; the positive control consisted of 2.5 μg of Jurkat nuclear extract; and the negative control consisted of complete lysis buffer (5 mM DTT, protease inhibitor cocktail, lysis buffer AM2) only. All samples were incubated with 30 μl of complete binding buffer (2 mM DTT, Herring sperm DNA, binding buffer AM3) for 1 h at room temperature. The competitor and non-competitor reactions consisted of 20 pmol of wild-type and mutated consensus oligonucleotides, respectively, in addition to the nuclear extract and complete binding buffer. The wells then were washed 3 times in 1X wash buffer AM2, followed by incubation with anti-p65 antibody diluted 1:1000 in 1X antibody binding buffer AM2 for 1 h at room temperature. After another series of washes, a HRP-conjugated secondary antibody diluted 1:1000 was added to each well for 1 h at room temperature. Following incubation with the secondary antibody, colorimetric detection was carried out and the absorbance of each sample at 450 nm wavelength was taken using the Spectramax spectrophotometer (Molecular Devices, Sunnyvale, CA).

Electrophoretic Mobility Shift Assay (EMSA)

Mobility shift assays were performed on nuclear protein fractions using the NFκB Gel Shift Kit (Active Motif). Briefly, a wild-type NFκB oligonucleotide probe, containing the consensus sequence **5'-GGGGATCCC-3'**, was end-labeled with (γ- ^{32}P) ATP, and purified through spin column purification using MicroSpin™ G-25 columns

(Active Motif). The specific activity of the labeled probe was determined by taking a Cerenkov count to confirm an activity of >1 X 10^5 counts per minute (cpm)/µl. The extract premix consisted of 4 µl of 4X binding buffer B2, 2 µl of 8X stabilizing solution, 4 µg of nuclear protein and dH_2O to a final volume of 16 µl. The extract premix then was incubated at 4°C for 20 min. For super shift assays, 2 µl of rabbit anti-p65 or anti-p50 antibody was added to the extract premix. The probe premix was composed of 2 µl of 4X binding buffer C2, 1 µl of 8X stabilizing solution, and 1 µl (≥100,000 cpm) of ^{32}P-labeled NFκB probe in a total volume of 8 µl. The extract and probe premixes were added together, and the mixture was incubated at 4°C for 20 min. The cold competitor and non-competitor reaction probe premixes contained an excess of unlabeled wild-type and mutant NFκB oligos, respectively. Reaction mixtures were subjected to electrophoresis (1 h, 250V) on a native 5% polyacrylamide gel in 1X tris-glycine (TGE) buffer. Gels were vacuum-dried and exposed to X-ray film (PerkinElmer, Boston, MA) at -80°C.

NFκB Reporter Activity Assay

Transformation of Competent XL-1 Blue E. coli cells

The reporter plasmids pNFκB-Luc and pSV-β-galactosidase were employed in NFκB reporter activity assays. pNFκB-Luc is a 5.7 kb reporter plasmid (Figure 18)with the luciferase (*Luc*) reporter gene that is driven by a TATA box promoter element and a NFκB-specific enhancer element. The enhancer element contains 5 repeats of the

recognition sequence 5'-GGGACTTTCC-'3. Upon cell activation, NFκB will bind the enhancer element and drive the expression of the *Luc* gene. The reporter plasmid pSV-β-galactosidase (Figure 21) was used as a control plasmid to determine transfection efficiency. This 6.8 kb plasmid has a SV40 early promoter and enhancer that drive constitutive expression of the *LacZ* gene, thus producing the β-galactosidase enzyme. Both pNFκB-Luc and pSV-β-galactosidase were transformed into XL-1 Blue *E. coli* cells for long-term use. XL-1 Blue cells were thawed on ice and aliquoted in 100 µl volumes. β-mercaptoethanol was added to each aliquot of cells, and the mixture was incubated for 10 min. on ice with swirling every 2 min. The pNFκB-Luc and pSV-β-galactosidase plasmids were added separately to the XL-1 Blue cells and incubated on ice for 30 min. The cells were heat-pulsed in a 42°C water bath for 45 sec and then incubated on ice for 2 min. Super Optimal broth with Catabolite repression (SOC) medium, pre-heated to 42°C, was added to the cells, which were then incubated at 37°C for 1 h with gentle shaking. The transformation mixture (≤ 200 µl) was plated on LB-agar (10 g Bacto-tryptone; 5 g Bacto-yeast extract; 5 g NaCl; 12 g Bacto-agar per liter) plates containing ampicillin (amp) (100 µg/ml). The plates also contained 100 µl of 2% X-gal and 100 µl of 10 mM isopropyl-β-D-1-thiogalactopyranoside (IPTG) for blue-white screening. Cells properly transformed with each plasmid will appear as white colonies on the plate, and those that are not transformed will appear blue. The pSV-β-galactosidase transformed cells will grow as blue colonies if streaked on agar plates containing only IPTG, due to constitutive expression of the β-galactosidase gene. All plates were stored at 4°C.

A Maxi Prep Kit (Qiagen) was used to isolate the pNFκB-Luc and pSV-β-galactosidase expression vectors. XL-1 Blue E. coli cells, transformed with both expression vectors, were cultured overnight in 250 ml of LB-amp (100 μg/ml) broth. Concentrations of all plasmids and DNA fragments were obtained using a Biophotometer (Eppendorf, Westbury, NY). Glycerol stocks of each plasmid were made stored at -80°C. Freshly streaked LB-amp agar plates with the pNFκB-Luc and pSV-β-galactosidase cultures were sent to the Molecular Biology Core Facility (Virginia Commonwealth University) for plasmid isolation. Maxi plasmid preparations were performed as described previously. The isolated pNFκB-Luc and pSV-β-galactosidase plasmids were restriction-enzyme digested with EcoRV and/or EcoRI. The digested plasmids were electrophoresed on a 1.5% agarose gel to reveal the linearized pNFκB-Luc and pSV- β-galactosidase plasmids (See Figures 19 and 22).

Transient Transfection/Luciferase Assay

To assay for NFκB transcriptional activity, BV-2 cells were transiently transfected with the pNFκB-Luc reporter plasmid (Stratagene, La Jolla, CA) using TransIT-Neural® transfection reagent (Mirus, Madison, WI). To normalize results from luciferase measurements, cells were co-transfected with pSV-β-galactosidase control plasmid (Promega, Madison, WI). BV-2 cells were seeded at 2 X 10^5cells/ml to achieve 50-70% confluency, and incubated overnight at 37°C with 5% CO_2. The transfection mixture per sample was prepared as follows: 6 μl of TransIT-Neural® reagent were added

to 250 µl of serum-free growth medium and the mixture was incubated for 20 min. at room temperature to allow for complex formation. Five micrograms (µg) of pNFκB-Luc and 5 µg of pSV-β-galactosidase plasmids were mixed together, and added to the transfection reagent/serum-free medium solution. The mixture was allowed to incubate for an additional 10 min. at room temperature. The transfection mixtures were added dropwise to each cell culture plate, and transfection was allowed to occur overnight at 37°C with 5% CO_2. Following transient transfection, the transfection medium was removed, and cells were pre-treated with drug or vehicle for 3 h and stimulated with 100 ng/ml LPS for 3 h. Cells then were lysed, and luciferase and beta-galactosidase activity was assayed using the Dual-Light® Luciferase and β-Galactosidase Reporter Gene Assay System (Applied Biosystems, Bedford, MA) with an Orion Microplate Luminometer (Berthold Detection Systems, Oakridge, TN).

Whole Cell Protein Extraction

Whole cell protein lysates of BV-2 cells were used in some Western blot assays. After drug treatment and stimulation, BV-2 cells were washed 2 times with room temperature 1X PBS. The cells were scraped from the culture flasks, collected and centrifuged at 400 x g for 10 min. The supernatant was aspirated and the cell pellets were resusupended in cold lysis buffer (50 mM Tris-HCl, pH 8.0; 150 mM NaCl and 1% NP-40) containing 1X protease inhibitor cocktail (Sigma). The resuspended cells were gently vortexed and incubated on ice for 30 min. with occasional mixing. The lysed cells were centrifuged at 10,000 x g for 15 min. at 4°C, and the supernatant (protein lysate) was

collected and stored at -80°C. A Bradford assay was performed to determine protein concentration.

SDS-Polyacrylamide Gel Electrophoresis (PAGE)/Western Immunoblotting

Protein samples (30-50 μg) were separated (1 h, 100V) on a 10% polyacrylamide gel. Gels were electroblotted onto nitrocellulose membranes (Biorad, Hercules, CA) which then were incubated in blocking buffer (1X Tris-buffered saline with 0.1% Tween-20 (TBS-T), and 5% nonfat dry milk) for 1h at room temperature. Immunodetection of the NFκB p65 subunit was performed overnight at 4°C with anti-phospho p65 and anti-p65 primary antibodies at 1:250 and 1:400 dilutions, respectively. After washing, membranes were incubated with secondary goat anti-rabbit HRP-conjugated antibody at a 1:750 dilution for 1 h at room temperature. Immunodetection of IκBα and phospho-IκBα was performed with the respective primary antibodies at 1:400 dilution, and secondary goat anti-rabbit HRP-conjugated and goat anti-mouse HRP-conjugated antibodies, respectively, at 1:750 dilution. Immunodetection of the CB_2 was carried out with a primary anti-human CB_2 antibody that was synthesized in rabbits, at a 1:100 dilution. The blots were then probed with goat anti-rabbit HRP-conjugated secondary antibody at a 1:400 dilution. Detection was carried out with chemiluminescence using ECL reagents (Amersham Biosciences, Piscataway, NJ), followed by exposure to X-ray film. To probe for equal protein loading, membranes were stripped with stripping buffer (62.5 mM Tris-HCl, pH 6.7; 2% SDS;100 mM 2-mercaptoethanol) for 30 min. at 50°C. Equal loading for whole protein lysates and cytoplasmic protein was determined using anti-β actin

primary antibody, and equal loading of nuclear protein was determined with anti-PCNA (proliferating cell nuclear antigen) primary antibody.

Southern Blot Analysis

PCR Synthesis of Digoxigenin-Labeled Probe

To confirm the Real-Time RT-PCR results, Southern blot analysis was performed on CB_1 and CB_2 amplicons. A Digoxigenin (Dig)-labeled probe (Roche, Indianapolis, IN) was employed in the Southern analyses instead of the standard radiolabeled probe. Digoxigenin (Dig) is a plant steroid hapten that is used in molecular biology techniques due to its high immunogenicity. Dig, like other haptens such as biotin and fluorescein, is used as a conjugation "tag" for the detection of nucleic acids for Southern and Northern blot analyses using anti-digoxigenin antibodies. The Dig-labeled probe was synthesized using PCR according to manufacturer's instructions. Synthesis was carried out in a 50 µl 1X PCR buffer, 200 µM of PCR Dig mix, 100 µg/ml each of downstream and upstream gene-specific primers, 5 U of polymerase enzyme, 500 pg of template DNA and sterile ddH_2O. The unlabeled control reaction mixture was carried out similarly, except that a standard dNTP mix (200 µM) was used instead of the Dig PCR mix. The probes were synthesized in the SmartCycler under the following settings: initial denaturation (95°C, 2 min.); 30 cycles of denaturation (95°C, 30 sec), annealing (60°C, 30 sec) and elongation (72°C, 1 min.); and a final elongation (72°C, 7 min.). A small aliquot of the PCR products was electrophoresed on a 1.5% agarose gel to confirm the presence of the unlabeled and Dig-labeled probes for both cannabinoid receptors. The Dig-labeled CB_1

was approximately 850 bp in size and the unlabeled probe was of a slightly smaller size of 650 bp (Figure 10A). The Dig-labeling of the CB_2 insert generated a 500 bp probe, while the unlabeled CB_2 probe was about 350 bp in size (Figure10B). The labeled probe was stored at -20°C until used in experiments.

Hybridization/Detection

The agarose gel containing the PCR products was incubated in denaturing solution (1.5 M NaCl; 0.5 M NaOH) for 30 min. at room temperature, followed by incubation in neutralization solution (1.5 M NaCl;1 M Tris, pH 8) for 30 min. The gel then was incubated in 20X Saline Sodium Citrate (SSC) buffer for 30 min. at room temperature. The transfer apparatus was set up and the PCR products were transferred to a nylon membrane overnight at room temperature. The following day the transferred products were UV crosslinked to the nylon membrane using a Stratalinker (Stratagene). Hybridization of the crosslinked membrane with a digoxigenin-labeled rat CB_1 or mouse CB_2 probe was carried out according to the manufacturer's (Roche) instructions. The membrane was pre-hybridized with hybridization buffer for 30 min. at 42°C, at which time the pre-hybridized membrane was incubated with either the CB_1 or CB_2 digoxigenin-labeled probe overnight at 40°C. The Dig-labeled probes were denatured in a boiling water bath for 5 min., followed by rapid cooling in an ice water bath. After the overnight hybridization, the membrane was stringently washed 2 times for 5 min. each at room temperature in 2X SSC with 0.1% SDS, followed by 2 washes for 15 min. each at 65°C in 0.5X SSC with 0.1% SDS. The membrane was briefly washed for 5 min. at

room temperature in 1X washing buffer (0.1 M maleic acid; 0.15 M NaCl; pH 7.5; 0.3% (v/v) Tween-20), followed by incubation in 100 ml of 1X blocking buffer (10X blocking solution diluted 1:10 in 1X maleic acid buffer) for 30 min. The blocked membrane was incubated with anti-digoxigenin antibody (75 mU/ml) for 30 min. at room temperature. The membrane underwent a couple of washes in 1X wash buffer as described previously, and then was equilibrated in 1X detection buffer (0.1 M Tris-HCl; 0.1 M NaCl; pH 9.5). The equilibrated membrane was placed in a plastic report cover, and incubated in 1X CPD-Star detection reagent (Roche, Indianapolis, IN) for 5 min. at room temperature. CDP-Star is a chemiluminescent substrate that is dephosphorylated by alkaline phosphatase, resulting in the formation of a dioxetane phenolate anion. The decomposition of this anion emits a light signal that can be detected on X-ray film. The membranes used in these Southern analyses were exposed to X-ray film (Perkin Elmer, Waltham, MA) for detection of CB_1 or CB_2 PCR products.

Statistical Analysis

All experiments were performed in triplicate and each experiment was repeated a minimum of two times. To evaluate homogenous data, an analysis of variance (ANOVA) was performed using Dunnett's test. These analyses were followed by a Student's t-test to compare vehicle control treatment group with the LPS/vehicle control group, and to compare LPS/vehicle treatment with drug treatment groups.

Results

EOC-20 Microglial-Like Cells Express the Cannabinoid Receptor CB_2 but do not Express the Cannabinoid Receptor CB_1.

The CB_1 is found predominantly in the brain and has been shown to be expressed in astrocytes, oligodendrocytes, neurons and microglia. While the CB_2 is found mainly in peripheral immune cells and testis, its expression can also be detected in the brain. In order to assess for cannabinoid receptor expression in EOC-20 microglial-like cells, Real-Time RT-PCR analysis was performed on total RNA isolated from unstimulated EOC-20 cells. The pCD-rSKR6 and pUC18-mCB_2 plasmids were restriction-enzyme digested to generate DNA inserts (Figure 2) that served as positive controls for CB_1 and CB_2 Real-Time RT-PCR assays, respectively. CB_1 mRNA was not detected in EOC-20 cells (Figure 3A), but these cells do express low levels of CB_2 mRNA (Figure 4A). The threshold cycle (C_t) was set at 30 fluorescence units, and this value is the minimum fluorescence level of DNA-bound SYBR green to be detected by a Cephid thermocycler. The PCR amplicons for both receptors were resolved by agarose gel electrophoresis, to confirm the presence of the 167 bp CB_1 amplicon (Figure 3B) and the 207 bp CB_2 amplicon (Figure 4B). These findings are not surprising for mouse EOC-20 microglial-

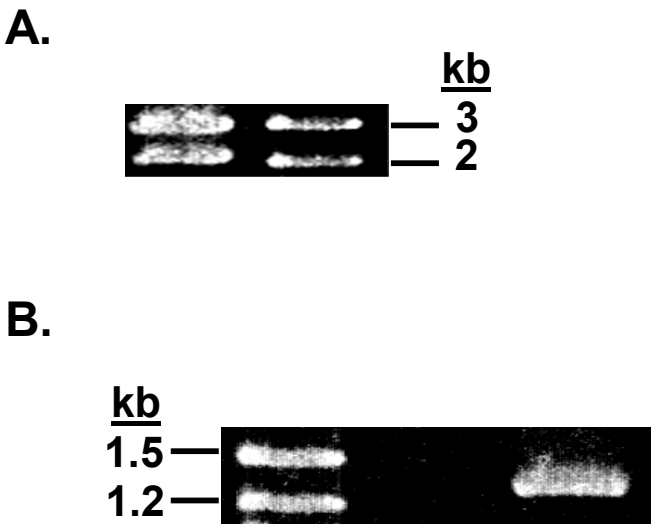

Figure 2. Restriction Enzyme Digestion of pCD-rSKR6 and pUC18-mCB_2. (A), The pCD-rSKR6 plasmid containing a DNA insert for the rat CB_1 was digested with BamHI and EcoRI to release the 2.4 kb CB_1 insert. A slightly larger DNA fragment (~3 kB) was also generated from the restriction digestion and represents the presence of additional restriction sites for BamHI and/or EcoRI. (B), The pUC18mCB_2 plasmid containing a DNA insert for the murine CB_2 also was digested with BamHI and EcoRI to release a 1.3 kb CB_2 fragment. Fragments from both plasmids were used as controls in Real-Time RT-PCR and Southern blot analyses.

A.

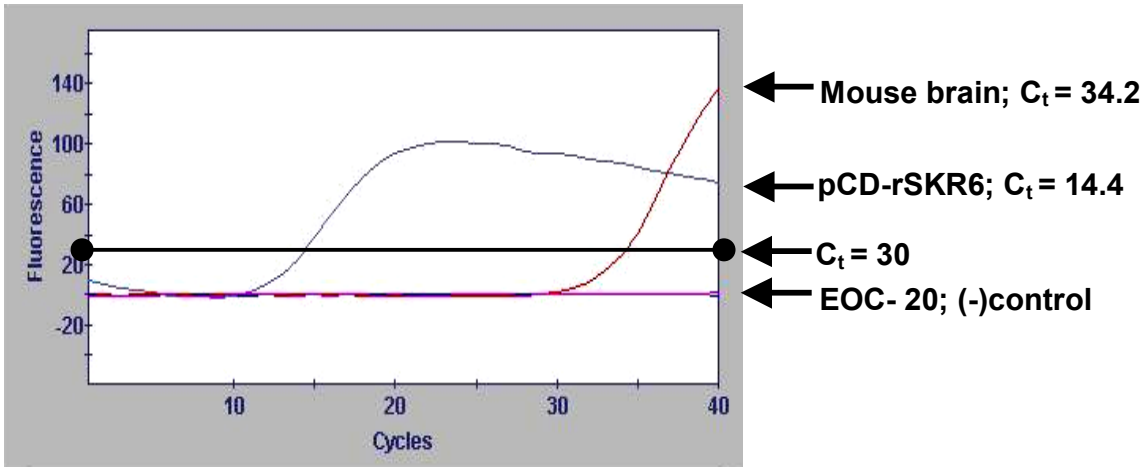

B.

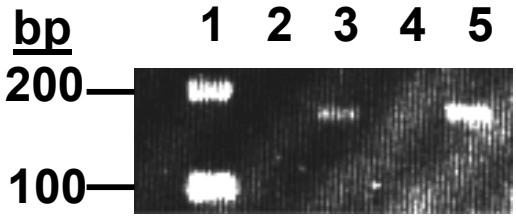

Figure 3. EOC-20 Cells Do Not Express CB_1 mRNA. Real-Time RT-PCR with SYBR green PCR mix was performed on total RNA isolated from unstimulated EOC-20 cells and whole mouse brain homogenate. A DNA fragment from the CB_1 plasmid pCD-rSKR6 was used as a positive control. (A), PCR amplification of CB_1 was detected in mouse brain homogenate (C_t = 34.2) and the positive control pCD-rSKR6 (C_t = 14.4). However, CB_1 expression was not detected in EOC-20 cells. The crossover threshold (C_t) was set at 30 fluorescence units. (B), PCR amplicons were electrophoresed on an agarose gel for confirmation. Lanes: 1, DNA ladder; 2, negative control; 3, positive control (pCD-rSKR6); 4, EOC-20 cells; 5, mouse brain homogenate. The 167 bp CB_1 amplicon was only detected in the positive control and mouse brain homogenate samples.

A.

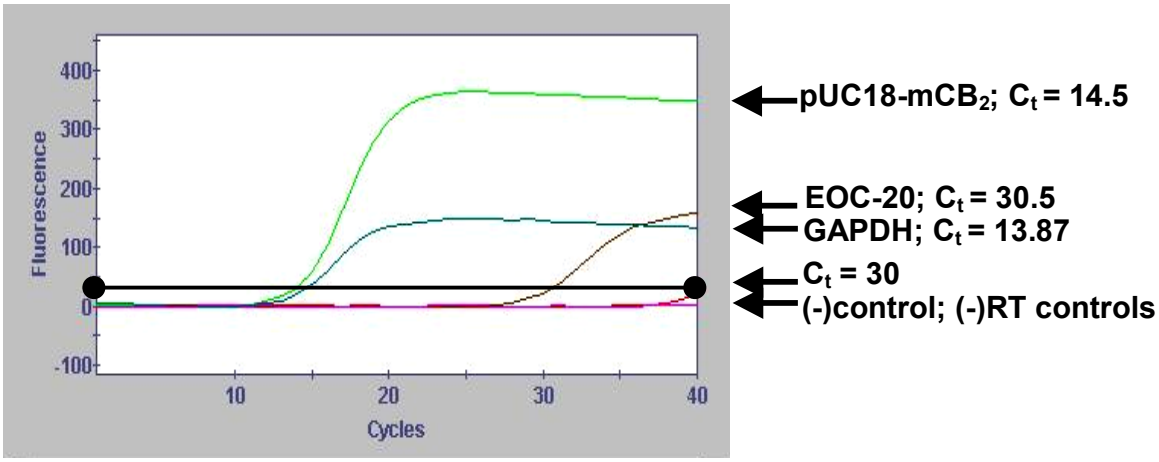

B.

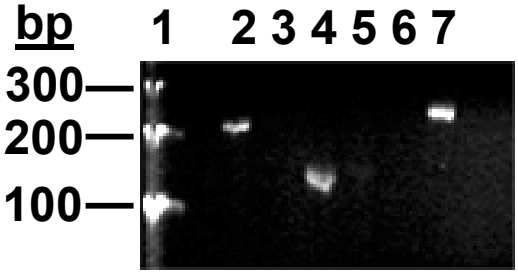

Figure 4. EOC-20 Cells Do Express CB_2 mRNA. Real-Time RT-PCR with SYBR green PCR mix was performed on total RNA isolated from unstimulated EOC-20 cells. A DNA fragment from the CB_2 plasmid pUC18-mCB_2 was used as a positive control. (A), PCR amplification of CB_2 mRNA was demonstrated in EOC-20 cells (C_t = 30.5) and the positive control pUC18-mCB_2 (C_t = 14.5). Primers for the housekeeping gene GAPDH was also used as a control (C_t = 13.9). The crossover threshold (C_t) was set at 30 fluorescence units. (B), PCR amplicons were electrophoresed on an agarose gel for confirmation of the 207 bp CB_2 amplicon. The smaller PCR product is amplification of the GAPDH gene. Lanes: 1, DNA ladder; 2, EOC-20 cells; 4, GAPDH; 6, negative control; 7, positive control (pUC18-mCB_2). Lanes 3 and 5 are (-)RT controls for EOC-20 cells and GAPDH, respectively.

like cells since primary microglia cells have been shown to have low levels of CB_1 expression while being a major contributor of CB_2 expression in the brain.

Stimulation of EOC-20 Cells with the Cytokines TNF-α or IFN-γ Increase p65 Production.

To further determine if the EOC-20 cells would be a suitable *in vitro* model to study the effects of cannabinoids on NFκB function in microglia cells, we analyzed NFκB activation by way of measuring levels of the p65 subunit upon cell stimulation. Induction of the p65 subunit was investigated instead of the p50 subunit because p65 plays the major role in NFκB activation and function, and it contains the transactivation domain responsible for the transcriptional activity of NFκB. TNF-α is a potent activator of microglial cells, thus using an ELISA-based binding assay, we assessed for NFκB induction upon stimulation with TNF-α. Nuclear extract (10 μg), from EOC-20 cells stimulated with various concentrations of TNF-α (10 ng/ml – 100 ng/ml) for 22 h, was added to wells of a 96-well plate pre-coated with a NFκB consensus oligonucleotide sequence. A p65-specific antibody was added to each well, followed by a HRP-conjugated secondary antibody. A colorimetric reaction was carried out to obtain a quantitative measure of p65 levels for each sample, extrapolated from a standard curve using recombinant p65 protein (Figure 5). Increasing levels of p65 were directly proportional to increasing concentrations of TNF-α (Figure 6). A two-fold increase (0.6 ng to 1.2 ng) of p65 levels was observed between the lowest TNF-α concentration (10

ng/ml) and the highest TNF-α concentration (100 ng/ml) used. A three-fold and six-fold increase of p65 concentration were observed between vehicle (0.2 ng) and 10 ng/ml TNF-α treated cells, and vehicle and 100 ng/ml TNF-α treated cells, respectively. For the Jurkat cell nuclear extract (2.5 μg) that served as the positive control, 0.8 ng of p65 was observed; and there were no measurable levels of p65 in the negative control. The competitor control, consisting of nuclear extract from the 100 ng/ml TNF-α sample incubated with 2 pmol of wild-type NFκB consensus oligonucleotide, demonstrated levels of p65 comparable to the vehicle (i.e., unstimulated) group. A seven-fold increase of p65 levels was observed between the competitor control and the non-competitor control (i.e., the 100 ng/ml TNF-α sample incubated with 2 pmol of a mutated NFκB consensus oligonucleotide). This analysis demonstrates that TNF- α could serve as an inducer for NFκB activation in our *in vitro* cell model. The same approach was used to analyze induction of p65 as it relates to NFκB activation in EOC-20 cells upon exposure to the cytokine IFN-γ. IFN-γ can activate macrophages and macrophage-like cells such as microglia, and prime them for antigen processing and presentation. EOC-20 cells were treated with 50 U/ml and 100 U/ml IFN-γ for 22 h, and the nuclear extract from these treated cells was assessed for NFκB activation. The TransAM NFκB ELISA demonstrated an increase in p65 production in EOC-20 cells upon IFN-γ-induced NFκB activation as compared to the vehicle-treated (i.e., unstimulated) cells; however, there was only a two-fold increase in p65 production between the stimulated and unstimulated cells (Figure 7). This is a striking difference from the ten-fold increase of p65 production

that was observed between vehicle-treated cells and cells stimulated with 100 ng/ml TNF-α (Figure 6). One explanation for the disparity in these results is that TNF-α and IFN-γ activate cells through two different signaling pathways. TNF-α activates cells through the induction of the transcription factor NFκB. IFN-γ, on the other hand, activates cells through the signal transducers and activator of transcription (STAT) family of proteins. Overall levels of p65 production were comparable between the two concentrations of IFN-γ. These results suggest that TNF-α rather than IFN-γ may serve as a better inducer of NFκB activity for our *in vitro* cell model.

Similar approaches were used to assess LPS-induced NFκB activation in EOC-20 cells. LPS is a classical cell activator and inducer of NFκB signaling. Previous studies performed in our laboratory as well as others investigated cannabinoid effects on pro-inflammatory cytokine gene expression in LPS-induced microglial or microglial-like cells. Assessing NFκB binding to its consensus sequence is another manner in which to study NFκB induction and any possible effects exerted by cannabinoids. Therefore, using Electrophoretic Mobility Shift Assays (EMSA), we assessed LPS-induced NFκB induction by way of binding to a synthetic DNA oligonucleotide containing the NFκB consensus sequence **5'-GGGGATCCC-3'**. EOC-20 cells were either vehicle-treated or stimulated with 100 ng/ml LPS for 1 h, and the nuclear extracts from these samples were assayed. Conflicting results were obtained from these analyses, for levels of LPS-induced NFκB binding were comparable to unstimulated cells (Figure 8). FACScan analysis was performed on EOC-20 cells in the laboratory of Dr. Kathleen McCoy, and it

was determined that these cells have a mutation in the cytoplasmic tail of TLR-4, thus causing these cells to be non-responders to LPS. TLR-4 is the pattern recognition receptor that interacts with LPS and leads to activation of NFκB. We determined that the EOC-20 cells may not represent the best cell model for our *in vitro* studies due to their lack of responsiveness to LPS. In reading through the literature, it was observed that the microglial cell line BV-2 had been used widely in studies examining microglial function and neuropathology. Therefore, these cells subsequently were assessed as a model for NFκB induction.

Mouse BV-2 Microglial Cells do not Express mRNA for the Cannabinoid Receptor CB_1.

A frozen stock of BV-2 cells was obtained from Dr. Michael McKinley of the Mayo Clinic (Jacksonville, FL). The microglial cell line BV-2 has been used as an *in-vitro* model for studying microglial function. These cells possess functional and phenotypic properties common to primary microglia including phagocytic ability, secretion of pro-inflammatory cytokines and expression of surface receptors and antigens (Blasi et al., 1990). We initially performed experiments with the BV-2 cells to determine if they would be a suitable cell model for our studies. To determine whether BV-2 cells can express CB_1, we performed Real-Time RT-PCR on RNA isolated from BV-2 cells to assess for the presence CB_1 mRNA in unstimulated and activated cells. Complementary DNA (cDNA) was synthesized and used in concert with SYBR green PCR mix and primers for murine CB_1. BV-2 cells have been shown to become activated by IFN-γ and

the bacterial toxin LPS (Blasi et al., 1990; Han et al., 2002; Hwang et al., 2004). Thus, BV-2 cells were seeded overnight in either complete growth medium, IFN-γ (100 U/ml) or LPS (1 μg/ml and 10 ng/ml). CB_1 mRNA was neither detected in unstimulated BV-2 cells nor in stimulated BV-2 cells stimulated with IFN-γ (100 U/ml) and LPS (1 μg/ml or 10 ng/ml) (Figure 9A). The pCD-rSKR6 plasmid containing CB_1 DNA was used as a positive control.

The 167bp PCR amplicons were resolved on a 4% OmniPure agarose gel (Figure 9B, *top panel*) in 1X TBE buffer, and transferred to a nylon membrane in 20X SSC buffer. The transferred DNA was UV crosslinked to the membrane, which was analyzed by Southern blot analysis. An insert from the CB_1 plasmid pCD-rSKR6 was isolated and labeled with digoxigenin (Figure 10A) to be used as a CB_1-specific probe in Southern blot analysis to confirm the results of our Real-Time RT-PCR analyses. Positive hybridization was obtained only with the pCD-rSKR6 DNA insert (Figure 9B, *bottom panel*). All assay controls, including RT-PCR reactions lacking the reverse transcriptase enzyme (-RT) and GAPDH controls, were electrophoresed as well.

Mouse BV-2 Microglial Cells Demonstrate A Baseline Level of Expression for Cannabinoid Receptor CB_2 mRNA.

The CB_2 is localized primarily in peripheral immune cells, but also has been identified within the CNS, with microglial cells being the major contributors of CB_2 expression. We assessed for CB_2 mRNA expression using Real-Time RT-PCR analysis with SYBR green PCR mix and primers specific for murine CB_2. BV-2 cells were seeded

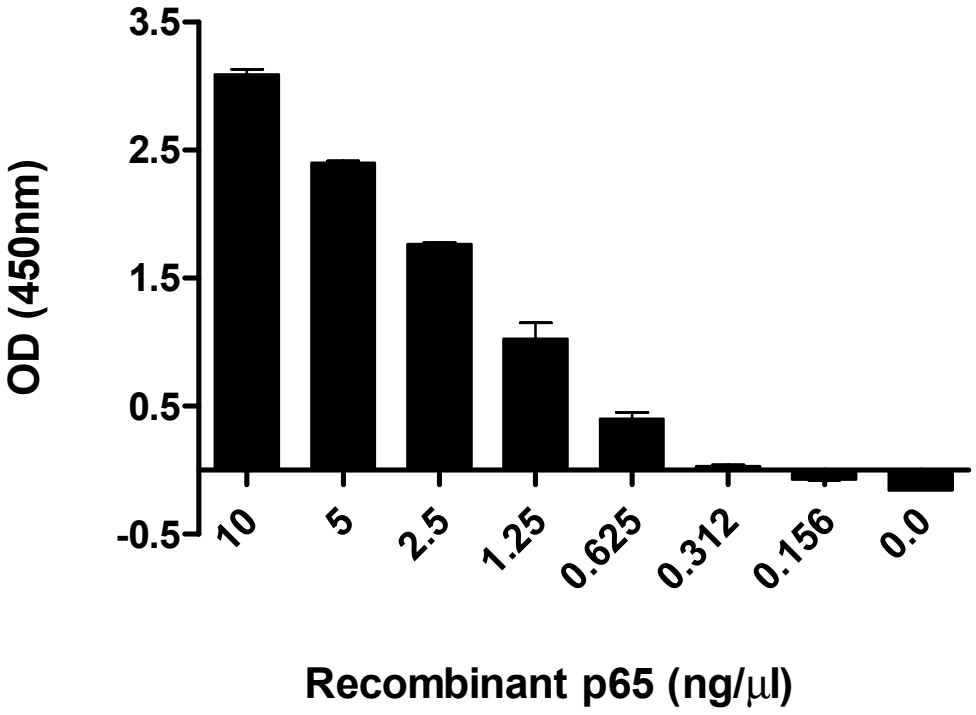

Figure 5. Standard Curve of Recombinant p65. TransAM ELISA (Active Motif) using antibodies specific for the p65 subunit demonstrated the detection of serially diluted (10 ng to 0.156 ng) recombinant p65 protein. Such standard curves were used to extrapolate concentrations of the p65 protein in experimental samples. Results are presented as ± SEM, n=2.

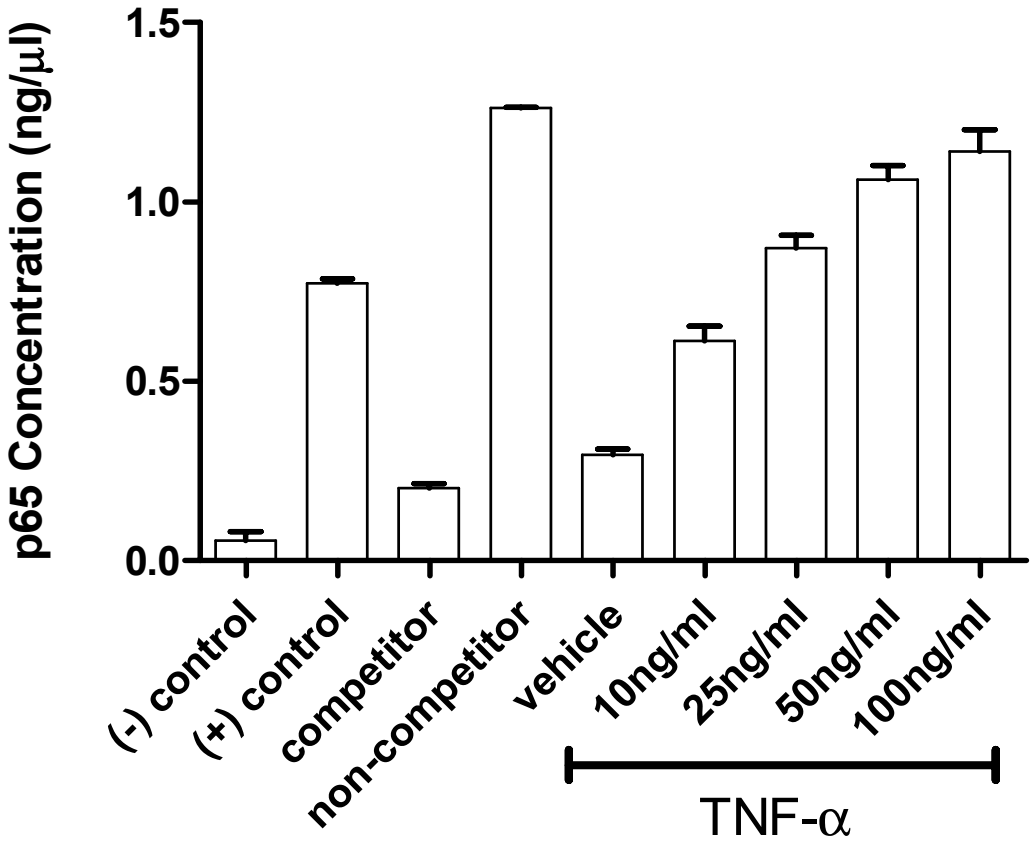

Figure 6. TNF-α-induced Production of p65 Protein in EOC-20 cells. The TransAM NFκB ELISA (Active Motif) demonstrated TNF-α-induced NFκB activation through an increase of p65 production. EOC-20 cells were treated with varying concentrations of TNF-α overnight. The nuclear extracts from these samples were used in ELISA assay. TNF-α exerted a concentration-related increase of p65 production in EOC-20 microglial-like upon stimulation with TNF-α. Results are presented as ± SEM, n=2.

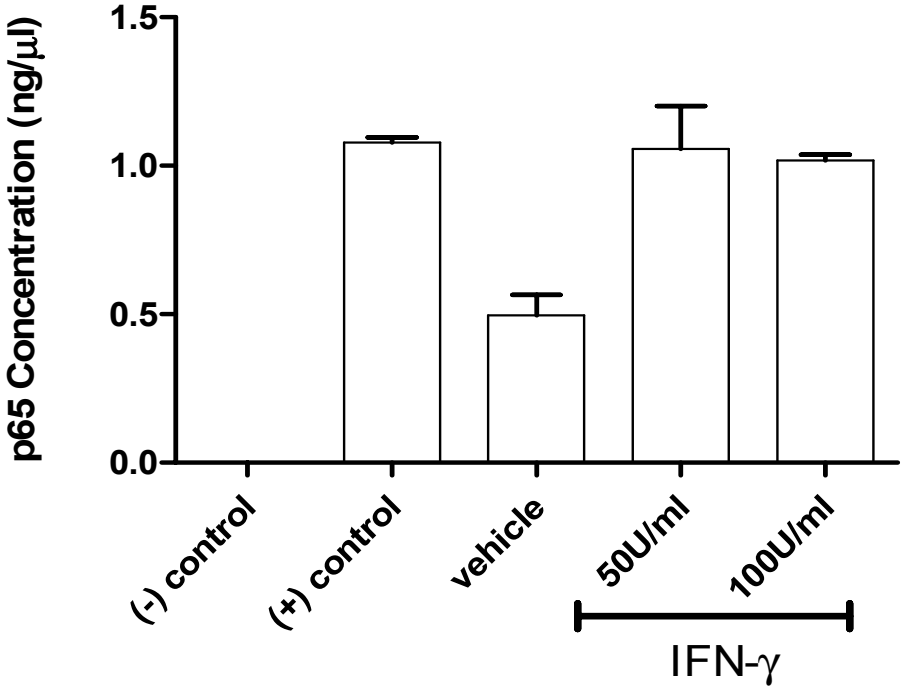

Figure 7. IFN-γ-induced Production of p65 Protein in EOC-20 Cells. The TransAM NFκB ELISA (Active Motif) was employed to assay IFN-γ-induced NFκB activation by way of measuring p65 production. EOC-20 cells were treated with 50 U/ml and 100 U/ml of IFN-γ overnight. The nuclear extracts from these samples were used in the ELISA assay. A two-fold increase of p65 concentrations was observed between the IFN-γ treated cells and the vehicle treated cells. Both concentrations of IFN-γ gave comparable levels of p65 concentration in the EOC-20 cells. The level of p65 in the negative (-) control was undetectable in this assay. Result presented as ± SEM, n=2.

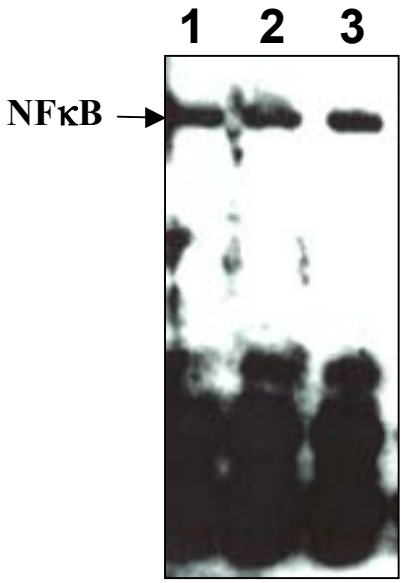

Figure 8. NFκB Binding is Exhibited in Unstimulated and LPS-stimulated EOC-20 Cells. EOC-20 cells were treated for 1 h with complete DMEM, 100 ng/ml LPS, and 100 ng/ml LPS with vehicle (0.01% ethanol). The nuclear extracts from these treatment groups were assessed for NFκB binding to a synthetic radiolabeled DNA oligonucleotide probe. Comparable levels of NFκB binding were observed in all treatment groups. Lanes: 1, unstimulated; 2, LPS alone; 3, LPS and vehicle.

overnight in either complete growth medium, IFN-γ (100 U/ml), or LPS (1 μg/ml and 10 ng/ml). As described previously, a DNA insert from the CB_2 plasmid pUC18-mCB_2 served as the positive control and a PCR reaction mixture lacking cDNA served as the negative control (Figure 11A). CB_2 mRNA expression was observed in unstimulated BV-2 cells, indicating that these cells have a baseline level of CB_2 mRNA expression (Figure 11B). Primary microglia cells *in vitro* have demonstrated differential gene expression of the CB_2 during their various activation states (Carlisle et al., 2002). microglial cells have an increased level of CB_2 gene expression during primed and responsive states of activation, and a lower level of gene expression once these cells are fully activated. Based on the fluorescence levels of the different treatment groups, we observed an augmented level of CB_2 mRNA expression, when compared to the baseline level, in BV-2 cells treated with 100 U/ml IFN-γ, which drives microglial cells into a responsive state of activation (Figure 11B). The lowest levels of fluorescence were observed in cells treated with 1 μg/ml LPS and 10 ng/ml LPS, which can fully activate microglia cells. Gel electrophoresis of the RT-PCR amplicons also reflects the differential expression of CB_2 mRNA among the different cell treatments (Figure 12A, *top panel*). Southern blot analysis was performed to confirm the Real-Time RT-PCR results using a digoxigenin-labeled probe generated from the pUC18-mCB_2 plasmid (Figure 10B). Positive CB_2 hybridization was observed for all treatment groups (Figure 12A, *bottom panel*). Western blot analysis was carried out to assess expression of CB_2 at the protein level in untreated and stimulated BV-2 cells. A human anti-CB_2 antibody synthesized in rabbits (Nowell KW, 1998) was used to detect CB_2 protein expression in all treatment groups (Figure

A.

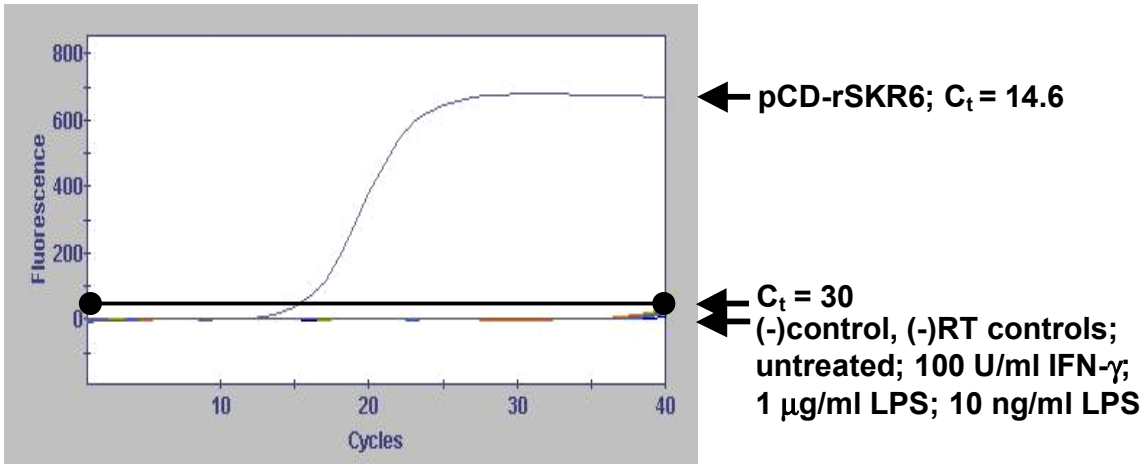

B.

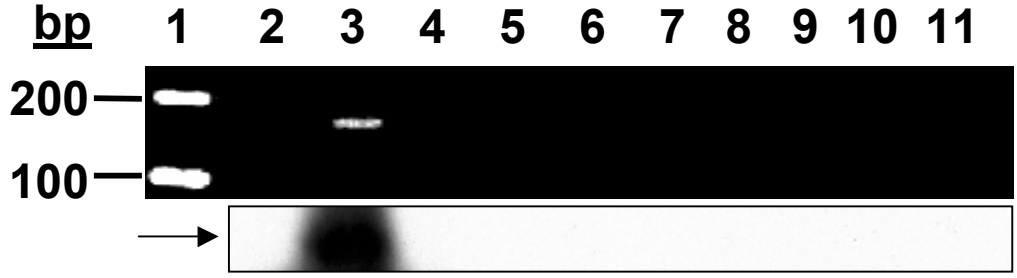

Figure 9. BV-2 Microglial-like Cells Do Not Express CB_1. BV-2 cells were stimulated overnight with complete DMEM, 100 U/ml IFN-γ, 1 μg/ml LPS or 10 ng/ml LPS. (A), Real-Time RT-PCR analysis was performed on total RNA isolated each group using CB_1 specific primers and SYBR green PCR mix. CB_1 mRNA was not detected in untreated or stimulated BV-2 cells. The CB_1 plasmid pCD-rSKR6 (C_t=14.6) served as the positive control. (B), *Top panel*, PCR reactions were resolved by agarose gel electrophoresis. *Bottom panel*, Southern blot analysis using a digoxigenin-labeled mouse CB_1 specific probe. Hybridization was obtained only for the CB_1-positive control (arrow). Lanes: 1, DNA ladder, 2, negative control; 3, positive control (pCD-rSKR6 plasmid); 4, untreated; 6, 100 U/ml IFN-γ; 8, 1 μg/ml LPS; 10, 10 ng/ml LPS; Lanes 5, 7, 9 and 11, (-)RT controls, respectively. The crossover threshold (C_t) was set at 30 fluorescence units.

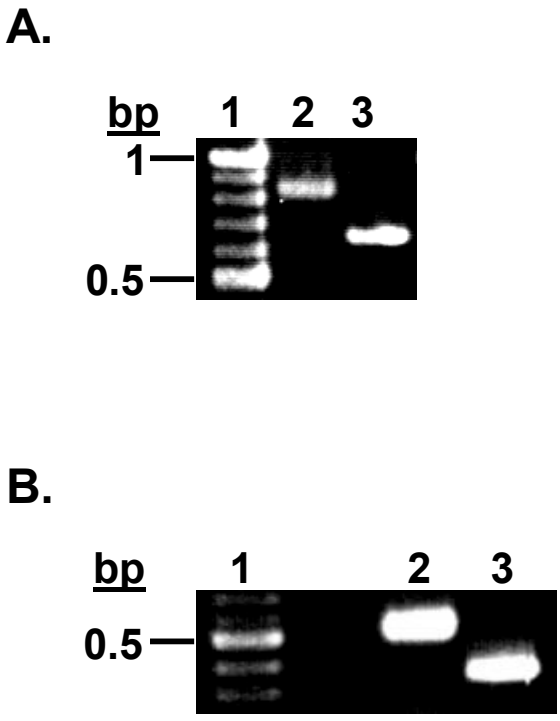

Figure 10. PCR Synthesis of Digoxigenin-Labeled CB_1 and CB_2 Probes. DNA inserts from pCD-rSKR6 (CB_1) and pUC18-mCB2 (CB_2) plasmids were PCR labeled with digoxigenin and used as specific probes for Southern blot analyses. The Dig labeling resulted in slightly larger amplicons than the unlabeled amplicons. (A), The Dig-labeled CB_1 and unlabeled CB_1 probes were approximately 850 bp and 650 bp in size, respectively. (B), Dig-labeled CB_2 and unlabeled CB_2 probes were approximately 500 bp and 350 bp in size, respectively. Lanes: 1, DNA ladder; 2, Dig-labeled probes; 3, unlabeled probes.

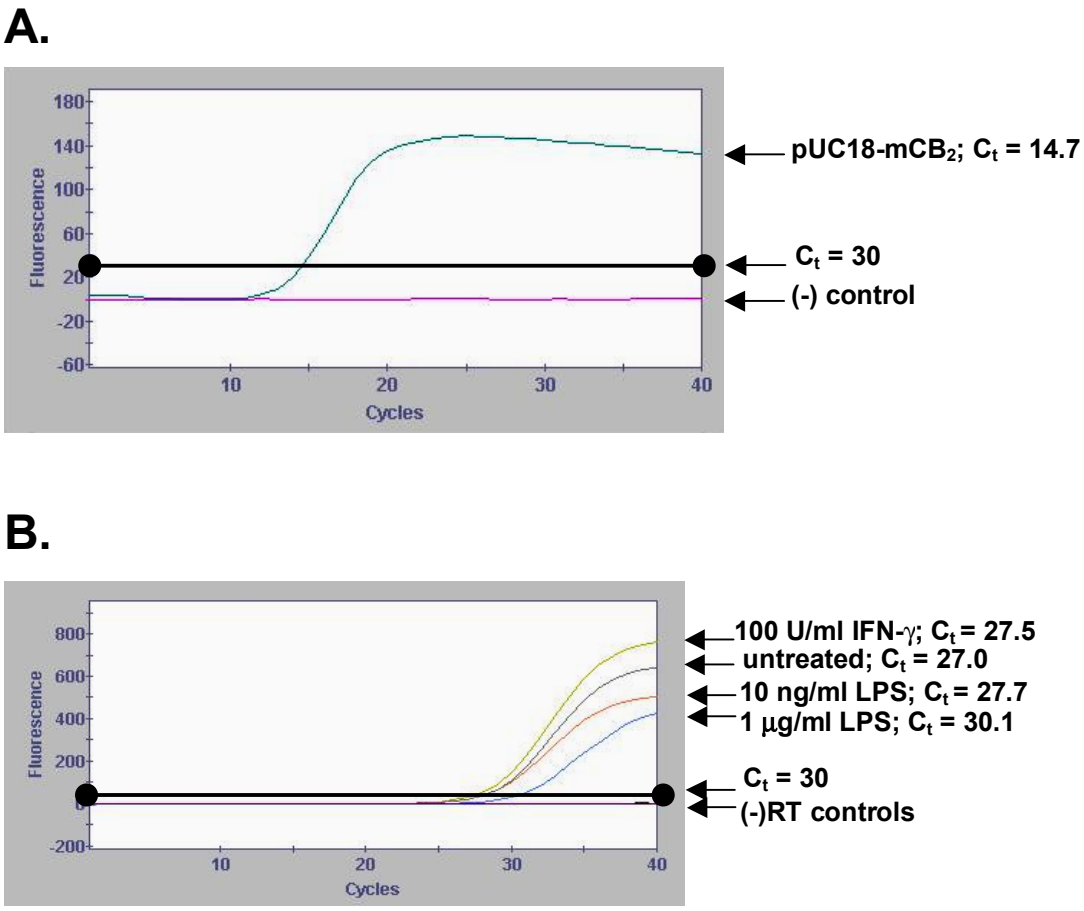

Figure 11. Untreated and Stimulated BV-2 Microglial-like Cells Express CB_2. BV-2 cells were stimulated overnight with complete DMEM, 100 U/ml IFN-γ, 1 μg/ml LPS or 10 ng/ml LPS. (A), The graphs depict the negative control and amplification of DNA from the CB_2 plasmid pUC18-mCB_2 (C_t = 14.7), which served as the positive control (B), Real-Time RT-PCR analysis was performed on total RNA isolated from each group using CB_2 specific primers and SYBR green PCR mix. CB_2 mRNA was detected in untreated cells (C_t = 27.5), 100 U/ml IFN-γ treated cells (C_t = 27.0), and cells stimulated with 1 μg/ml LPS (C_t = 30.1) and 10 ng/ml LPS (C_t = 27.7). There was no amplification detected in the (-)RT controls. The crossover threshold (C_t) was set at 30 fluorescence units.

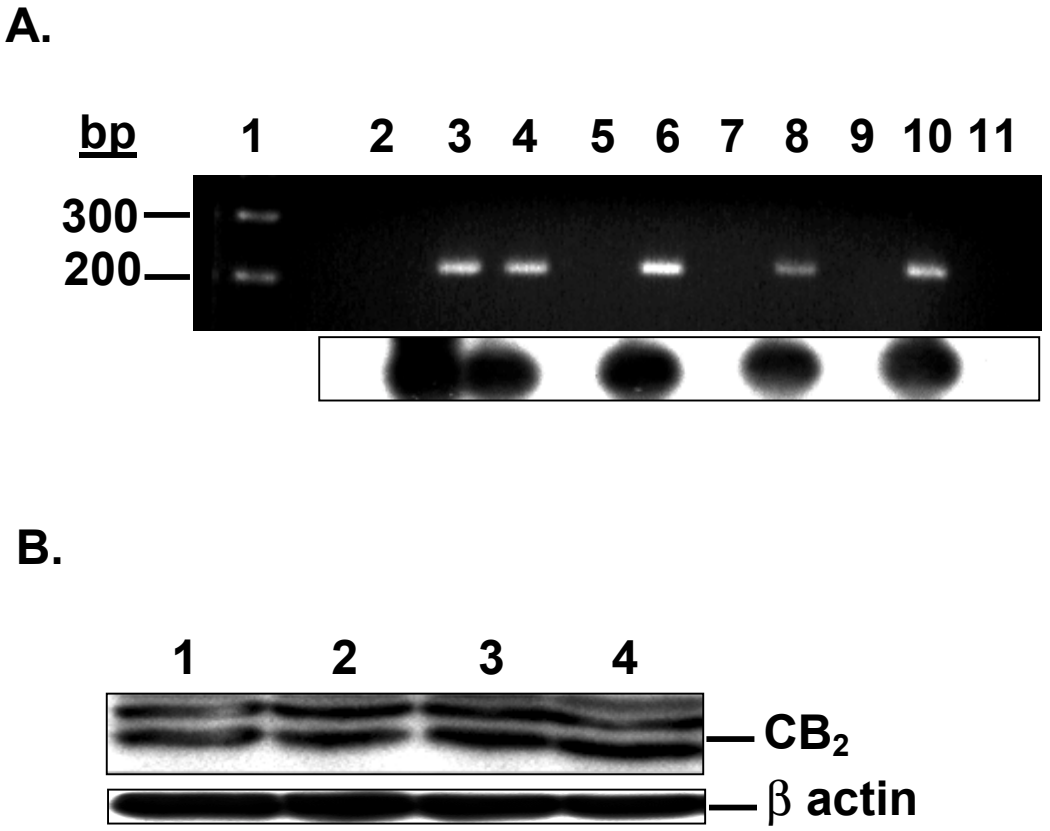

Figure 12. CB_2 Epression in BV-2 Cells. Agarose gel electrophoresis and Southern blot analysis were performed on Real-Time RT-PCR reactions to confirm the presence of the 204 bp CB_2 amplicon. (A), *Top panel*, Gel electrophoresis of RT-PCR amplicons resolved on a 4% agarose gel. CB_2 expression was observed in the positive control, untreated cells and cells stimulated with IFN-γ or LPS. *Bottom panel*, Southern blot analysis using a digoxigenin-labeled CB_2 specific probe. Positve hybridization was obtained for all samples. Lanes: 1, DNA ladder; 2, negative control; 3, positive control (pUC18-CB_2 plasmid); 4, untreated; 6, 100 U/ml IFN-γ; 8, 1 μg/ml LPS; 10, 10 ng/ml LPS. Lanes 5, 7, 9, and 11 are (-) RT controls, respectively. (B), *Top panel*, Western blot analysis of mouse CB_2; Lanes: 1, untreated; 2, 100 U/ml IFN-γ; 3, 1 μg/ml LPS; 4, 10 ng/ml LPS. *Bottom panel*, Equal protein loading control. The blot was stripped and reprobed with anti-β-actin antibody.

12B, *top panel*). Equal protein loading was assessed using a beta-actin antibody (Figure 12B, *bottom panel*).

LPS Induces NFκB Binding in BV-2 Microglial Cells.

The major objective for this study is to assess cannabinoid effects on NFκB activity and regulation upon LPS-induced cell activation. *In vitro*, full activation of microglia can be replicated using LPS, resulting in an induction of pro-inflammatory cytokine genes that are NFκB-regulated. Activation of the NFκB signaling cascade results in several downstream signaling events that culminate in the translocation of NFκB into the nucleus, binding to its gene promoter recognition site and gene transcription. Initially, we assessed for LPS-induced NFκB binding of BV-2 cells using electrophoretic mobility shift assays (EMSA). BV-2 cells were left untreated in complete growth medium or stimulated with 100 ng/ml LPS for various time intervals (5 min., 10 min., 15 min., 30 min., 60 min.) to determine the optimal time kinetics for NFκB binding to a synthetic oligonucleotide probe. The synthetic probe is representative of the NFκB cognate consensus sequence *in vivo*. The 100 ng/ml concentration of LPS was used based on published reports that demonstrated this concentration could robustly activate and elicit an immune response from BV-2 cells (Kim et al., 2005; Kremlev et al., 2004). To perform the EMSAs, binding reactions were made using 4 μg of nuclear protein extracted from each sample group and 1-2 μl of a ^{32}P-labeled probe with a Cerenkov count of $>1x10^5$cpm/μl. The DNA-protein complexes or "shifts" observed demonstrated LPS-induced NFκB binding as early as 10 min. and as late as 60 min. (Figure 13). There

was no binding observed in the untreated sample. Based on these results, it was determined that LPS stimulation for 30min. would be an optimum time to stimulate cells with LPS and investigate any possible cannabinoid-mediated modulation of LPS-induced NFκB binding.

The concentration of nuclear protein (4 μg) used in these assays was determined in a protein titration assay using several concentrations of nuclear protein (1 – 8 μg) extracted from LPS-stimulated BV-2 cells (Figure 14, *left panel*) and LPS-stimulated primary microglial cells (Figure 14, *right panel*). Based on the DNA-protein complexes formed in this experiment, it was determined that 4 μg of nuclear protein would be optimal for our binding assays.

To confirm specificity of the oligonucleotide probe used in the mobility shift assays, we performed cold competition and non-competition experiments using a two-fold increase of a wild-type NFκB probe which served as the competitor, and a two-fold increase of a mutated NFκB probe which served as the non-competitor. The excess of unlabeled wild-type probe competed with and prevented interaction of the ^{32}P-labeled probe with the nuclear extract, thus preventing formation of the DNA-protein complex (Figure 15A, *left lane*). A mutation in the recognition sequence of the mutated unlabeled probe does not prevent proper recognition and binding by NFκB, thus allowing the ^{32}P-labeled probe to bind to the nuclear protein as expected (Figure 15A**,** *right lane*). In addition, supershift assays were performed using antibodies against the p65 and p50 subunits of the NFκB heterodimer. The protein-DNA complexes formed larger

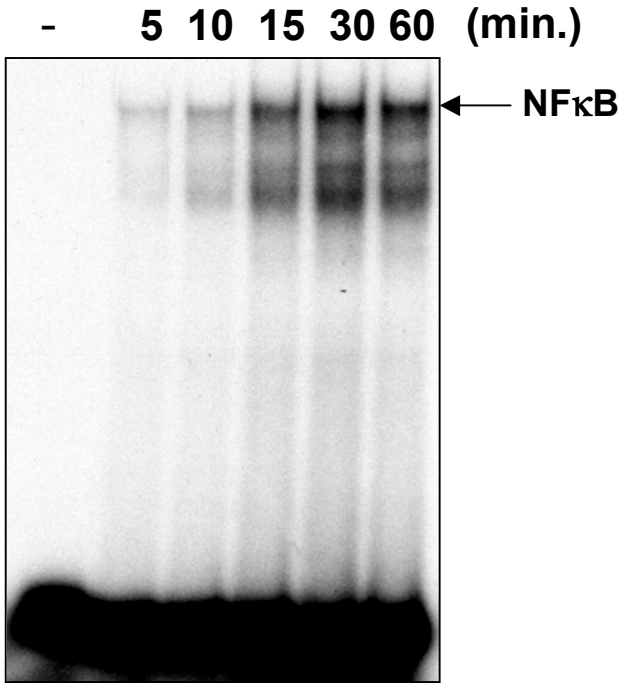

Figure 13. Time Kinetics of LPS-Induced NFκB Binding in BV-2 Cells. BV-2 cells were either untreated (-) or stimulated with 100 ng/ml of LPS for the indicated time intervals (5 min. – 60 min.). Nuclear protein was extracted from all treatment groups and assayed by electrophoretic mobility shift assay (EMSA) using a ^{32}P-labeled, NFκB oligonucleotide probe. Based on the time kinetics of LPS-induced NFκB binding in BV-2 cells, it was determined that the 30 min. time interval would be an optimal time to assess binding. The untreated cells did not demonstrate binding to the synthetic, radiolabeled probe as expected.

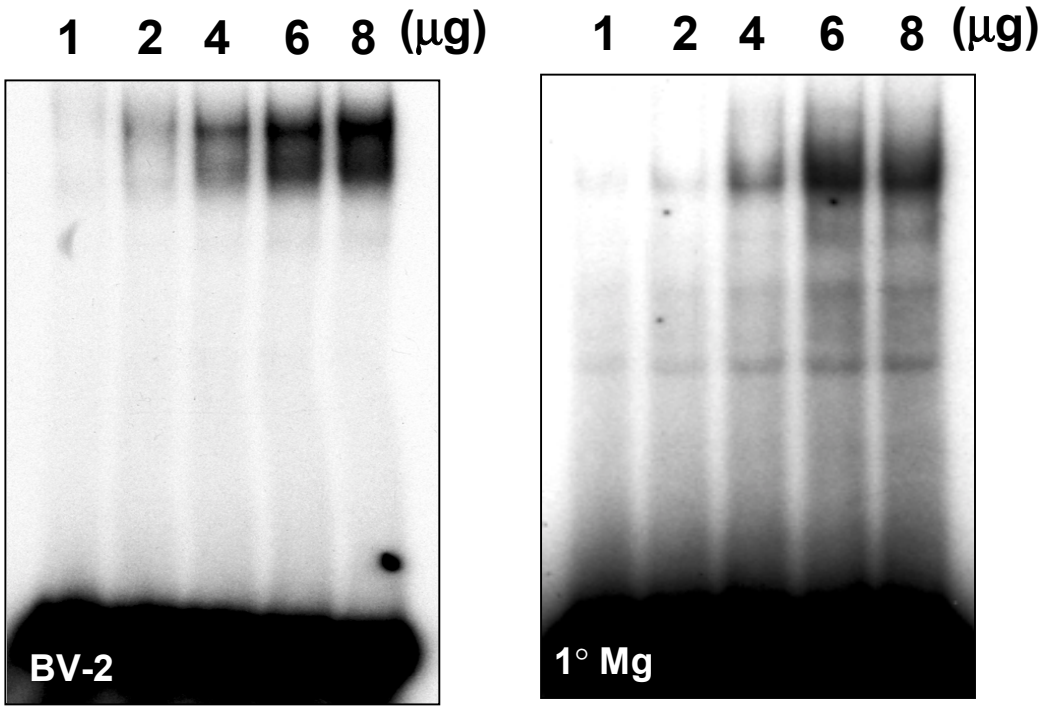

Figure 14. Nuclear Protein Titration of BV-2 Cells and Primary Microglia. BV-2 cells and primary microglia (1° Mg) cells were stimulated with 100 ng/ml LPS (30 min.). Varying concentrations (1 μg – 8 μg) of nuclear protein extracted from the stimulated cells were assessed for binding to a synthetic NFκB probe to determine the optimal protein concentration for the EMSAs. The results observed with both cell types indicate that 4 μg of nuclear protein was sufficient to form the protein-DNA complexes or "shifts".

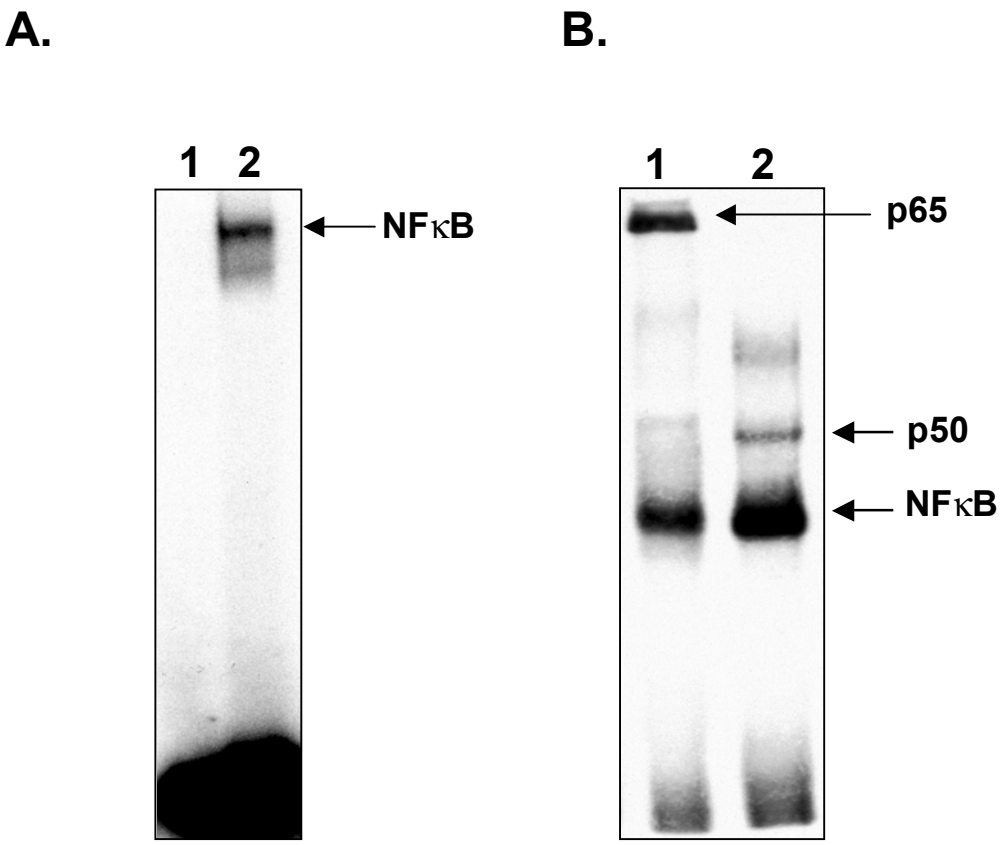

Figure 15. The Specificity of the Radiolabeled Probe Employed in the Mobility Shift Assays. (A), Cold competitor and non-competitor assays were performed on nuclear protein extracted from LPS-stimulated BV-2 cells. For the cold competitor analysis, a 2-fold increase of an unlabeled NFκB probe was incubated with the nuclear protein and the ^{32}P-labeled NFκB probe. The unlabeled probe prevented protein-DNA complex or "shift" formation (Lane 1). For the cold non-competitor analysis, the unlabeled mutant probe will not be recognized by NFκB, thus allowing shift formation of NFκB and the ^{32}P-labeled probe (Lane 2). (B), Supershift assays using antibodies against the p65 and the p50 subunits of NFκB were performed. The p65 antibody (Lane 1) and the p50 antibody (Lane 2) formed larger complexes or "super-shifts" through interaction with the NFκB-^{32}P-labeled probe shifts.

complexes or "supershifts" with the anti-p65 (Figure 15B, *left lane*) or anti-p50 antibody (Figure 15B, *right lane*).

The Partial Cannabinoid Receptor Agonist Δ^9-THC Exerts an Inhibitory Effect on NFκB Binding in LPS-Stimulated BV-2 Cells.

Cannabinoids such as Δ^9-THC have been shown to down-regulate the gene expression of pro-inflammatory cytokines (Puffenbarger et al., 2000; Curran et al., 2005), however such modulation is not due to message degradation (Fischer-Stenger et al., 1993; Puffenbarger et al., 2000). Thus, we examined if the partial cannabinoid receptor agonist Δ^9-THC affects pro-inflammatory cytokine gene expression at the promoter and/or transcriptional level by altering the ability of NFκB to bind to its cognate promoter binding sequence. BV-2 cells were pre-incubated with Δ^9-THC (3 h) and then stimuated with 100 ng/ml LPS for 30 min. Nuclear extracts were used to analyze the induction of NFκB binding to the synthetic DNA probe. EMSA analyses demonstrated that Δ^9-THC inhibited NFκB binding in LPS treated BV-2 cells in a concentration-related fashion. As concentrations approached the nanomolar level, inhibition of NFκB binding was increased as compared to the higher concentrations, with significant inhibition occurring at the 10^{-7}M and 10^{-8}M concentrations, and maximal inhibition occurring at the 10^{-8}M concentration (Figure 16A). This bimodal effect, typical of lipophilic cannabinoid compounds, is exemplified by the initial inhibition and subsequent dissipation of the inhibitory effect at the 10^{-5}M and 10^{-6}M concentrations, respectively. As decreasing

concentrations of Δ^9-THC approach the nanomolar level, inhibition of NFκB binding is observed once again. The 10^{-5}M concentration of Δ^9-THC is an extremely high concentration of this lipophilic compound, and effects observed at this concentration may reflect non-specific action through membrane activation and/or perturbation. High levels of Δ^9-THC also have been shown to cause apoptosis in microglial-like cells, suggesting that the lack of NFκB binding at 10^{-5}M may be due to a decreased number of viable cells. Responses observed approaching or at nanomolar levels are consistent with receptor-mediated effects. Densitometric measurements of the protein-DNA complexes were taken and percent binding of the treatment groups was calculated as compared to the LPS treatment group that served as the positive control (Figure 16B).

The Full Cannabinoid Receptor Agonist CP55940 Exerts an Inhibitory Effect on LPS-Induced NFκB Binding in BV-2 Cells.

The synthetic agonist CP55940 also has been shown to inhibit gene expression of pro-inflammatory cytokines (Puffenbarger et al., 2000). Similarly to Δ^9-THC, we assessed the effects of CP55940 on NFκB binding in LPS-stimulated BV-2 cells. CP55940 inhibited the binding activity of NFκB in a concentration-related fashion comparable to that observed with Δ^9-THC (Figure 17A*)*. Significant inhibition of NFκB binding ranged from 10^{-7}M to 10^{-9}M concentrations of CP55940. The maximal inhibitory effect of CP55940 on NFκB binding was observed at 10^{-9}M concentration, distinct from the maximal inhibitory effect of Δ^9-THC at the 10^{-8}M concentration. These results were not unexpected, for CP55940 acts as a full agonist to both cannabinoid

receptors and therefore would have greater efficacy than the partial agonist Δ^9-THC upon receptor interaction. As observed with Δ^9-THC, inhibition of NFκB binding was observed at the 10^{-5}M concentration of CP55940, which dissipated at the 10^{-6}M concentration, once again demonstrating the biphasic effects of cannabinoid compounds. Densitometric measurements of the protein-DNA complexes were taken and percent binding of the treatment groups was calculated as compared to the LPS treatment group that served as the positive control (Figure 17B).

Time Dependent NFκB Transcriptional Activity in LPS-Stimulated BV-2 Cells.

We have demonstrated that both Δ^9-THC and CP55940 inhibit the binding of NFκB to a synthetic oligonucleotide probe that contains its cognate consensus sequence. We next determined a functional linkage of cannabinoid-mediated inhibition of consensus sequence binding to NFκB transcriptional activity. Using a luciferase-based reporter activity assay, we investigated the ability of NFκB to induce the transcription of the luciferase gene (*Luc*) upon LPS stimulation. BV-2 cells were transiently transfected with the pNFκB-Luc reporter plasmid that contains the *Luc* gene, which is driven by a basic TATA box promoter element (Figures 18 and 19). Directly upstream from the TATA box is an inducible NFκB enhancer element that contains 5 copies of the NFκB consensus sequence. Upon binding of NFκB to this enhancer element, the *Luc* gene is transcribed and ultimately results in the production of the luciferase protein. The level of luciferase measured is directly proportional to NFκB transcriptional activity. We initially

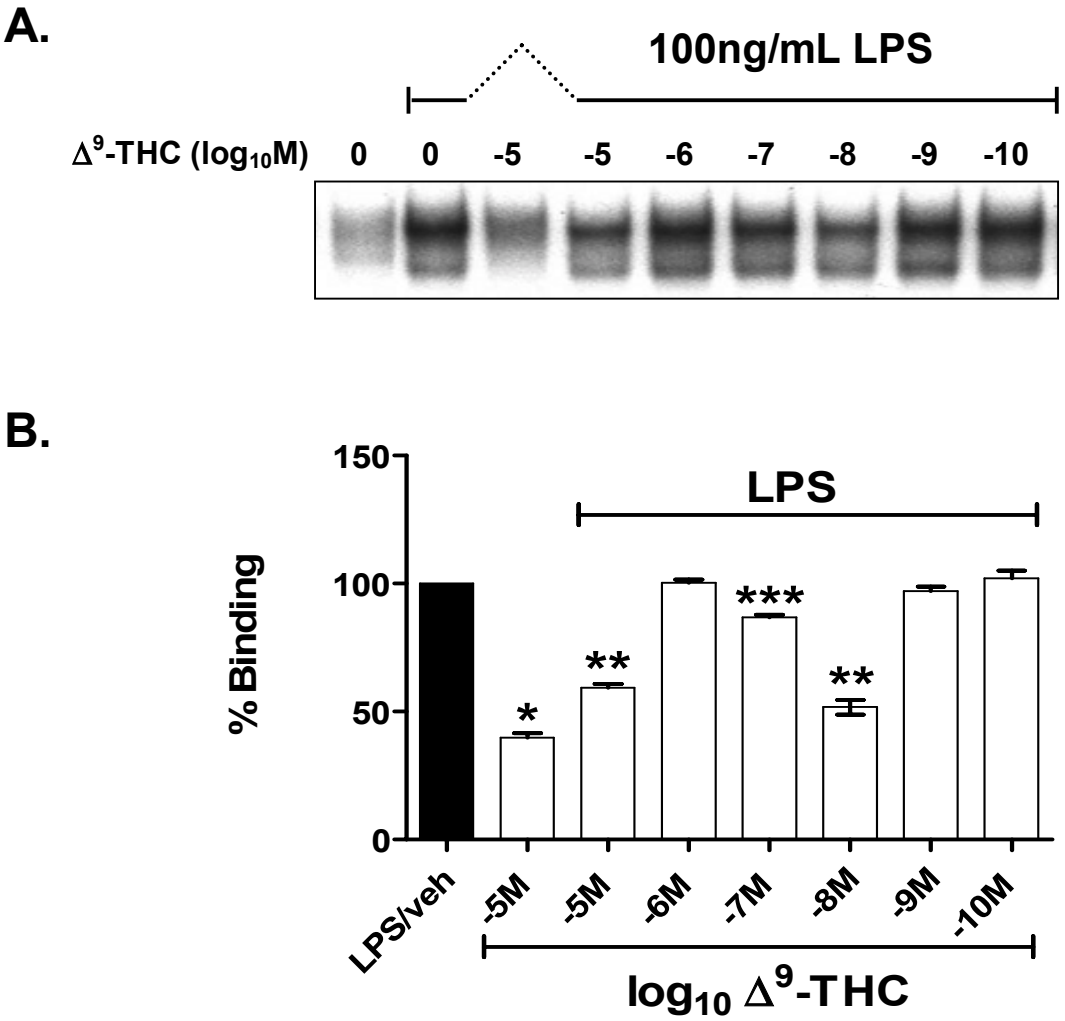

Figure 16. The Partial Cannabinoid Receptor Agonist Δ^9-THC Inhibits LPS-induced NFκB Binding in BV-2 cells. BV-2 cells were pre-treated (3 h) with vehicle (0.01% ethanol) or Δ^9-THC at the indicated concentrations. Binding of nuclear extracts to the ^{32}P-labeled, oligonucleotide NFκB probe then was analyzed by EMSA. Δ^9-THC inhibited NFκB binding in a concentration-related fashion. (A), A representative autoradiogram of NFκB EMSA analysis. (B), Densitometric representation depicting percent binding as compared to the LPS/vehicle positive control treatment group. Densitometric measurement of the vehicle treatment was substracted as the background from each group. Results are presented as the mean ± SD, *p<0.001; **p<0.01; ***p<0.05.

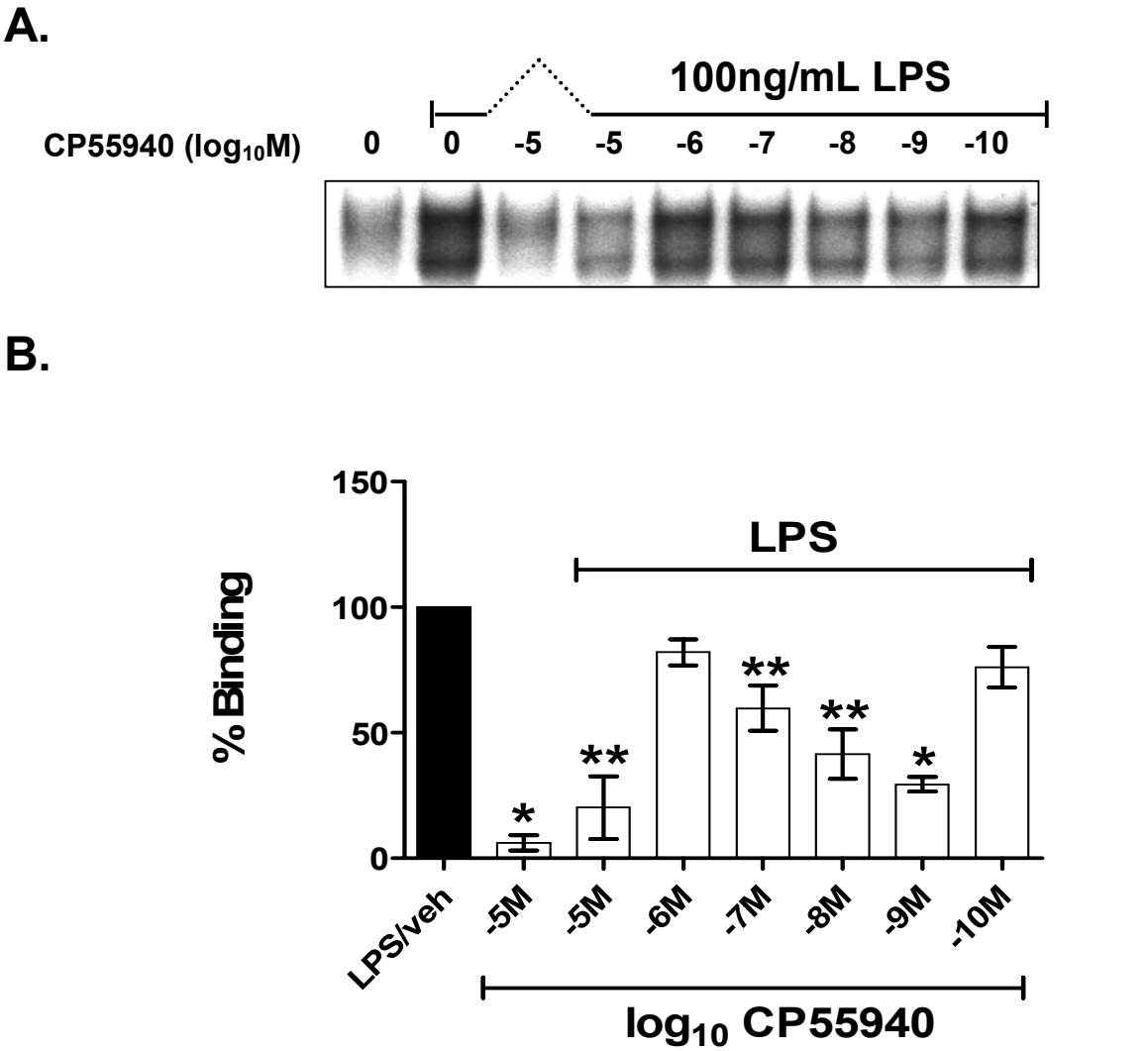

Figure 17. The Full Cannabinoid Receptor Agonist CP55940 Inhibits LPS-induced NFκB Binding in BV-2 Cells. BV-2 cells were pre-treated (3 h) with vehicle (0.01% ethanol) or CP55940 at the indicated concentrations. Binding of nuclear extracts to the ^{32}P-labeled, oligonucleotide NFκB probe then was analyzed by EMSA. CP55940 inhibited NFκB binding in a concentration-related fashion. (A), A representative autoradiogram of NFκB EMSA analysis. (B), Densitometric representation depicting percent binding as compared to the LPS/vehicle positive control treatment group. Densitometric measurement of the vehicle treatment was substracted as the background from each group. Results are presented as the mean ± SD, *p<0.01; **p<0.05.

assessed the time kinetics of LPS-induced NFκB transcriptional activity as it relates to the production of luciferase. Actual protein synthesis occurs further downstream from receptor-ligand interaction, cell activation, and signaling events that lead to gene transcription. BV-2 cells transfected with the pNFκB-Luc plasmid were either treated with vehicle (0.01% ethanol) or 100 ng/ml LPS for various time periods (1 h, 3 h, 8 h and overnight). The amount of luciferase produced from each treatment sample was measured, and from this analysis it was determined that LPS stimulation for 3 h provided distinguishable measurements of luciferase protein when compared to vehicle treated samples of that same time point (Figure 20).

The Exogenous Cannabinoids Δ^9-THC and CP55940 Exert Inhibitory Effects on the Transcriptional Activity of NFκB in LPS-Stimulated BV-2 Cells.

To assess the effects of cannabinoids on LPS-induced NFκB transcriptional activity, BV-2 cells transfected with the pNFκB-Luc reporter plasmid were treated (3 h) with varying concentrations of the partial cannabinoid agonist Δ^9-THC or the full agonist CP55940 prior to stimulation with LPS (3 h). These cells were co-transfected with the control reporter plasmid pSV-β-gal (Figures 21 and 22). The pSV-β-gal plasmid has constitutive expression of the β-gal gene, therefore levels of the β-galactosidase enzyme can be measured to determine transfection efficiency and/or normalization. After drug treatment and LPS stimulation, cells were lysed and luciferase and β-galactosidase levels were measured using a luminometer. Δ^9-THC exerted a concentration-related inhibition

of NFκB transcriptional activity, with a significant decrease in the transcription of the *Luc* gene occurring from the 10^{-7}M to the 10^{-9}M concentrations (Figure 23). The greatest inhibitory effect on transcriptional activity occurred at 10^{-8}M concentration of Δ^9-THC, which is the same concentration of Δ^9-THC that exhibited maximum inhibition of NFκB binding demonstrated in the EMSA analyses (Figure 16). These observations suggest that there is a functional linkage between the diminished ability of NFκB to bind to its cognate promoter site and its ability to mediate gene expression. Similar effects were observed with CP55940. The greatest CP55940-mediated inhibition of transcriptional activity occurred at the 10^{-9}M concentration (Figure 24), but significant down-regulation of NFκB transcriptional activity also was observed at the 10^{-7}M and 10^{-8}M concentrations. In both the Δ^9-THC and CP55940 assays, minimal levels of the luciferase reporter were detected in the vehicle and cannabinoid treated cells lacking LPS stimulation. As with the EMSA analyses, the 10^{-6}M and 10^{-10}M concentrations of either cannabinoid did not have inhibitory effects on transcriptional activity and were similar to the level of activity observed with the LPS control treatment group. As demonstrated previously with the binding studies, the results from the reporter activity assays demonstrate the biphasic manner in which cannabinoids are exerting their effects on NFκB activity. The effects of Δ^9-THC and CP55940 on NFκB binding and transcriptional as concentrations approach the nanomolar level suggest that their effects are receptor-mediated.

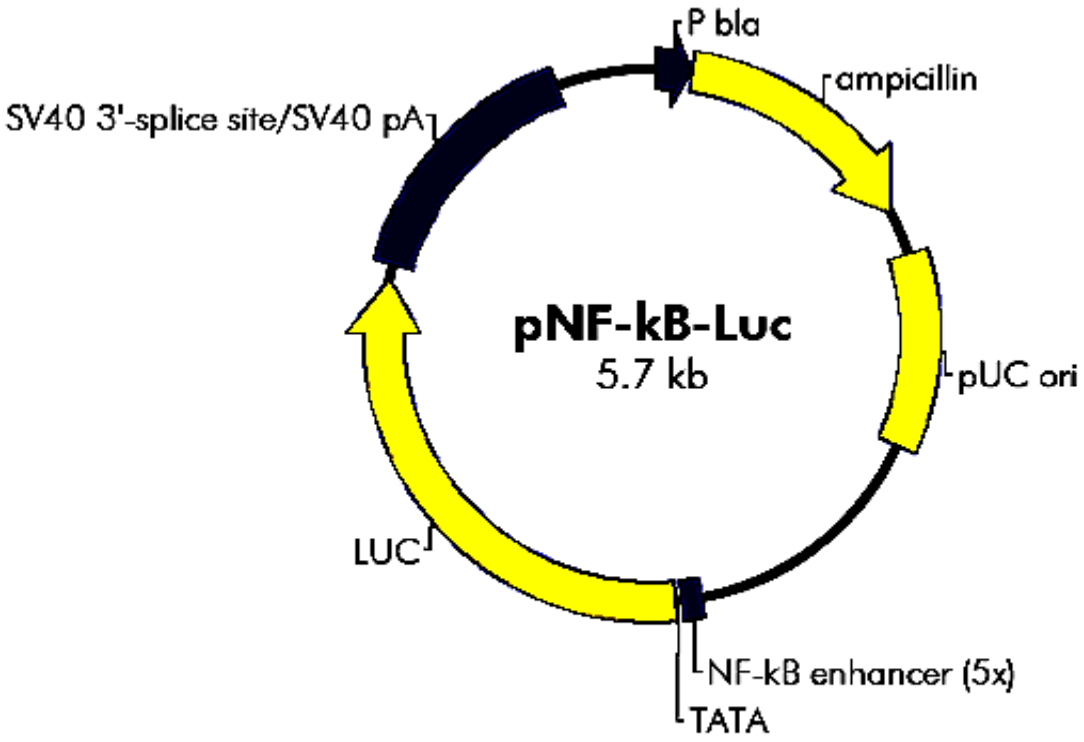

Figure 18. The pNFκB-Luc Reporter Plasmid (Stratagene). The 5.7 kb plasmid has an ampicillin resistance ORF (*bla*), which confers resistance to transformed bacterial cells, and a pUC origin of replication. The reporter gene *Luc* is driven by a basic TATA box promoter element and the NFκB enhancer. The enhancer contains 5 repeats of the consensus sequence 5'-TGGGGACTTTCC**GC-3'.**

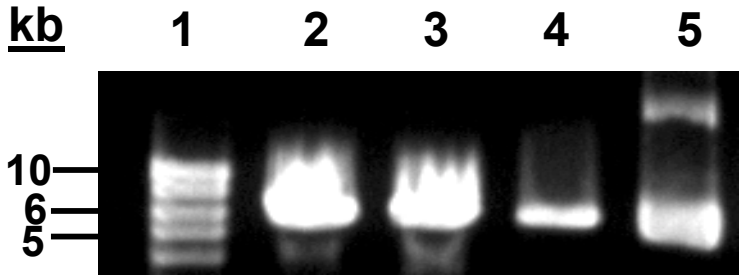

Figure 19. EcoRV Digestion of pNFκB-Luc. The reporter plasmid pNFκB-Luc was digested with EcoRV restriction enzyme. Gel electrophoresis of purified plasmid samples were of the same size as the 5.7 kb stock pNFκB-Luc plasmid. Lanes: 1, DNA ladder; 2, EcoRV digestion of purified pNFκB-Luc (Sample A); 3, EcoRV digestion of purified pNFκB-Luc (Sample B); 4, EcoRV digestion of stock pNFκB-Luc plasmid (Stratagene); 5, undigested stock pNFκB-Luc plasmid.

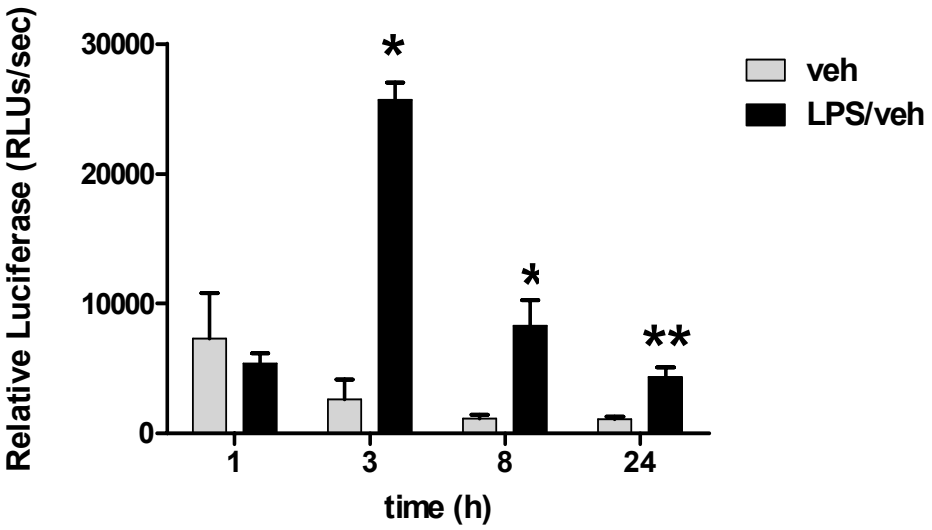

Figure 20. Time Kinetics of NFκB-Induced Luciferase Production in LPS Stimulated BV-2 Cells. BV2 cells were transfected with pNFκB-Luc reporter plasmid in complete growth medium. Time kinetics of LPS-induced NFκB transcriptional activity was determined (24 h post transfection) by stimulating cells with 100 ng/mL LPS for the indicated time intervals. The (3 h) time interval was chosen for all subsequent drug experiments because of the significant distinguishable increase of luciferase levels as compared to the vehicle treatment at 3 h. *P <0.001; **P = 0.014.

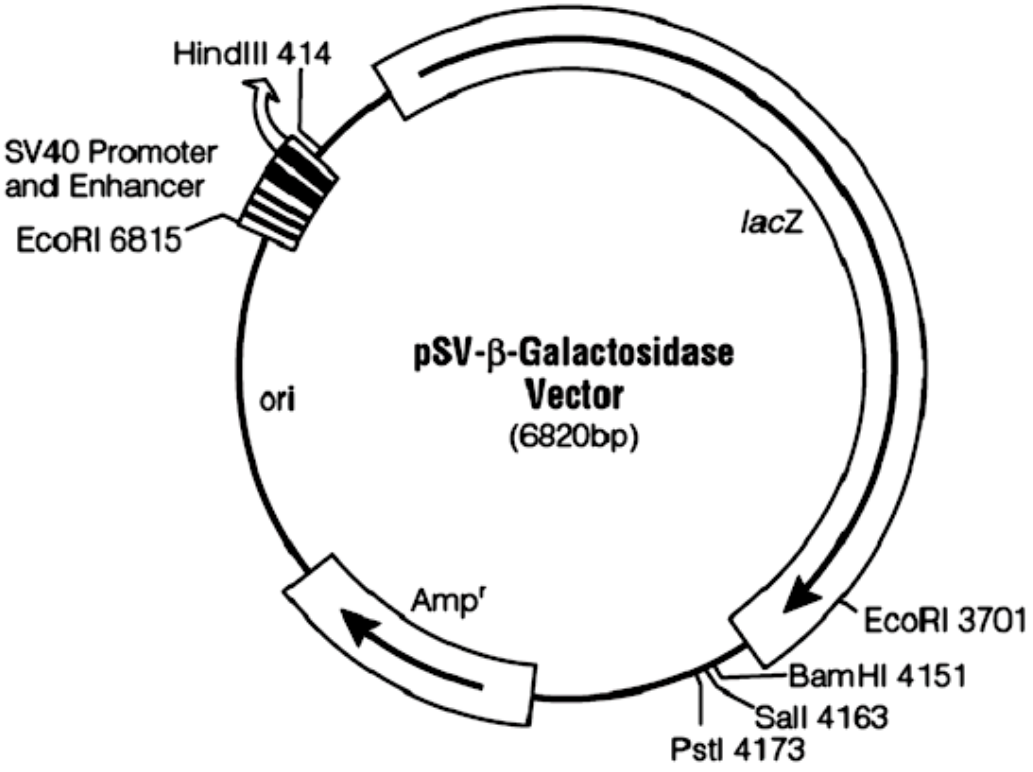

Figure 21. The pSV-β-gal Control Plasmid (Promega). This 6.8 kb plasmid also confers ampicillin resistance (*Ampr*) to transformed bacterial cells, and also has the *lacZ* gene, the coding sequence for the beta-galactosidase enzyme. In addition to multiple restriction sites, pSV-β-gal has a SV40 promoter and enhancer site, and *E. coli* cells transformed with this plasmid will display constitutive expresion of *lacZ* due to the *E. coli gpt* promoter (coding region 428-433).

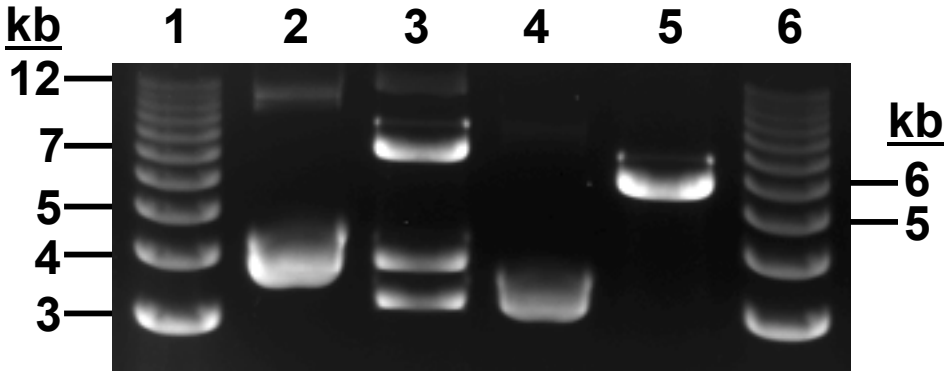

Figure 22. EcoRI Digestion of pSV-βgal and EcoRV Digestion of pNFκB-Luc. The restriction enzyme digestions of both pSV-βgal and pNFκB-Luc were performed at the Molecular Biology Core Facility at VCU. Lanes: 1, DNA ladder; 2, plasmid prep sample of the undigested pSV-βgal plasmid; 3, EcoRI digestion of pSV-βgal that generated a 6.8 kb DNA fragment, which is the size of the plasmid, as well as two smaller fragments that are approximately 4 kb and 3.5 kb in size; 4, plasmid sample of the undigested pNFκB-Luc plasmid; 5, EcoRV digestion of pNFκB-Luc that generated a 5.7 kb DNA fragment, the size of the pNFκB-Luc plasmid; 6, DNA ladder.

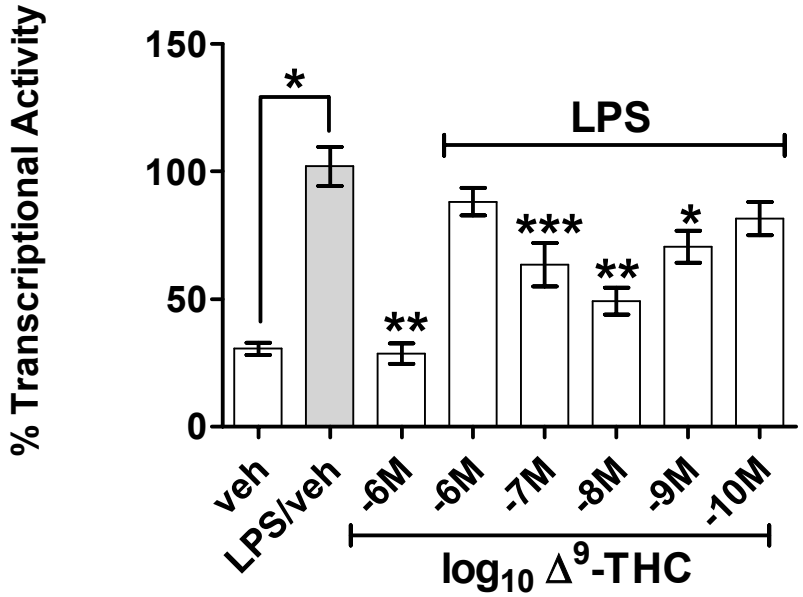

Figure 23. Δ^9-THC Down-Regulates the Transcriptional Activity of NFκB in BV-2 Cells. At 24 h post transfection, BV-2 cells were treated (3 h) with vehicle (0.01% ethanol) and Δ^9-THC at the indicated concentrations, followed by stimulation (3 h) with 100 ng/mL LPS. After LPS treatment, cells were collected, luciferase was extracted from lysed cells and measured. Background luciferase levels were substracted from each sample and normalized to β-galalctosidase levels. Percent activity of all treatment groups was determined. Δ^9-THC inhibited the transcription of the NFκB-regulated luciferase gene (*Luc*) in a concentration-related manner. The greatest inhibitory effect was observed at the 10^{-8}M concentration. The assays were repeated three times in triplicate. The results are presented as the mean ± SD. *p<0.01, **p<0.001, ***p<0.05.

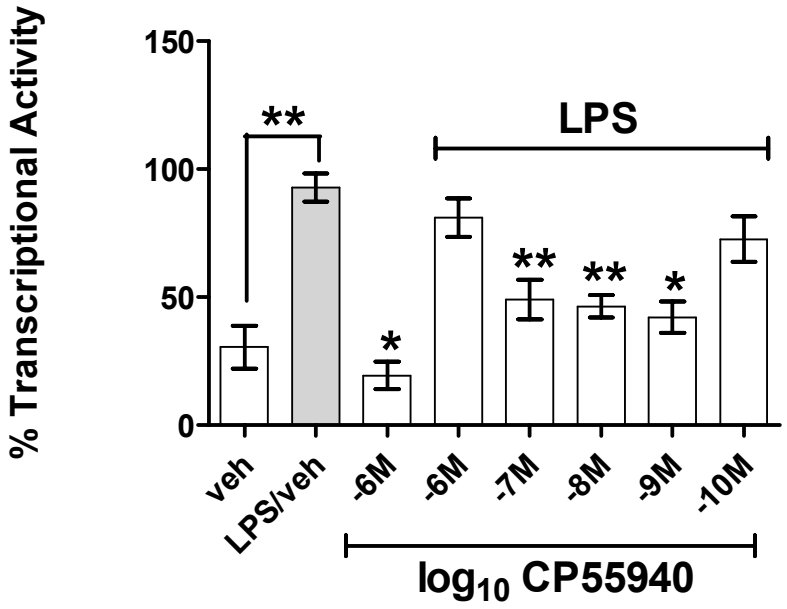

Figure 24. CP55940 also Down-Regulates the Transcriptional Activity of NFκB in BV-2 Cells. At 24 h post transfection, BV-2 cells were treated (3 h) with vehicle (0.01% ethanol) and CP55940 at the indicated concentrations, followed by stimulation (3 h) with 100 ng/mL LPS. After LPS treatment, cells were collected, luciferase was extracted from lysed cells and measured. Background luciferase levels were substracted from each sample and normalized to β-galalctosidase levels. Percent activity of all treatment groups was determined. CP55940 inhibited the transcription of the NFκB-regulated luciferase gene (*Luc*) in a concentration-related manner. The greatest inhibitory effect was observed at the 10^{-9}M concentration. The assays were repeated three times in triplicate. The results are presented as the mean ± SD. *p<0.01, **p<0.05.

The Inhibitory Effects on NFκB Binding and Transcriptional Activity are not Mediated through CB_1.

Both the EMSA analyses and the NFκB reporter activity assays demonstrate that both Δ^9-THC and CP55940 down-regulate binding and transcriptional activity of NFκB in LPS-stimulated BV-2 cells. We investigated the specificity in which both exogenous cannabinoids are exerting inhibitory effects by determining if the effects are mediated through CB_1, CB_2 or in a non-CB_1/non-CB_2 mode. Through Real-Time RT-PCR analysis, BV-2 cells were shown to express CB_2 mRNA but not CB_1 mRNA (Figures 9 and 11). Although BV-2 cells did not exhibit detectable levels of CB_1, we performed reporter activity assays on BV-2 cells treated with the CB_1 selective agonist ACEA and the CB_1 selective antagonist SR141716A. Inhibitory effects and the blocking of such inhibitory effects exerted by ACEA and SR141716A, respectively, could possibly give insight as to whether another cannabinoid receptor is involved. BV-2 cells were pre-treated with decreasing concentrations of ACEA (3 h) 24 h-post transfection, followed by stimulation with 100 ng/ml for 3 h. The level of transcriptional activity of ACEA-treated samples were comparable to that of the LPS treated positive control group (Figure 25); thus, ACEA did not exert an inhibitory effect on NFκB transcriptional activity. We complemented these studies with competition assays using the CB_1 antagonist SR141716A in concert with the full agonist CP55940. Twenty-four hours post transfection, BV-2 cells were treated with SR141716A (10^{-6}M) for 1 h, and with CP55940 (10^{-7}M) for 3 h prior to stimuation with LPS. The 10^{-7}M concentration of CP55940 was used because a significant decrease of transcriptional activity was

consistently observed at this concentration. BV-2 cells treated with vehicle and LPS/vehicle served as the negative and positive controls, respectively. LPS-stimulated BV-2 cells pre-treated with CP55940 without prior exposure to the antagonist SR141716A was used as the comparative group for assessing the effects of SR141716A. The exposure to SR141716A prior to cannabinoid treatment did not block the inhibitory effect of CP55940 (Figure 26); thus, comparable levels of activity were observed between SR141716A and CP55940 treated, stimulated BV-2 cells and CP55940 treated, stimulated cells. The results from these studies demonstrate that Δ^9-THC and CP55940 exert effects in a CB_1-independent manner.

The Cannabinoid-Mediated Inhibitory Effects on NFκB Binding and Transcriptional Activity are Mediated, In Part, Through CB_2.

We have demonstrated through receptor specificity studies that the inhibitory effects exerted by Δ^9-THC and CP55940 are not mediated through CB_1. Those findings were expected, for Real-Time RT-PCR analysis revealed that BV-2 microglial cells do not express mRNA for CB_1. We then performed receptor specificity studies to determine if the effects of Δ^9-THC and CP55940 are exerted by CB_2. As described previously with the CB_1 specificity studies, transfected BV-2 cells were pre-treated (3 h) with the CB_2-selective ligand O-2137 or the CB_2-selective antagonist SR144528 in concert with CP55940. There was a significant decrease in transcriptional activity observed in the O-0137 treated cells ranging from the 10^{-7}M to 10^{-10}M concentrations, with the 10^{-8}M concentration exhibiting the maximum down-regulation (Figure 27). It was observed that

the level of inhibition of NFκB transcriptional activity was not as profound with O-2137 as was observed with Δ^9-THC and CP55940. The selectivity of O-2137 is based on its affinity to bind to CB_2 and not its responsiveness upon interaction with the receptor, and therefore O-2137 may not be as efficacious as Δ^9-THC and CP55490. To further investigate the involvement of CB_2, we exposed BV-2 cells to the CB_2-selective antagonist SR144528 (10^{-6}M) for one hour prior to CP55940 (10^{-7}M) treatment and LPS stimulation. As described previously, treatment with CP55940 resulted in a significant decrease in transcriptional activity as compared to LPS treated cells; however, treatment with SR144528 prior to incubation with CP55940 blocked the inhibitory effect of CP55940 (Figure 28). The level of transcriptional activity observed in SR144528-treated cells was not returned to the level of activity observed with LPS-stimulated cells, but there was a significant increase of transcriptional activity when compared to CP55940-treated cells that were not exposed to SR144528. The combined results of the CB_1 and CB_2 specificity studies suggest that Δ^9-THC and CP55940 are exerting inhibitory effects on NFκB binding and activity through interaction with the CB_2.

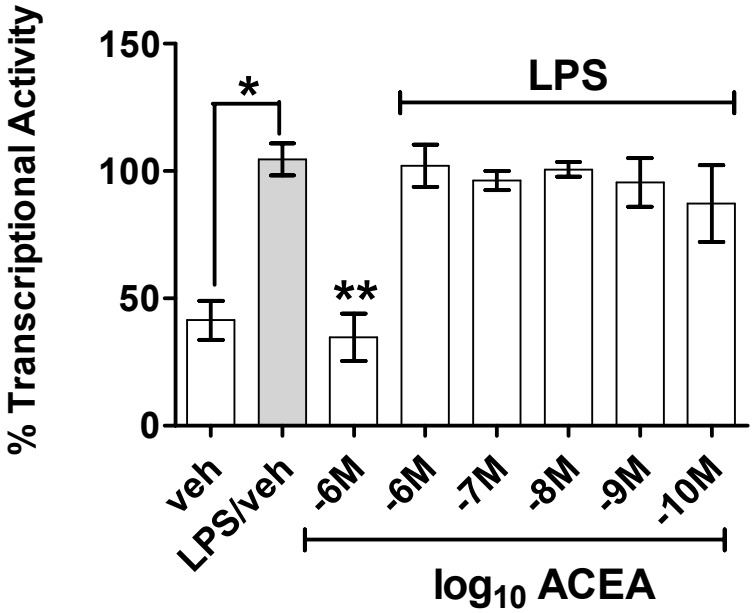

Figure 25. The CB_1-Selective Agonist ACEA Does Not Inhibit the Transcriptional Activity of NFκB in BV-2 Cells. At 24 h post transfection, BV-2 cells were treated (3 h) with vehicle (0.01% ethanol) and ACEA at the indicated concentrations, followed by stimulation (3 h) with 100 ng/mL LPS. After LPS treatment, cells were collected, luciferase was extracted from lysed cells and measured. Background luciferase levels were substracted from each sample and normalized to β-galalctosidase levels. Percent activity of all treatment groups was determined. Comparable levels of transcriptional activity were observed between the ACEA-treated, LPS-stimulated BV-2 cells and LPS-stimulated BV-2 cells. All assays were performed twice in triplicate. The results are presented as the mean ± SD. *p<0.01, **p<0.05.

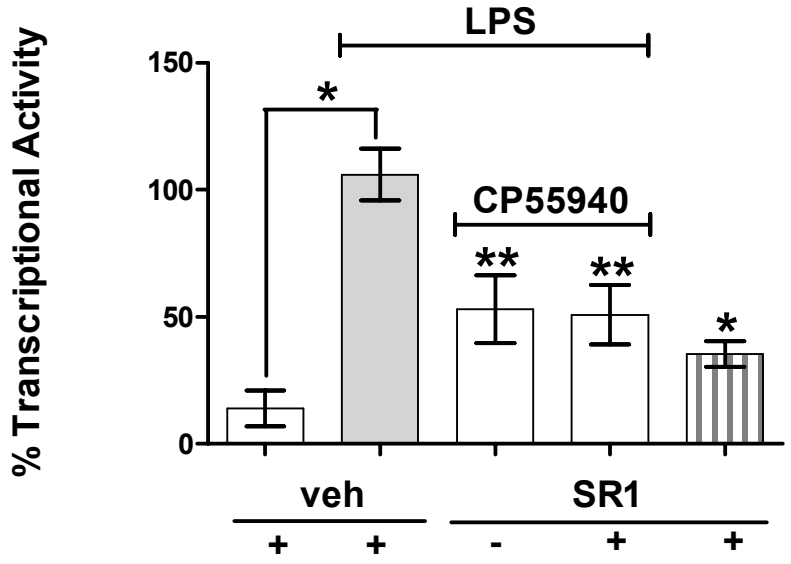

Figure 26. The CB_1-Selective Antagonist SR141716A (SR1) Does Not Block the Inhibitory Effects of CP55940 on NFκB Transcriptional Activity. NFκB reporter activity assays were performed on LPS-stimulated BV-2 cells pre-treated separately with the CB_1 antagonist SR141716A at 10^{-6}M (1 h) and CP55940 at 10^{-7}M (3 h). After LPS treatment, cells were collected, luciferase was extracted from lysed cells and measured. Background luciferase levels were substracted from each sample and normalized to β-galalctosidase levels. Percent activity of all treatment groups was determined. CP55940 exhibited an inhibitory effect on transcriptional activity but that effect was blocked by SR141716A. The results are presented as the mean ± SD, *p<0.01, **p<0.05.

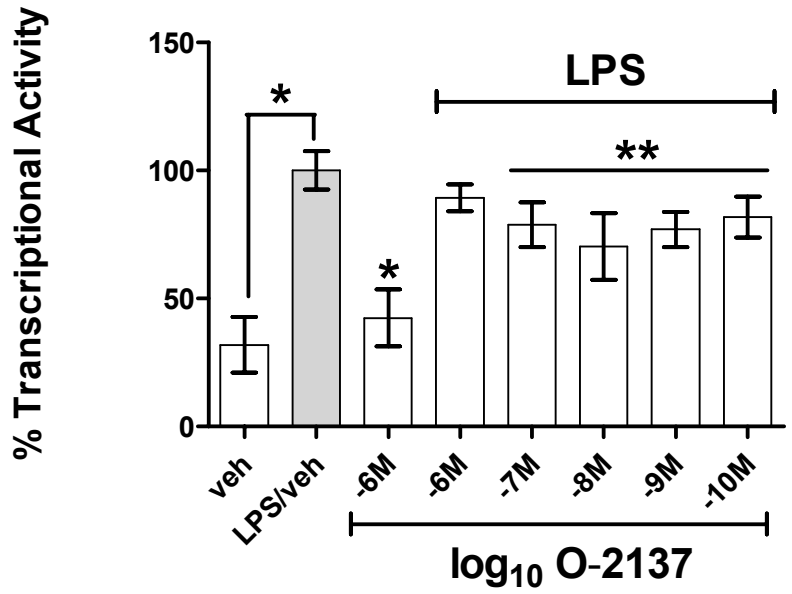

Figure 27. The CB_2-Selective Ligand O-2137 Partially Inhibits the Transcriptional Activity of NFκB in BV-2 Cells. At 24 h post transfection, BV-2 cells were treated (3 h) with vehicle (0.01% ethanol) and O-2137 at the indicated concentrations, followed by stimulation (3 h) with 100 ng/mL LPS. After LPS treatment, cells were collected, luciferase was extracted from lysed cells and measured. Background luciferase levels were substracted from each sample and normalized to β-galalctosidase levels. Percent activity of all treatment groups was determined. Although on a smaller scale, O-2137 significantly inhibited the transcriptional activity of NFκB, with maximum inhibition occurring at the 10^{-8}M concentration. All assays were performed twice in triplicate. The results are presented as the mean ± SD. *p<0.001, **p<0.05.

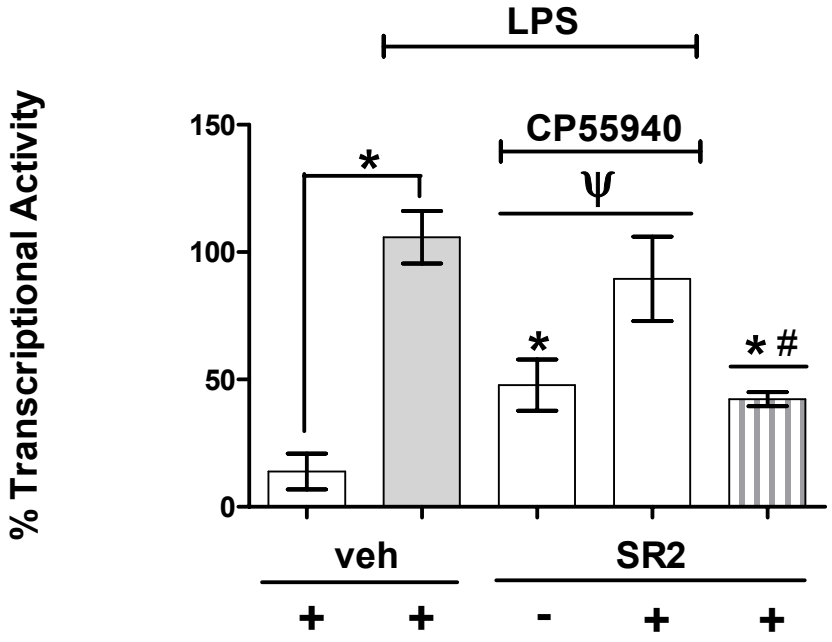

Figure 28. The CB_2-Selective Antagonist SR144528 (SR2) Blocks the CP55940-Mediated Inhibition of NFκB Transcriptional Activity. NFκB reporter activity assays were performed on LPS-stimulated BV-2 cells pre-treated separately with the CB_2 antagonist SR144528 at 10^{-6}M (1 h) and CP55940 at 10^{-7}M (3 h). After LPS treatment, cells were collected, luciferase was extracted from lysed cells and measured. Background luciferase levels were substracted from each sample and normalized to β-galalctosidase levels. Percent activity of all treatment groups was determined. CP55940 exhibited an inhibitory effect on transcriptional activity, and that inhibition was blocked by SR144528. The results are presented as the mean ± SD, n=4. *$p<0.01$, for treatment groups compared with the LPS/vehicle control treatment. $^{\psi}p<0.01$, for CP55940-treated cells compared to CP55940-treated cells exposed to SR2. $^{\#}p<0.05$, for SR2 alone treated cells compared to CP55940-treated cells exposed to SR2.

The Non-CB_1/Non-CB_2 Selective Agonist O-2095 does not Exert Inhibitory Effects on NFκB Transcriptional Activity.

The results of our studies thus far suggest that Δ^9-THC and CP55940 are exerting effects at least in part through the CB_2. We investigated whether another cannabinoid subtype could also mediate the effects observed with Δ^9-THC and CP55940.

The synthetic cannabinoid agonist O-2095 does not exhibit selectivity to either CB_1 or CB_2 but elicits a pharmacological response (Ng et al., 1999). O-2095 does demonstrate selectivity to vanilloid receptors, and it has been suggested that the vanilloid receptor TRVP-1 functions as a cannabinoid receptor (Smart et al., 2000; Ross, 2003). Any O-2095-mediated effects on the activity of NFκB may suggest the involvement of another cannabinoid receptor subtype. To determine if cannabinoid-mediated inhibition of NFκB activity also may be exerted through another cannabinoid receptor subtype, transfected BV-2 cells were treated with O-2095 as described previously. O-2095 did not elicit an inhibitory response on NFκB transcriptional activity, and the level of transcriptional activity in O-2095-treated cells was comparable to levels observed with the LPS control treatment group (Figures 29). Interestingly, cells treated with 10^{-6}M concentration of O-2095 without LPS stimulation demonstrated elevated levels of transcriptional activity, suggesting that O-2095 may participate in signaling events that induce the activation of NFκB.

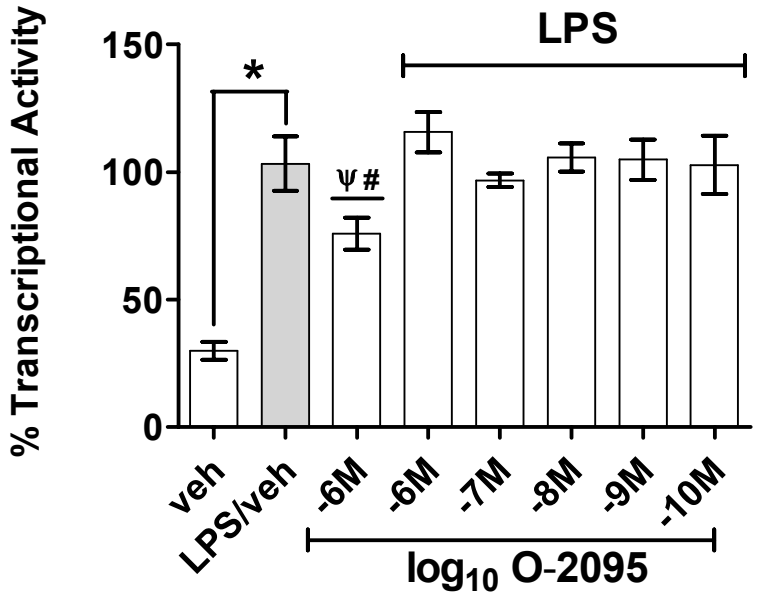

Figure 29. The Non-CB_1/Non-CB_2 Selective Agonist O-2095 Does Not Inhibit the Transcriptional Activity of NFκB. NFκB reporter activity assays were performed on LPS-stimulated BV-2 cells pre-treated O-2095 (3 h) at the indicated intervals. After LPS treatment, cells were collected, luciferase was extracted from lysed cells and measured. Background luciferase levels were substracted from each sample and normalized to β-galalctosidase levels. Percent activity of all treatment groups was determined. O-2095 treated BV-2 overall exhibit the same level of transcriptional activity as LPS alone treated BV-2 cells. The results are presented as the mean ± SD, n=3. *$p<0.01$, for vehicle treated cells compared with LPS/vehicle treated cells. $^{\Psi}p<0.01$ and $^{\#}p<0.05$, for drug alone treated cells compared with vehicle treated and LPS/vehicle treated cells, respectively.

LPS-Induced Phosphorylation and Degradation of IκBα are Time-Specific.

In addition to determining the specificity in which Δ^9-THC and CP55940 down-regulate NFκB activity, we also set out to determine the sites of action in which Δ^9-THC and CP55940 inhibit NFκB function. We proposed to determine whether cannabinoids inhibiting the binding and activity of NFκB through modulation of its conformation, or are affecting cellular events in the cytoplasm such as protein synthesis, phosphorylation, degradation and transport. NFκB activation is rigorously controlled both extracellularly and intracellularly, and the rate-limiting step of NFκB activation is the phosphorylation and subsequent degradation of the inhibitor protein IκBα. Prior to cell activation, IκBα sequesters NFκB in the cytoplasm by masking its nuclear localization signal, and upon cell activation, IκBα is phosphorylated at serine residues 32 (Ser32) and 36 (Ser36). Phosphorylated IκBα is then polyubiquitinated, and the ubiquitination of this protein marks it for degradation by the 26S proteasome. The degradation of IκBα allows NFκB to translocate into the nucleus, bind to its cognate promoter binding sites and induce gene expression. Since these early signaling events that result in the activation of NFκB take place rapidly, we first determined the time kinetics of IκBα phosphorylation. For these experiments BV-2 cells were treated with vehicle or 100 ng/ml LPS for 5, 7.5, 10, 15, and 30 min. Cytoplasmic and nuclear protein were extracted for analysis, and the cytoplasmic fractions were assessed for the phosphorylation and degradation of IκBα using antibodies specific for IκBα phosphorylated at Ser32/Ser36 and endogenous IκBα, respectively. Phosphorylation of IκBα was observed as early as 5 min. post LPS

stimulation and was barely detectable by the 15 min. time point (Figure 30, *top panel*). There was no major induction of IκBα phosphorylation in the vehicle treated samples at the 5 min. and 30 min. time intervals. To confirm equal protein loading, the blots were stripped and reprobed with beta-actin antibody (Figure 30, *bottom panel*). Cytoplasmic protein fractions from the LPS-stimulated BV-2 cells also were analyzed by Western immunoblot analysis for LPS-induced degradation of IκBα. Degradation of IκBα was observed 15 min. post LPS stimulation (Figure 31, *top panel*), which is complementary to the results obtained from Western immunoblot analysis of phosphorylated IκBα (Figure 30). Again, the blots were stripped and reprobed with a beta-actin antibody to assess for equal protein loading (Figure 31, *bottom panel*).

Δ^9-THC and CP55940 do not Inhibit LPS-Induced Phosphorylation of IκBα.

After determining the time kinetics of IκBα phosphorylation and degradation, we employed Western immuoblot analysis to determine if Δ^9-THC and CP55940 modulate the phosphorylation and/or degradation of IκBα. BV-2 cells were pre-treated with Δ^9-THC or CP55940 and then stimulated with 100 ng/ml LPS for 5 min. As described previously, cytoplasmic protein was resolved by SDS-Page electrophoresis, electroblotted and probed with IκBα antibodies. Results from these analyses demonstrated that phosphorylation of IκBα was not detected in unstimulated cells, as seen with vehicle and cannabinoid alone treated cells (Figures 32A and 32B**)**. Phosphorylation of IκBα occurred upon LPS stimulation and the same overall level of phosphorylation was

observed in cells pre-treated with Δ^9-THC (Figure 32A, *top panel*) or CP55940 (Figure 32B, *top panel*). These results suggest that the inhibitory effects of Δ^9-THC and CP55940 on NFκB function are independent of IκBα phosphorylation.

Δ^9-THC and CP55940 Partially Inhibit the Degradation of IκBα Upon LPS Stimulation.

We also performed Western blot analysis on the endogenous IκBα protein to assess degradation of this protein and the possible cannabinoid effects on this cellular process. IκBα is ultimately degraded by the 26S proteasome upon cell stimulation, and we demonstrated previously that this process occurs within 15 min. after LPS-induced cell activation. BV-2 cells were pre-treated (3 h) with Δ^9-THC or CP55940, followed by stimulation with 100 ng/ml LPS (15 min.). Western immunoblot analyses were performed on cytoplasmic protein fractions using the anti-IκBα antibody described previously, and we observed IκBα degradation in LPS-stimulated BV-2 cells (Figures 33A and 33B). However, Δ^9-THC (Figure 33A) and CP55940 (Figure 33B) treatment prior to LPS stimulation resulted in a decrease in the degradation of IκBα. Cells that were treated with cannabinoids without LPS stimulation exhibited the same amount of IκBα in the cytoplasm as the untreated cells. These results demonstrate that while Δ^9-THC and CP55940 do not affect the phosphorylation of IκBα, these compounds are able to diminish the LPS-induced, proteolytic degradation of this protein. The ability of Δ^9-THC and CP55940 to inhibit degradation of IκBα suggests that these compounds may

affect actual proteolytic activity of the 26S proteosome or affect a regulatory event that happens after phosporylation, but prior to degradation, such as ubiquitination.

Δ^9-THC does not Affect Synthesis and Phosphorylation of the p65 Subunit

We investigated overall levels of p65 in both the cytoplasm and nucleus through Western immunoblot analyses. BV-2 cells were pre-treated with Δ^9-THC (3 h) and stimulated with 100 ng/ml LPS for 30 min. Cytoplasmic and nuclear proteins were extracted and resolved by SDS-Page electrophoresis. Western immunoblot analysis was performed using an anti-p65 antibody for detection in both the cytoplasm and nucleus. The levels of cytoplasmic p65 were comparable in all samples, demonstrating that synthesis of this protein is not affected by Δ^9-THC (Figure 34A, *top panel*). In nuclear samples, we observed a LPS-induced increase of p65 in the stimulated cells when compared to vehicle treated or cells treated only with cannabinoids, demonstrating apparent adequate transport of p65 into the nucleus upon cell activation. The levels of nuclear p65 in cells treated with Δ^9-THC were also comparable to those for the LPS treated samples (Figure 34B, *top panel*), suggesting that these exogenous cannabinoids do not affect the transport of p65 into the nucleus. The blots were stripped and reprobed with beta-actin (Figure 34A, *bottom panel*) and proliferating cell nuclear antigen (PCNA) (Figure 34B *bottom panel*) antibodies to assess for equal cytoplasmic and nuclear protein, respectively.

Complete NFκB activation necessitates phosphorylation of the p65 subunit, which is carried out by several stimulant-specific serine kinases. Serine residue 536 is located

in the transactivation domain of p65 and is phosphorylated by the IκB kinase (IKK) (Sakurai et al., 1999; Sakurai et al., 2003; Sizemore et al., 2002; Yang et al., 2003). We assessed the time kinetics of LPS-induced p65 phosphorylation at Ser536, and the effects that cannabinoids may exert on its phosphorylation and transport into the nucleus. Cytoplasmic protein was assessed for the time kinetics of p65 phosphorylation using antibodies specific for p65 phosphorylated at Ser536, which is located in the transactivation domain of p65 and specifically phosphorylated by IKK. BV-2 cells were treated with vehicle or 100 ng/ml LPS for 2.5, 5, 7.5, 10, 15 and 30min. Cytoplasmic protein fractions were resolved by SDS-Page electrophoresis and electroblotted onto nitrocellulose membranes. The LPS-induced phosphorylation of p65 at Ser536 was detected as early as 5 min. post LPS-stimulation, and was still detectable 30 min. post cell activation, although the level of phosphorylation has diminished some as compared to the earlier time points (Figure 35, *top panel*). Basal levels of phosphorylation at this serine residue were detected in the vehicle treated cells, and cells stimulated with LPS for 2.5 min. Equal protein loading was assessed by probing the membranes with a beta-actin antibody (Figure 35, *bottom panel*). We examined the effects that Δ^9-THC may have on the cytoplasmic and nuclear levels of phospho (Ser536)-p65 using Western blot analysis. As described previously, BV-2 cells were pre-treated with Δ^9-THC (3 h) followed by stimulation with 100 ng/ml LPS (15 min.). Cytoplasmic and nuclear proteins were fractionated by SDS-Page electrophoresis, electroblotted onto nitrocellulose membranes and probed with the phospho-p65 antibody described previously. In the cytoplasm, comparable levels of this phospho-protein were observed in all treatment groups (Figure

36A, *top panel*). These results suggest that Δ^9-THC does not modulate the phosphorylation of p65. In the nucleus, we observed a LPS-induced increase of phospho-p65 in LPS-stimulated cells as compared to the vehicle and Δ^9-THC-treated cells (Figure 36B, *top panel*). Furthermore, levels of phospho-p65 in Δ^9-THC-treated cells were similar to levels of phospho-p65 in LPS-stimulated cells, suggesting that Δ^9-THC does not affect the transport of phosphorylated p65 into the nucleus. The blots were stripped and reprobed with beta-actin (Figures 36A *bottom panel*) and proliferating cell nuclear antigen (PCNA) (Figures 36B *bottom panel*) antibodies to assess for equal cytoplasmic and nuclear protein, respectively.

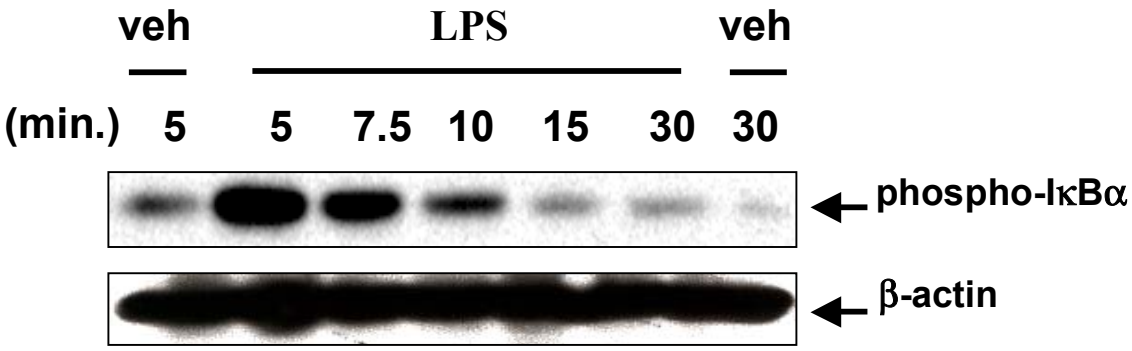

Figure 30. Rapid LPS-Induced Phosphorylation of IκBα in BV-2 Cells. BV-2 cells were stimulated with vehicle (0.01% ethanol) or 100 ng/mL LPS for the indicated time intervals. Cytoplasmic and nuclear protein was extracted from the cells, and the cytoplasmic fractions were resolved by SDS-PAGE. The resolved proteins were electroblotted onto to a nitrocellulose membrane and Western immunoblot analysis was performed using a phospho-IκBα antibody that detects IκBα when phosphorylated at serine residues 32 and 36. The results from this analysis demonstrate that IκBα is phosphorylated as early as 5 min. post LPS-induced cell activation. The membrane was stripped and reprobed with a beta-actin antibody to assess for equal protein loading.

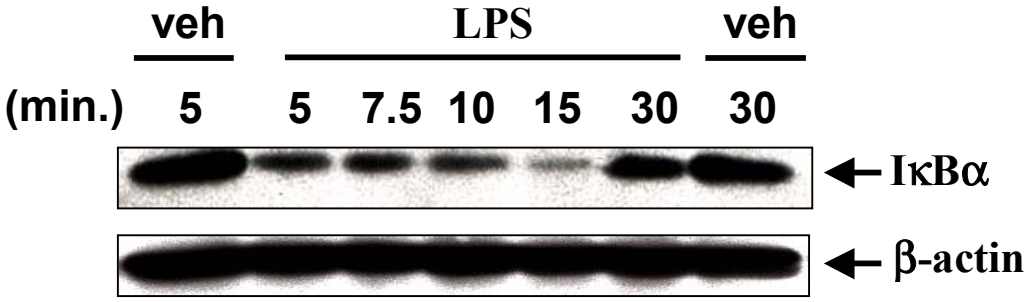

Figure 31. Degradation of IκBα is Time Specific. BV-2 cells were stimulated with vehicle (0.01% ethanol) or 100 ng/mL LPS for the indicated time intervals. Cytoplasmic and nuclear protein was extracted from the cells, and the cytoplasmic fractions were resolved by SDS-PAGE. The resolved proteins were electroblotted onto a nitrocellulose membrane and Western immunoblot analysis was performed using an IκBα antibody that detects the endogenous IκBα protein. The results from this analysis demonstrate that complete degradation of IκBα takes place 15 min. after LPS-induced cell activation. The membrane was stripped and reprobed with a beta-actin antibody to assess for equal protein loading.

A.

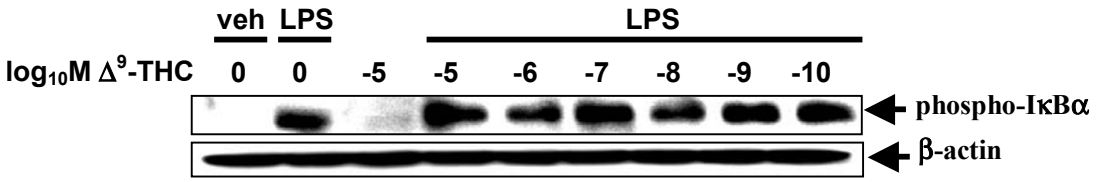

B.

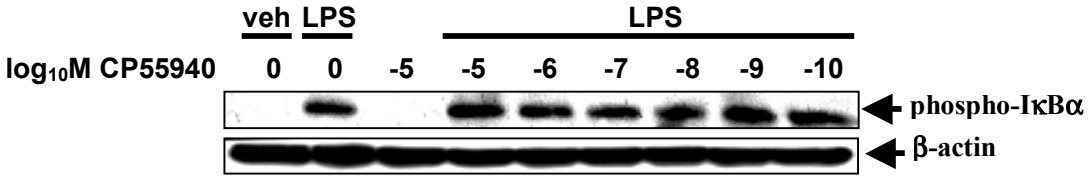

Figure 32. Δ^9-THC and CP55940 do not Affect the LPS-Induced Phosphorylation of the NFκB inhibitor IκBα. BV-2 cells were pre-treated (3 h) with Δ^9-THC (A) or CP55940 (B) at the indicated intervals and stimulated (5 min.) with 100 ng/ml LPS. Cytoplasmic protein extracts were subjected to Western blot analysis using an anti-phospho IκBα antibody which detects phosphorylated serine residues 32 and 36. Treatment with either Δ^9-THC (panel A) or CP55940 (panel B) did not affect the phosphorylation of IκBα. Blots were stripped and reprobed for β-actin for assessment of equal protein loading.

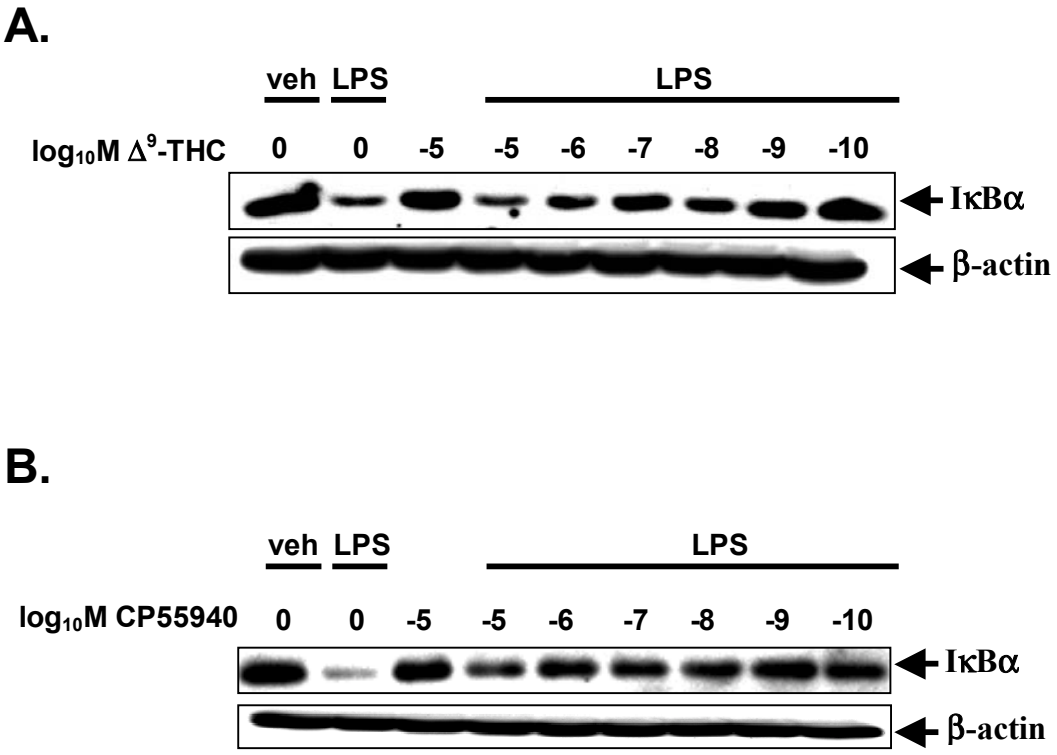

Figure 33. Δ^9-THC and CP55940 Partially Inhibit LPS-Induced Degradation of IκBα. BV-2 cells were pre-treated (3 h) with Δ^9-THC (A) or CP55940 (B) at the indicated intervals and stimulated (15 min.) with 100 ng/ml LPS. Cytoplasmic protein extracts were subjected to Western blot analysis using an anti-IκBα antibody which detects the endogenous IκBα protein. Degradation of IκBα was observed in LPS stimulated cells, however treatment with either Δ^9-THC (panel A) or CP55940 (panel B) resulted in decreased degradation of IκBα when compared to the LPS treated cells. Blots were stripped and reprobed for β-actin for assessment of equal protein loading.

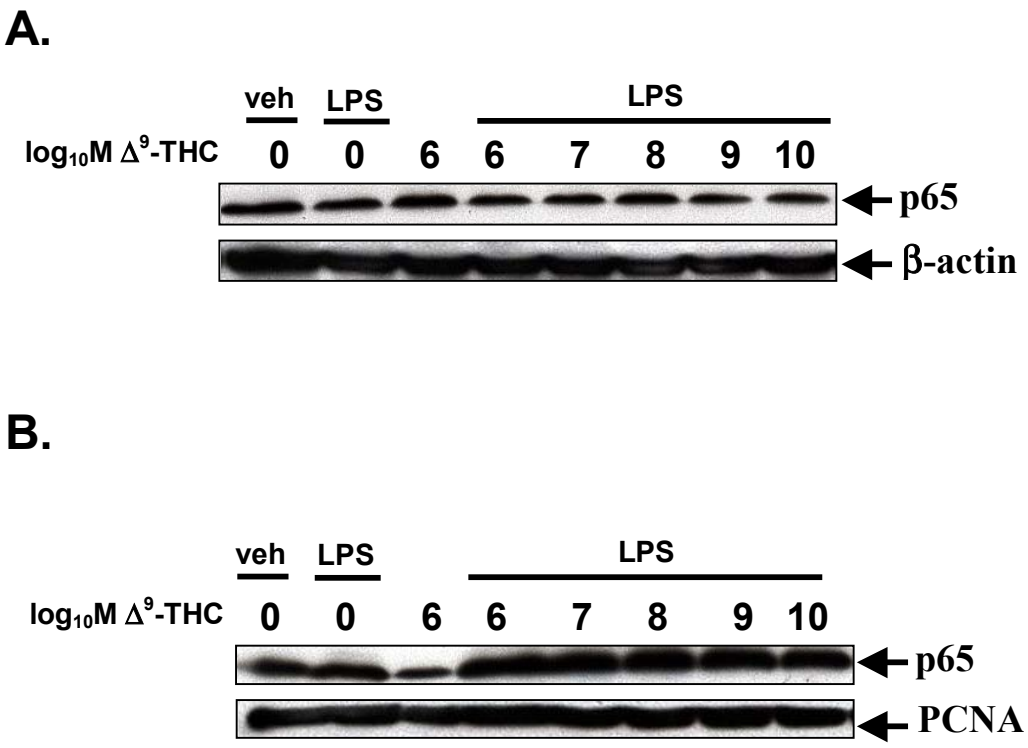

Figure 34. Protein Expression of Cytoplasmic and Nuclear p65. BV-2 cells were pre-treated with vehicle (0.01% ethanol) or Δ^9-THC (3 h) at the indicated intervals, followed by stimulation with 100 ng/mL LPS (30 min.). Cytoplasmic and nuclear protein were extracted from the cells, and both fractions were resolved by SDS-PAGE. The resolved proteins were electroblotted onto a nitrocellulose membrane and Western immunoblot analysis was performed using specific a p65 antibody that detects the endogenous p65 protein. (A), Cytoplasmic p65. Treatment with Δ^9-THC did not affect the synthesis of p65 as comparable levels of protein expression were observed in all treatment groups. (B), Nuclear p65. Treatment with Δ^9-THC did not affect the translocation of p65 into the nucleus, nuclear protein expression of p65 in the cannabinoid-treated cells was similar if not greater than the LPS-stimulated cells. The membranes were stripped and reprobed with a beta-actin and proliferating cell nuclear antigen (PCNA) antibodies to to assess for equal cytoplasmic and nuclear protein loading, respectively.

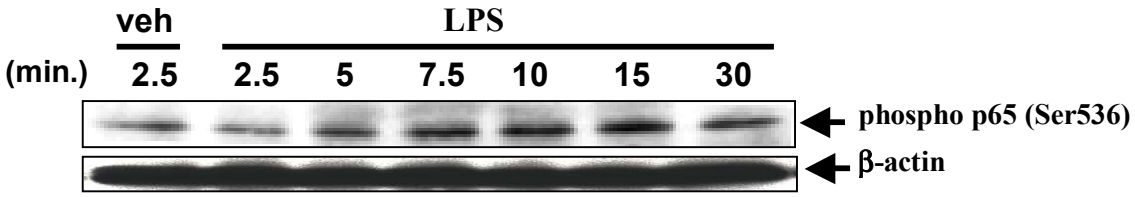

Figure 35. LPS-Induced Phosphoryation of the NFκB p65 Subunit at Serine 536. BV-2 cells were stimulated with vehicle (0.01% ethanol) or 100 ng/mL LPS for the indicated time intervals. Cytoplasmic and nuclear protein was extracted from the cells, and the cytoplasmic fractions were resolved by SDS-PAGE. The resolved proteins were electroblotted onto a nitrocellulose membrane and Western immunoblot analysis was performed using specific phospho-p65 antibody that detects p65 when phosphorylated at Ser536. Stimulus-induced phosphorylation at this residue begins as early as 5 min. post LPS stimulation and as late as 30 min. post stimulation. The level of phosporylation is diminished by the time the 30 min. interval was reached. Basal levels of phosphorylation at this residue were observed in the vehicle treated cells and at 2.5 min. post LPS stimulation. The membranes were stripped and reprobed with a beta-actin antibody to assess for equal protein loading.

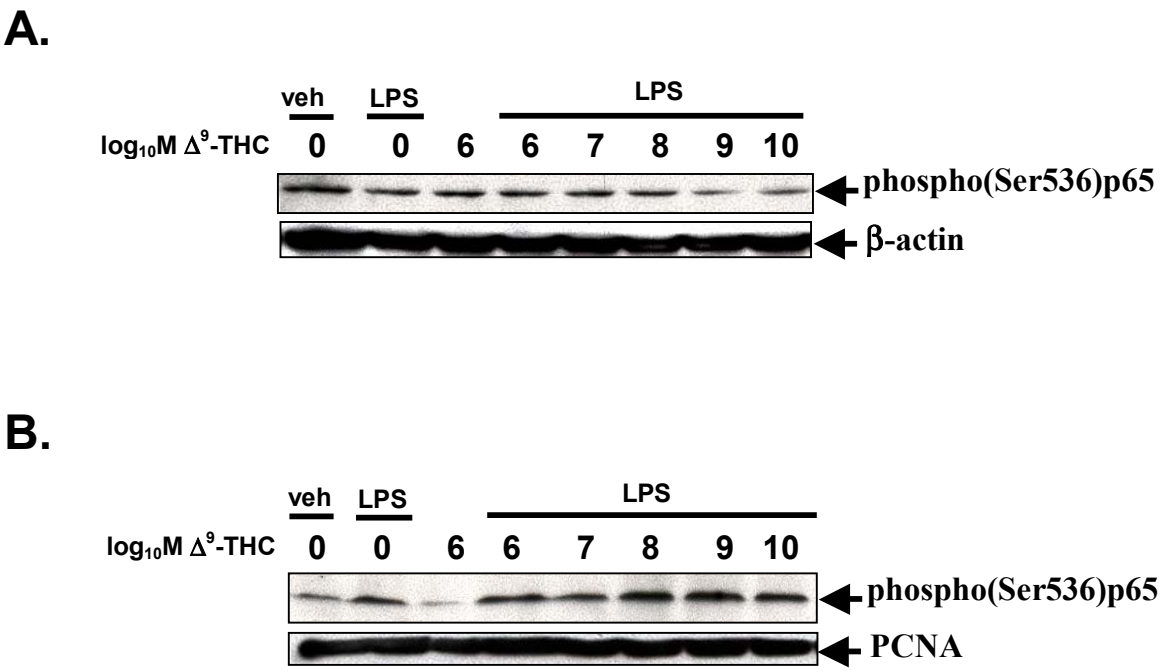

Figure 36. Δ^9-THC does not Affect LPS-Induced Phosphoryation of p65 at Serine 536 and its Nuclear Translocation. BV-2 cells were pre-treated with vehicle (0.01% ethanol) or Δ^9-THC (3 h) at the indicated intervals, followed by stimulation with 100 ng/mL LPS (15 min.). Cytoplasmic and nuclear protein was extracted from the cells, and the cytoplasmic fractions were resolved by SDS-PAGE. The resolved proteins were electroblotted onto a nitrocellulose membrane and Western immunoblot analysis was performed using specific phospho-p65 antibody that detects p65 when phosphorylated at Ser536. (A), Phoshorylation of phospho-p65. Stimulus-induced phosphorylation at this residue was not affect by the treatment with Δ^9-THC. (B), Nuclear translocation of phosphor-p65. The transport of this phosphorylated protein into the nucleus was not inhibited by Δ^9-THC, as similar levels of protein expression were observed in all LPS-stimulated cells. The membranes were stripped and reprobed with a beta-actin and proliferating cell nuclear antigen (PCNA) antibodies to assess for equal cytoplasmic and nuclear protein loading.

Discussion

Microglia, as the resident macrophage of the central nervous system (CNS), have the critical role of remodeling and regenerating cells as well as providing the first line of defense against infection and injury (Cabral and Marciano-Cabral, 2005; Perry, 2004; Facchinetti et al., 2003; Aloisi, 2001; Blasi et al., 1990). While the combined roles of microglia cells are to maintain an immunological homeostatic balance in the CNS, these cells also have been pathologically linked to the degeneration of the CNS. Microglia become fully activated upon infection or injury and are able to elicit a whole host of pro-inflammatory cytokines and other mediators as part of a typical immune response. However, activated microglia have been associated as a direct cause of, or a contributor to exacerbating a multitude of chronic neurodegenerative diseases that are pathologically hallmarked by an atypical production of pro-inflammatory factors. These chronic diseases include Alzheimer's disease (AD), Multiple Sclerosis (MS) and Human Immunodeficiency Virus encephalitis (HIVE). The elicitation of pro-inflammatory factors from other cells within the CNS, and from infiltrated peripheral immune cells, also contributes to the pathology of neurodegenerative and neuroinflammatory diseases.

It has been well documented that cannabinoids can alter immune function of macrophages and macrophage-like cells such as microglia (Cabral andGriffin-Thomas,

2008; Cabral and Griffin-Thomas, 2009). Thus, cannabinoid receptors have been explored for their therapeutic potential to serve as molecular targets for exogenous cannabinoids for the treatment of neuropathological disorders (Cabral and Griffin-Thomas, 2008; Cabral and Griffin-Thomas, 2009). *In vitro* and *in vivo* studies of MS and AD demonstrated that exogenous cannabinoids prevented activation of primary microglia and cognitive impairment in AD, and improved the motor function of mice suffering from a virus-induced demylinating disease that resembles MS (Arevalo-Martin et al., 2003; Croxford and Miller, 2003; Ramirez et al., 2005a). Immune modulation exerted by exogenous cannabinoids is believed to be consequential to the inhibition of adenylate cyclase activity, a primary effect of cannabinoid receptor signaling. One of the important immune modulatory effects of exogenous cannabinoids such as Δ^9-THC, the major psychoactive component of marijuana, is the modulation of gene expression of pro-inflammatory cytokines. Δ^9-THC and the synthetic exogenous cannabinoids WIN55,212-2 and CP55940 have been shown in microglia, astrocytes and macrophages to inhibit LPS-induced pro-inflammatory cytokine (IL-1α, IL-1β, IL-6 and TNF-α) mRNA expression, ablate TNF-α release (Puffenbarger et al., 2000; Facchinetti et al., 2003) and inhibit production of nitric oxide (NO) through modulating the expression of inducible nitric oxide synthase (iNOS) (Coffey et al., 1996; Jeon et al., 1996; Molina-Holgado et al., 2002; Ross et al., 2000; Waksman et al., 1999). The specific mechanisms in which exogenous cannabinoids reduce or inhibit the inducible expression of pro-inflammatory cytokine genes, particularly in microglial cells, have yet to be fully defined. The goal of the present study was to define the mechanisms of cannabinoid-mediated down-

regulation of the inducible expression of pro-inflammatory cytokine genes in microglial cells. Previous studies have shown that overall mRNA degradation is not the causative factor for cannabinoid-mediated reduction in mRNA expression (Fischer-Stenger et al., 1993; Puffenbarger et al., 2000). Therefore, we proposed that the modulation of pro-inflammatory gene expression takes place at the transcriptional level.

Δ^9-THC has been shown to modulate the activity of transcription factors to bind to specific cognate consensus binding sites in the promoter regions of specific genes (Kaminski, 1996). This modulation of transcription factor activity was attributed to a down-stream effect of cannabinoid-mediated adenylate cyclase inactivity (Kaminski, 1996). One important transcription factor that binds to specific sites in the promoter region of pro-inflammatory cytokine genes is NFκB, a major role player in the inflammatory immune response. NFκB can be activated by various stimuli, including bacterial LPS. Initially, we entertained the use of mouse EOC-20 microglial cells as targets for assessing effects of cannabinoids on NFκB binding in response to stimulation with LPS. Treatment of EOC-20 cells with TNF-α or IFN-γ resulted in an increase in p65 levels in the nucleus which is indicative of NFκB activation. However, NFκB binding in EOC-20 cells stimulated with LPS was comparable to NFκB binding exhibited by unstimulated cells. Ultimately, these cells were shown to lack expression of CD14, the co-receptor to TLR-4, and the lack of a complete TLR-4/CD14 complex prevents EOC-20 cells from signaling specifically through TLR-4 upon exposure to LPS. Therefore, subsequent experiments were performed using mouse BV-2 microglial-like cells. BV-2 cells are phenotypically and functionally similar to primary microglia which

includes their ability to phagocytize, secrete cytokines and chemokines, and express a host of cell surface receptors. Furthermore, our studies have demonstrated that these cells express CB_2 at the mRNA and protein levels.

Using the BV-2 cells, we first demonstrated LPS-induced binding of NFκB *in vitro* in both neonatal rat primary microglial cells and the BV-2 microglial cell line. Upon LPS stimulation, NFκB binding to a synthetic DNA probe that contains its cognate consensus sequence was observed as early as 15 min. post stimulation and more robustly at 30 min. post stimulation, which was the time point used in all subsequent binding studies. We then analyzed the effects of the partial cannabinoid receptor agonist Δ^9-THC on LPS-induced NFκB binding to nuclear promoter elements, which is critical for the induction of gene transcription. It was observed that Δ^9-THC inhibited NFκB binding in a biphasic, concentration-related manner. BV-2 cells treated with a 10^{-5}M concentration of Δ^9-THC displayed decreased levels of NFκB binding as compared to cells stimulated with LPS alone. We accounted this phenomenon to the toxic effects of such a high concentration of the highly lipophilic Δ^9-THC compound, which has been shown to perturb lipid-bilayers of cellular membranes (Makriyanni et al., 1990; Martin 1986), and cause apoptosis in microglial-like BV-2 cells (data not shown). The 10^{-6}M concentration did not exert an effect on NFκB binding when compared to BV-2 cells treated with LPS alone, suggesting that the inhibitory effect observed at the 10^{-5}M concentration was no longer established at the more diluted 10^{-6}M concentration. Δ^9-THC exerted inhibitory effects at the 10^{-7}M and 10^{-8}M concentrations, with the greatest inhibition occurring at 10^{-8}M. The level of NFκB binding at the 10^{-9}M and 10^{-10}M concentrations was

comparable to that of LPS-stimulated cells at the 10^{-6}M concentration. The response pattern that Δ^9-THC exerted on NFκB binding is consistent with that from published studies that report biphasic effects exerted by cannabinioids (Little and Martin, 1991; Kujtan et al., 1993; Berdyshev et al., 1997). Cannabinoids, at higher concentrations, can display a pattern of responsiveness that is the result of non-specific modes of action, such as perturbation of cellular membranes and/or cell apoptosis. The inhibitory responses elicited as concentrations approach nanomolar levels are indicative of a more specific mode of action such as receptor-mediated. Further indication of concentration-related, receptor- mediated effects exerted by lower concentrations of Δ^9-THC is the observation that the inhibitory effects taper off as the concentrations are further diluted (10^{-9}M and 10^{-10}M concentrations). In agreement with previous studies, the results of these binding experiments demonstrate the dual mode of action of Δ^9-THC on LPS-induced NFκB binding.

A similar mode of action on NFκB binding was exhibited with the full cannabinoid receptor agonist CP55940. As described with Δ^9-THC, we observed attenuated levels of NFκB binding at the 10^{-5}M, which dissipated at the 10^{-6}M concentration. However, CP55940 exerted a concentration-related inhibition of NFκB binding over an extended range (10^{-7}M – 10^{-9}M), with maximum inhibition occurring at the 10^{-9}M concentration. The level of binding at the 10^{-10}M concentration was comparable to that of the LPS treatment group. CP55940, as a full agonist, has greater efficacy than Δ^9-THC which is a partial agonist, so the extended inhibitory effect on NFκB binding exerted by CP55940 was not surprising. The results from the Δ^9-THC and

CP55940 studies demonstrate cannabinoid-mediated effects on NFκB binding, but do not indicate whether these effects are functionally linked to the transcriptional activity of NFκB.

Exogenous cannabinoids and the endogenous cannabinoid anandamide have been shown to inhibit the transcriptional activity of NFκB in cell types other than microglia (Sancho et al., 2003; Curran et al., 2005). Our study represents the first analysis of the effects of cannabinoids on microglial-like cells. In initial studies, BV-2 microglial-like cells upon LPS-stimulation for 3h, 8h and overnight exhibited a significant increased level of NFκB transcriptional activity as compared to unstimulated cells. A robust increase in transcriptional activity at the 3h time interval was observed and therefore, was used in all subsequent reporter activity studies. BV-2 cells exposed to Δ^9-THC prior to stimulation with LPS exhibited attenuated levels of LPS-induced transcriptional activity in a concentration-related fashion (10^{-7}M - 10^{-9}M). Maximum inhibition occurred at the 10^{-8}M concentration, consistent with results obtained in the NFκB binding assays. The level of transcriptional activity at the 10^{-6}M and 10^{-10}M concentrations were comparable to those of the LPS-treated cells; again, this pattern of responsiveness demonstrated a biphasic mode of action of Δ^9-THC. Similarly, CP55940 inhibited the transcriptional activity of NFκB over the same concentration range (10^{-7}M - 10^{-9}M) but the extent of the inhibition was greater with the more efficacious CP55940 compound. The concentration-related effects that both Δ^9-THC and CP55940 are exerting on the functional activity of NFκB suggest a specific mode of action that is receptor-mediated. In order to establish a

linkage to either of the two cannabinoid receptors, we performed a series of experiments to determine the specificity in which these inhibitory effects are occurring.

Real-Time RT-PCR analysis revealed that mRNA for CB_1 is not detected in unstimulated BV-2 cells and cells activated with IFN-γ or LPS. Southern blot analysis confirmed the absence of CB_1 mRNA. However, Real-Time RT-PCR analysis demonstrated that BV-2 cells exhibit a base-line level of expression of the CB_2, as detection of CB_2 mRNA was observed in unstimulated cells. BV-2 cells stimulated with either IFN-γ or LPS exhibited variable expression of CB_2 mRNA, consistent with reports that microglial differentially express the CB_2 based on their different activation states (Carlisle et al., 2002). Southern blot analysis confirmed the presence of CB_2 mRNA in both unstimulated and stimulated BV-2 cells. To further elucidate the specificity in which Δ^9-THC and CP55940 are inhibiting NFκB function, we again performed NFκB reporter activity assays using CB_1 and CB_2 selective agonists and antagonists. The CB_1 selective agonist ACEA did not inhibit the transcriptional activity of NFκB, which was not surprising since BV-2 cells were shown to not express CB_1 at the mRNA and protein levels. In addition, the inhibitory effect of 10^{-7}M CP55940 on transcriptional activity was not reversed by the CB_1-selective antagonist SR141716A, thus further confirming the lack of involvement of the CB_1. These finding are consistent with published reports that indicate that the CB_1 is not linked to the modulation of most immune responses, (Cabral and Griffin-Thomas, 2009). However, the CB_2 has been functionally linked to the modulation of inflammatory immune responses in both the periphery and the CNS (Cabral and Griffin-Thomas, 2008; Cabral and Griffin-Thomas, 2009).

Reporter activity assays performed with the CB_2 selective ligand O-2137 indicated that this compound exerted an inhibitory effect on transcriptional activity. However, while the inhibitory effect of O-2137 was significant from the 10^{-7}M - 10^{-10}M range, the percentage of inhibition when compared to LPS-stimulated cells was not robust. To further explore whether the CB_2 played a role in modulating the function of NFκB, we employed the CB_2-selective antagonist SR144528 in concert with CP55940 for a subsequent set of reporter activity studies. The CB_2-selective antagonist was able to block CP55940-mediated inhibition of NFκB transcription. These findings are contrary to other published reports that indicate that exogenous and endogenous cannabinoids inhibit inducible NFκB transcriptional activity independent of either cannabinoid receptor. Curran and colleagues reported that the exogenous cannabinoid WIN55212,2 inhibits IL-1 signaling in astrocytes, which prevents induction of cell adhesion molecules and the chemokine IL-8 (Curran et al., 2005). They attributed WIN55212,2-mediated inhibition of IL-1 signaling to WIN55212,2 suppressing NFκB transcriptional activity. However, they reported that neither CB_1 or CB_2 was involved in the process since the astrocyte cell line used in the studies does not express mRNA for either receptor and CB_1 and CB_2 -selective antagonists did not block the inhibitory effects of WIN55212,2 on the induction of adhesion molecules. Sancho and colleagues reported that the endogenous cannabinoid anandamide inhibits NFκB activity in a cannabinoid-receptor independent manner (Sancho et al., 2003). The Jurkat 5.1 clone was used as their cell model, a clone that was shown to express CB_2 but not CB_1 mRNA. NFκB reporter activity assays demonstrated that anandamide exerted a concentration-related inhibition on

transcriptional activity, although it should be noted that relatively high levels of anandamide range from 5μM to 25μM ($5x10^{-6}M – 2.5x10^{-5}M$) were used to obtain such an effect. This inhibition of transcriptional activity was not blocked by the CB_1 and CB_2 antagonists SR141716A and SR144528, respectively. There are several explanations that may account for our disparate results. First, the findings reported in this dissertation versus those of Curran and colleagues (Curran et al., 2005), and Sancho and colleagues (Sancho et al., 2003) may indicate that the specificity of action for exogenous cannabinoids may be cell-specific. Second, it should also be considered that inhibitory effects observed around the non-pharmacological range such as 10μM ($10^{-5}M$) may be due to non-receptor specific action such as membrane perturbation and toxicity that may cause apoptosis. In this context, cannabinoid-mediated effects observed in our studies were in the range of 0.1μM to 0.001μM ($10^{-7}M – 10^{-9}M$), and the CB_2 antagonist SR144528 was able to block the effects of 0.1μM CP55940. Our findings, however, are consistent with other reports that show that the CB_2 more than the CB_1 is involved in ablating the production of pro-inflammatory mediators in microglia cells. Eljaschewitsch and colleagues reported that anandamide attenuated the production of nitric oxide (NO) via reducing iNOS gene expression (Eljaschewitsch et al., 2006). While CB_1 antagonism provided a minor reversal of NO inhibition, antagonizing the CB_2 completely abolished the anti-inflammatory effects of anandamide. Also consistent with our findings are reports that demonstrate CB_2-mediated attenuation of TNF-α, IL-1, IL-6 and IL-8 production in macrophages (Klegeris et al., 2003; Berdyshev et al., 1997; Gallily et al., 2000). The elicitation of TNF-α and IL-1 has been shown to induce NFκB activation,

thus participating in an autoregulatory feedback loop that regulates and deregulates NFκB activity (Blackwell and Christman, 1997; Lawrence et al., 2001; Ye and Johnson, 2001).

In addition to defining the specificity of action in which the exogenous cannabinoids Δ^9-THC and CP55940 inhibit NFκB activity, our studies also involved identifying the site of action of these compounds. It has been reported that both cannabinoid receptors play a role in activating or regulating signaling pathways involving adenylate cyclase/cAMP, mitogen-activated protein kinase (MAPK), cAMP-dependent protein kinase (PKA) and a host of transcription factors and their specific regulators (Howlett and Mukhopadhyay, 2000; Demuth and Molleman, 2006). CB_1 and CB_2 are negatively coalesced to adenylate cyclase, which results in a decreased production of cAMP. Upon cannabinoid binding to either cannabinoid receptor, the activated, heterotrimeric G-protein uncouples into alpha (α) and beta/gamma ($\beta\gamma$) subunits, and the $\beta\gamma$ subunit participates in signaling cascades distinct from those of the α subunit, such as the MAPK cascade (Howlett and Mukhopadhyay, 2000). The inhibitory α subunit is responsible for the stifling of adenylate cyclase activity and production of cAMP. This lack of cAMP production impedes downstream cAMP-mediated signaling events such as PKA catalytic activity, and transcription factor activation. These specific sites may represent target points for cannabinoid-mediated action that could ultimately result in the down-regulation of immune function, particularly pro-inflammatory cytokine expression in microglia cells.

The transcription factor NFκB plays a major role in inducing the inflammatory response, so stringent control of its activation is required for proper immune function (Blackwell and Christman, 1997). Prior to translocating into the nucleus, binding to specific promoter elements, and inducing transcription of NFκB-regulated genes, NFκB is retained in the cytoplasm by its inhibitor protein IκBα. Upon cell activation, IκBα is rapidly phosphorylated, ubiquitinated and degraded by the 26S proteosome, thereby allowing for the nuclear translocation of NFκB. In order to address whether cannabinoids altered any of these events, we first performed a set of experiments to determine if the specific site in which cannabinoids act to inhibit NFκB function involved IκBα. Since the phoshorylation of IκBα at serine residues 32 and 36 initiates its ubiquitination and degradation, we assessed the effects of Δ^9-THC and CP55940 on this regulatory event. Both cannabinoid compounds were shown not to inhibit LPS-induced phosphorylation of IκBα. In concert with the previous set of experiments, we also determined if Δ^9-THC and CP55940 inhibited the degradation of IκBα. We observed that both compounds inhibited full degradation of IκBα upon LPS-induced cell activation. These findings are consistent with reports from Sancho and colleagues (Sancho et al., 2003) that indicated that anandamide inhibited the transcriptional activity of NFκB in part by inhibiting TNF-α-induced degradation of IκBα. However, Sancho and colleagues also reported that the lack of IκBα degradation was due to anandamide inhibiting the catalytic activity of IκB kinase (IKK), the kinase responsible for the phosphorylation of IκBα (Sancho et al., 2003). These results should be considered in the

context that the anandamide-mediated effects on NFκB activity and regulation observed with Sancho's group were indicated to be independent of cannabinoid receptor signaling. Since our studies demonstrated a linkage of the CB_2 in the inhibition of NFκB activity, we have to consider that the lack of IκBα degradation is a consequence of cannabinoid-mediated adenylate cyclase inhibition which modulates further downstream signaling events, thus resulting in a defect in ubiquitination and/or proteolytic degradation. As described previously, adenylate cyclase inhibition results in a lack of cAMP production that stifles the catalytic activity of PKA. The ubiquition-proteasome pathway has been shown to be dependent on and regulated by PKA (Hoang et al., 2004; Zhang et al., 2007). Specific serine phosphorylation of one the 26S proteasome ATPases by PKA stimulates the activity of the proteasome. Our findings also are consistent with a study that demonstrated that Δ^9-THC, with the involvement of the CB_2 receptor, may interfere with the enzyme activity of some proteases in macrophages and prevent proper antigen processing for T cell stimulation (McCoy et al., 1995; McCoy et al., 1999). However, further studies are required in order to establish a link between Δ^9-THC and CP55940-mediated inhibition of IκBα degradation and modulation of the ubiquitin/ proteasome pathway.

Another regulatory component for complete NFκB activation requires phosphorylation of the p65 subunit at serine residues 276, 529 and 536. Serine residue 536, phosphorylated by IKK upon TNF-α or LPS stimulation, is located in the transactivation domain (TAD) of p65 and is important for the activation and transcriptional activity of NFκB. Using an antibody specific for the detection of p65

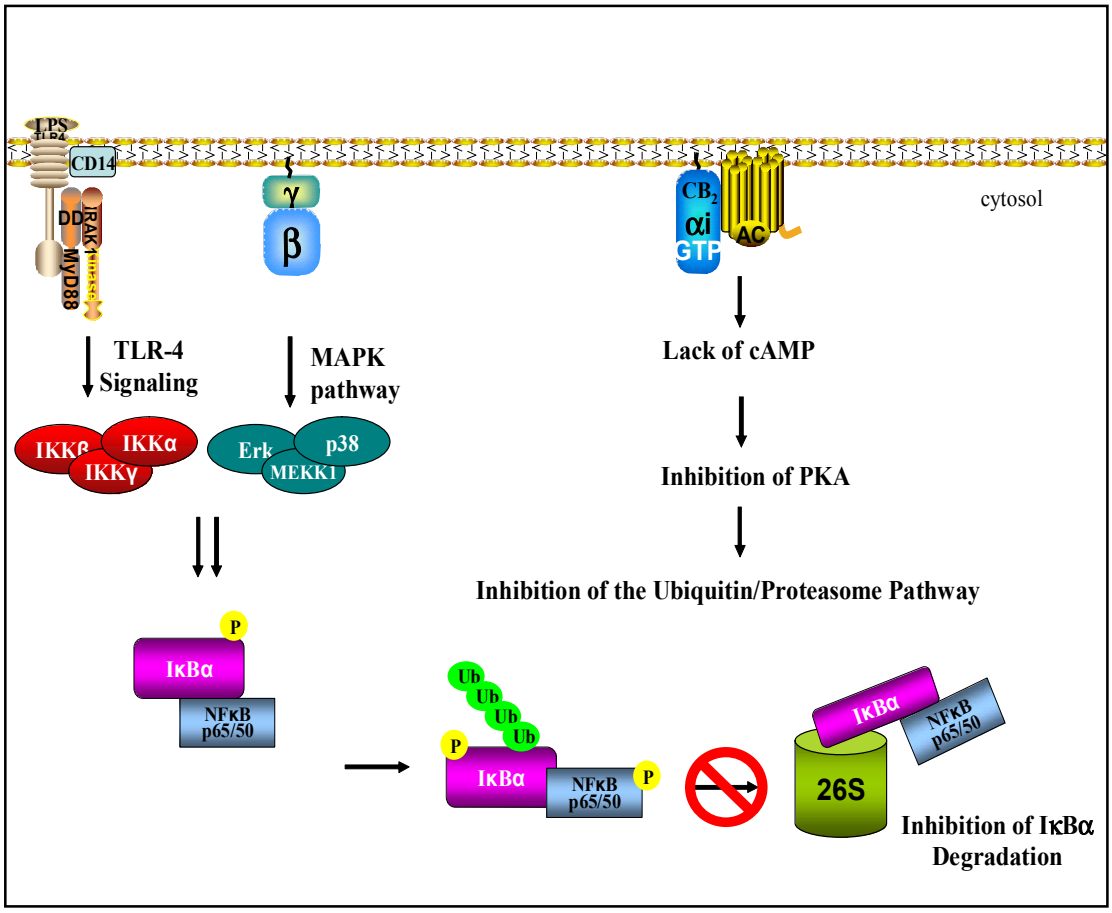

Figure 37. Cannabinoid-Mediated Inhibition of LPS-Induced NFκB Activity in BV-2 Cells. The exogenous cannabinoids Δ^9-THC and CP55940 inhibit NFκB activity, in part, by signaling through the CB_2. Upon treatment of BV-2 cells with either Δ^9-THC or CP55940, activation of the CB_2 commences with the dissociation of the inhibitory G-protein into β/γ and α subunits. The α subunit binds to adenylate cyclase and prevents the production of cAMP, and the kinase activity of PKA. Once cannabinoid-treated BV-2 cells are stimulated with LPS, a stimulatory signaling pathway is initiated through TLR-4. Concurrently with TLR-4 signaling, the β/γ subunit can induce activation of MAPK signaling, which can also activate NFκB. From our studies, it was demonstrated that Δ^9-THC and CP55940 did not inhibit phosphorylation of the inhibitor protein IκBα but inhibited its degradation. Therefore, we propose that CB_2 signaling superimposes an inhibitory effect on TLR-4 and/or MAPK signaling at the ubiquitin/proteasome degradative pathway, thus preventing IκBα degradation and ultimately NFκB activity.

when phosphorylated at serine 536, we observed that LPS-induced phosphorylation of this residue is not affected by Δ^9-THC. Furthermore, Δ^9-THC did not affect the translocation of phospho-p65, as comparable levels of this phospho-protein were detected in the nuclear protein extracted from LPS-stimulated and Δ^9-THC-treated BV-2 cells. Δ^9-THC also did not affect overall synthesis or transport of the endogenous p65 protein as seen in both cytoplasmic and nuclear protein fractions. Consistent with our findings, Curran and colleagues reported that, while WIN55212,2 inhibited the transcriptional activity of NFκB, it did not affect translocation of activated p65 into the nucleus (Curran et al., 2005).

The inhibition of NFκB binding and transcriptional activity exerted by Δ^9-THC and CP55940 appears to be a consequence of these compounds inhibiting the degradation of IκBα which would constitute retainment of the IκBα/NFκB complex in the cytoplasm, and result in a lack of unbound, activated NFκB translocating to the nucleus. However, results from Western immunoblot analyses demonstrated that phosphorylation and nuclear translocation of the p65 subunit was not modulated by cannabinoids. Therefore, we postulate that multiple signal transduction cascades are involved in cannabinoid-mediated modulation of LPS-induced NFκB binding and activity. Eljaschewitsch noted that inhibition of signal transduction in microglial cells requires parallel activation of multiple signaling cascades, including signaling of pattern recognition receptors, such as the Toll-like receptor 4 (TLR-4), which recognizes and binds to bacterial LPS (Eljaschewitsch et al., 2006). In our *in vitro* cell model, LPS-induced signaling followed cannabinoid receptor activation in which distinct signaling pathways are activated by the

α and βγ subunits of the cannabinoid-receptor coupled G_i protein. As described previously, signal transduction of the α subunit, which inhibits adenylate cyclase activity and cAMP production, modulate further downstream cAMP and/or PKA-dependent signaling events that ultimately affects the ubiquitin/proteasome pathway. Concurrent with G_i-α inhibitory signaling, G_i-βγ and LPS-mediated stimulatory signaling lead to the activation of NFκB through the MAPK signaling and TLR-4 signaling networks, respectively. These signaling cascades allow phosphorylation and activation of specific kinases (i.e., IKK, MAPK) that result in the normal phosphorylation of the p65 subunit and IκBα but not its degradation, as observed in cannabinoid-treated BV-2 cells. It is likely that G_i-α signaling converges onto the stimulatory signaling that results in NFκB activation at the ubiquitin/proteasome step and superimposes an inhibitory effect on one or both of these processes (Figure 37). While the convergence of these signaling cascades may explain the cannabinoid-mediated modulation of IκBα degradation observed in our studies, its does not fully explain how activated NFκB, in terms of the p65 subunit, is still able to translocate into the nucleus, and possibly induce gene expression. One explanation is that there is still some nominal level of NFκB occurring, which is demonstrated by the fact that Δ^9-THC or CP55940 did not completely inhibit NFκB activity. Furthermore, it was demonstrated that the CB_2 antagonist SR144528 did not fully reconstitute the transcriptional activity of NFκB when inhibited by CP55940. It should be noted that one of the genes that can be induced by this nominal level of NFκB activity is its inhibitor IκBα. Indeed, reports have demonstrated that newly synthesized

IκBα can translocate into the nucleus, bind to NFκB and prevent its transcriptional activity (Arenzana-Seisdedos et al., 1997; Chiao et al., 1994; Sachdev et al., 2000; Rodriguez et al., 1999; Huang et al., 2000). The consequent binding of IκBα to NFκB interferes with the conformation of NFκB in that proper binding to its DNA promoter cannot be established. This phenomena may detail an additional mechanism of action located specifically in the nucleus that would further inhibitory NFκB binding and transcriptional activity (Figure 38).

Another explanation as to how cannabinoids may affect the activity of NFκB once it has localized to the nucleus is the involvement of glucocorticoid receptors. Glucocorticoids are steroid hormones that bind to, and activate, glucocorticoid receptors (GCR). GCRs have been shown to exhibit anti-inflammatory modes of action upon activation by translocating into the nucleus and repressing gene transcription of pro-inflammatory cytokines and chemokines (Adcock, 2001a; Adcock and Caramori, 2001b). It has been reported that GCRs have direct protein-protein interactions with transcription factors involved in inducing the inflammatory response such as NFκB, and alter their ability to bind to DNA promoter elements and induce gene expression (Karin M, 1998; Kagoshima et al., 2003). Endogenous cannabinoids, as well as the exogenous cannabinoids Δ^9-THC and cannabidiol, have been shown to bind to GCRs due to their structural similarity to steroid hormones (Eldridge et al., 1991). Δ^9-THC has been shown to displace binding of steroid hormones to GCRs, thus serving as a potential competitor to these compounds. The effects elicited from Δ^9-THC-GCR interaction have been reported to be similar to those effects observed in glucocorticoid-GCR interactions

(Eldridge and Landfield, 1990; Eldridge, 1991). Thus, Δ^9-THC in exhibiting agonist-like behavior for GCRs could activate these receptors. The activation of GCRs by Δ^9-THC and CP55940 may describe another mode of action in which cannabinoids down-regulate the activity and function of NFκB (Figure 39). The results of our studies demonstrate that more than one role player is involved in cannabinoid-mediated inhibition of NFκB activity. However, further studies are required in order to establish whether these multiple signaling cascades are involved and are acting in concert with, or independently of, one another.

In summary, we have demonstrated that the exogenous cannabinoids Δ^9-THC and CP55940 inhibit the functional activity of the universal transcription factor NFκB. Both Δ^9-THC and CP55940 were found to diminish the binding of NFκB to synthetic DNA probes containing its consensus sequence. In addition, the ability of NFκB to transcribe a reporter gene (*Luc*) was attenuated by these compounds. This inhibitory effect was linked functionally to the CB_2, for the inhibitory effects of CP55940 on transcriptional activity was significantly blocked by the CB_2-selective antagonist SR144528. To define the site of action in which CB_2 signaling results in NFκB malfunction, we examined the effects of Δ^9-THC and CP55940 on the IκBα protein that strictly regulates its activation. Neither cannabinoid compound had an affect on the phosphorylation of this regulatory protein which constitutes an initial step in activating NFκB upon cell stimulation. However, Δ^9-THC and CP55940 were found to inhibit the degradation of IκBα which entails the rate-limiting step in NFκB activation. These results suggest that cannabinoids

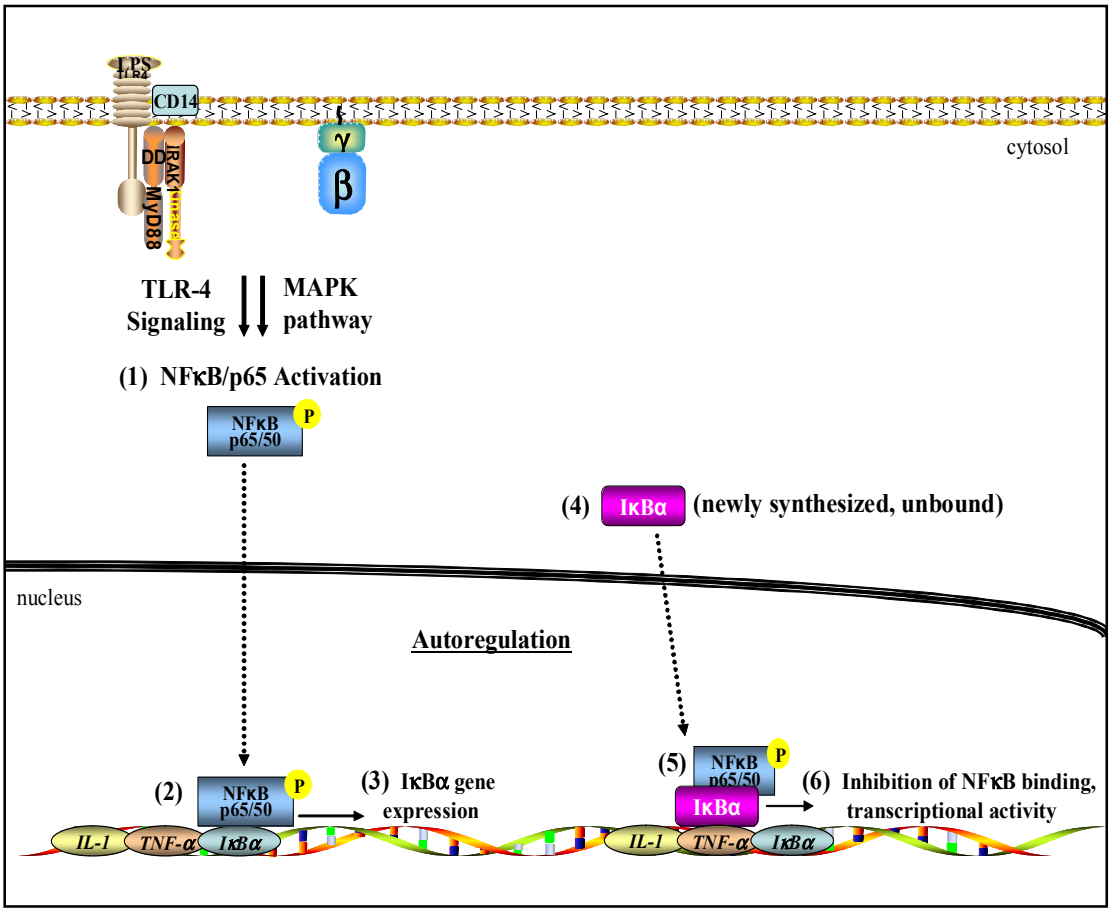

Figure 38. Inhibition of NFκB Binding and Transcriptional Activity in BV-2 Cells via Autoregulation. Our results indicate that a nominal level of NFκB activity persists by way of TLR-4 or MAPK signaling (1). This was demonstrated by the lack of inhibition that Δ^9-THC exerted on the translocation of activated phospho-p65 into the nucleus (2), and by the fact that neither Δ^9-THC nor CP55940 fully inhibited NFκB transcriptional activity. We postulate that there may be other mechanisms of action that also inhibit NFκB binding and transcriptional activity, despite the presence of some level of NFκB activity. We further speculate that this nominal level of NFκB activity results in gene expression of NFκB -regulated genes, such as the gene for its inhibitor IκBα (*NFKBIA*) (3). Expression of *NFKBIA* results in newly synthesized protein that has yet to bind to NFκB (4). It has been shown that newly synthesized, unbound IκBα can translocate into the nucleus and bind to activated NFκB (5). The binding of IκBα to NFκB prevents its binding and subsequent transcriptional activity (6), thus NFκB autoregulates itself by inducing gene expression of its inhibitor, IκBα.

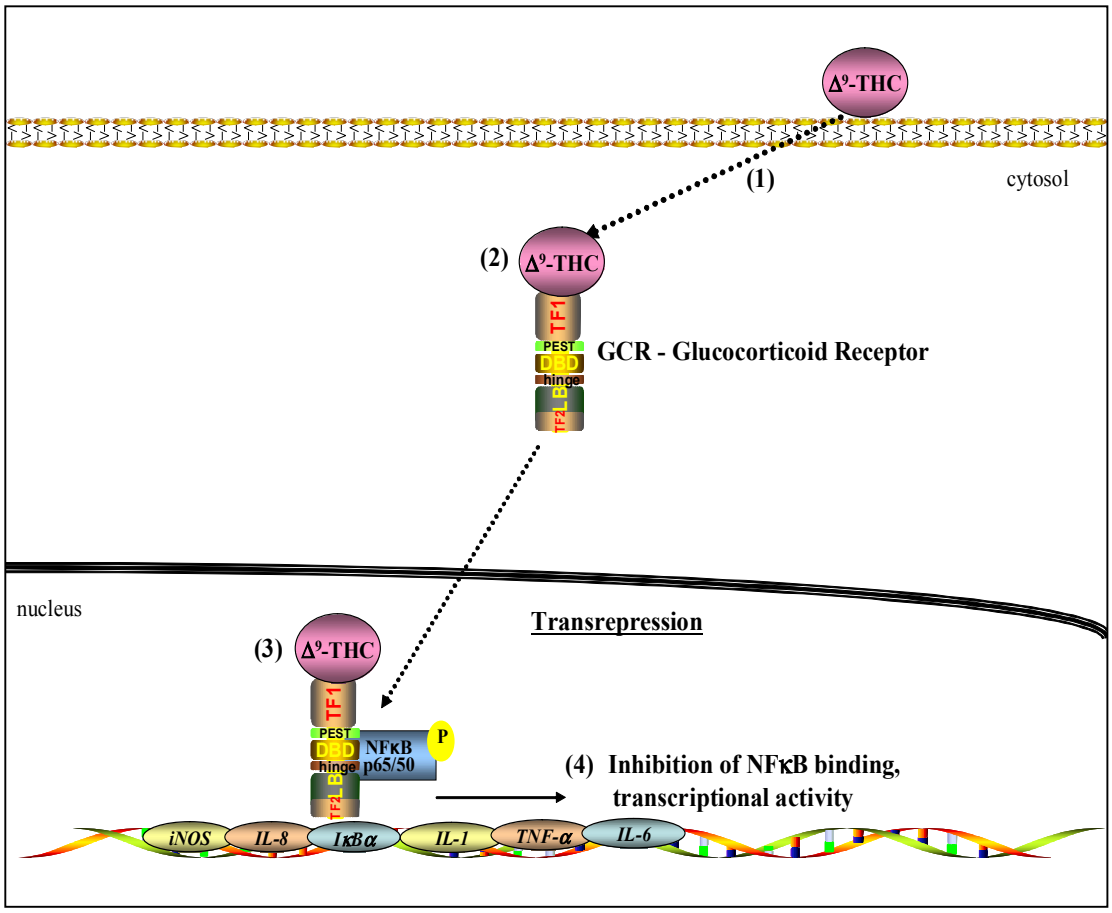

Figure 39. Inhibition of NFκB Binding and Transcriptional Activity in BV-2 Cells via Transrepression. Our results indicate that there still is a nominal level of NFκB activity occurring by way of TLR-4 or MAPK signaling. This was demonstrated by the lack of inhibition that Δ^9-THC exerted on the translocation of activated phospho-p65 into the nucleus, and by the fact that neither Δ^9-THC nor CP55940 fully inhibited NFκB transcriptional activity. One explanation is that NFκB may autoregulate itself by inducing gene expression of its inhibitor IκBα, which can translocate into the nucleus, bind to NFκB, and prevent its binding and activity (Figure 38). We also postulate that NFκB activity may be repressed through interaction with glucorticoid receptors (GCR). Cannabinoids such as Δ^9-THC can readily pass through cellular membranes and enter the cytosol (1). Specifically, Δ^9-THC has been shown to bind and activate GCRs (2), which reside in the cytosol. The activated GCR, complexed with Δ^9-THC, can translocate to the nucleus and bind to NFκB (3). Binding of GCRs to NFκB prevents the proper binding and subsequent transcriptional activity of NFkB, thus repressing NFκB activity (4).

degradation by the 26S proteasome, or have an affect on the proteolytic activity of the 26S proteasome. We also determined the effect of Δ^9-THC and CP55940 on the p65 subunit of NFκB, which plays a critical role in DNA binding and transcriptional activity. Overall synthesis and transport of p65 was not affected by Δ^9-THC and CP55940. In addition, neither Δ^9-THC nor CP55940 had an effect on the phosphorylation of p65 at its serine 536 site and its translocation into the nucleus, both of which is required for complete transactivation of NFκB.

Collectively, our results suggest that in addition to the exogenous cannabinoids Δ^9-THC and CP55940, through the CB_2, mediating the modulation of NFκB function in microglial-like cells in part by inhibiting the proteolytic degradation of IκBα, there is also a mechanism of action in the nucleus by which these exogenous cannabinoid compounds prevent the proper binding and subsequent transcriptional activity of NFκB, the major inducer of the inflammatory immune response. Importantly, these studies demonstrate the therapeutic potential of cannabinoids and the CB_2 as a molecular target for ablating neuropathies and other neurodegenerative disorders that are pathologically hallmarked by a chronic elicitation of pro-inflammatory mediators in large part by activation of microglia cells that is mediated through NFκB.

Literature Cited

Literature Cited

1. Adcock IM (2001a) Glucocorticoid-regulated transcription factors. *Pulm Pharmacol Ther* 14:211-219.

2. Adcock IM and Caramori G (2001b) Cross-talk between proinflammatory transcription factors and glucorticoids. *Immunol Cell Biol* 79:376-384.

3. Aloisi F (2001) Immune function of microglial. *Gli*a 36:165-179.

4. Arata S, Newton C, Klein T and Friedman H (1991) Tetrahydrocannabinol treatment suppresses growth restriction of *Legionella pneumophila* in murine macrophage cultures. *Life Sci* 49:473-479.

5. Arata S, Newton C, Klein T and Friedman H (1992) Enhanced growth of *Legionella pneumophila* in tetrahydrocannabinol-treated macrophages. *Proc Soc Exp Biol Med* 199:65-67.

6. Arenzana-Seisdedos F, Turpin P, Rodriguez M, Thomas D, Hay RT, Virelizier JL and Dargemont C (1997) Nuclear localization of I kappa B alpha promotes active transport of NF-kappa B from the nucleus to the cytoplasm. *J Cell Sci* 110:369-378.

7. Arevalo-Martin A, Vela JM, Molina-Holgado E, Borrell J and Guaza C (2003) Therapeutic action of cannabinoids in a murine model of multiple sclerosis. *J Neurosci* 23:2511-2516.

8. Arimoto T and Bing G (2003) Up-regulation of inducible nitric oxide synthase in the substantia nigra by LPS causes microglial activation and neurodegeneration. 2003. *Neurobiol Dis* 12:35-45.

9. Auphan N, DiDonato JA, Rosette C, Helmberg A and Karin M (1995) Immunosuppression by glucocorticoids: inhibition of NF-kappa B activity through induction of I kappa B synthesis. *Science* 270:286-290.

10. Baker D, Pryce G, Davies WL and Hiley CR (2006) In silico patent searching reveals a new cannabinoid receptor. *Trends Pharmacol Sci* 27:1-4.

11. Basu A, Krady JK, Enterline JR and Levison SW (2002) TGFβ1 prevents IL-1β induced microglial activation whereas TNFα and IL-6 stimulated activation are not antagonized. *Glia* 40:109-120.

12. Benveniste EN (1997) Role of macrophages/microglial in multiple sclerosis and experimental allergic encephalomyelitis. *J Mol Med* 75:165-173.

13. Berdyshev EV, Boichot E, Germain N, Allain N, Anger JP and LagenteV (1997) Influence of fatty acid ethanolamides and delta9-tetrahydrocannabinol on cytokine and arachidonate release by mononuclear cells. *Eur J Pharmacol* 330:231-240.

14. Blackwell TS, Holden EP, Blackwell TR, De Larco JE and Christman JW (1994) Cytokine-induced neutrophil chemoattractant mediates neutrophilic alveolitis in rats: association with nuclear factor kappa B. *Am J Respir Cell Mol Biol* 11:464-472.

15. Blackwell TS, Holden EP, Blackwell TR, Christman BW and Christman JW (1996) Activation of NF-κB in rat lungs by treatment with endotoxin: modulation by treatment with N-acetylcysteine. *J Immunol* 157:1630-1637.

16. Blackwell TS and Christman JW (1997) The role of nuclear factor-κB in cytokine gene regulation. *Am J Respir Cell Mol Biol* 17:3-9.

17. Blasi E, Barluzzi R, Bocchini V, Mazzolla R and Bistoni F (1990) Immortalization of murine microglial cells by a v-raf/v-myc carrying retrovirus. *J Neuroimmunol* 27:229-237.

18. Breivogel CS, Griffin G, Di Marzo V and Martin BR (2001) Evidence for a new G protein-coupled cannabinoid receptor in mouse brain. *Mol Pharmacol* 60:155-163.

19. Brostjan C, Anrather J, Csizmadia V, Stroka D, Soares M, Bach FH and Winkler H (1996) Glucocorticoid-mediated repression of NFkappaB activity in endothelial cells does not involve induction of IkappaBalpha synthesis. *J Biol Chem* 271:19612-19616.

20. Burnette-Curley D, Marciano-Cabral F, Fisher-Stenger K and Cabral GA (1993) Delta-9-tetrahydrocannabinol inhibits cell contact-dependent cytotoxicityof BacillusCalmette-Guerin-activated macrophages. *Int J Immunopharmacol* 15:371-382.

21. Burnette-Curley D and Cabral GA (1995) Differential inhibition of RAW264.7 macrophage tumoricidal activity by delta 9tetrahydrocannabinol. *Proceedings of the Society for Experimental Biology and Medicine* 210:64-76.

22. Cabral GA and Dove-Pettit DA (1998) Drugs and immunity: cannabinoids and their role in decreased resistance to infectious disease. *J Neuroimmunol* 83:116-123.

23. Cabral GA and Marciano-Cabral F (2004) Cannabinoid-mediated exacerbation of brain infection by opportunistic amebae. *J Neuroimmunol* 147:127-130.

24. Cabral GA and Marciano-Cabral F (2005) Cannabinoid receptors in microglial of the central nervous system: immune functional relevance. *J Leukoc Biol* 78:1192-1197.

25. Cabral GA and Staab A (2005) Effects on the immune system. *Handb Exp Pharmacol* 168:385-423.

26. Cabral GA, Raborn ES, Griffin L, Dennis, J and Marciano-Cabral, F (2008) CB2 receptors in the brain:role in central immune function. *Br J Pharmacol* 153:240-251.

27. Cabral GA and Griffin-Thomas L (2008) Cannabinoids as therapeutic agents for ablating neuroinflammatory disease. *Endocrine, Metabolic & Immune Disorders – Drug Targets* 8:159-172.

28. Cabral GA and Griffin-Thomas L (2009) Emerging role of the cannabinoid receptor CB2 in immune regulation: therapeutic prospects for neuroinflammation. *Expert Rev Mol Med* 11:e3.

29. Carayon P, Marchand J, Dussossoy D, Derocq JM, Jbilo O, Bord A, Bouaboula M, Galiègue S, Mondière P, Pénarier G, Fur GL, Defrance T and Casellas P (1998) Modulation and functional involvement of CB2 peripheral cannabinoid receptors during B-cell differentiation. *Blood* 92:3605-3615.

30. Carlisle SJ, Marciano-Cabral F, Staab A, Ludwick C and Cabral GA (2002) Differential expression of the CB2 cannabinoid receptor by rodent macrophages and macrophage-like cells in relation to cell activation.*Int Immunopharmacol* 2:69-82.

31. Chakrabarti, A.; Onaivi, E. and Chaudhuri, G. (1995) Cloning and sequencing of a cDNA encoding the mouse brain-type cannabinoid receptor protein. *DNA Seq* 5:385-388.

32. Chiao PJ, Miyamoto S and Verma IM (1994) Autoregulation of I kappa B alpha activity. *Proc Natl Acad Sci USA* 91:28-32.

33. Cho S, Urata Y, Iida T, Goto S, Yamaguchi M, Sumikawa K and Kondo T (1998) Glutathione downregulates the phosphorylation of I kappa B: autoloop regulation of the NF-kappa B-mediated expression of NF-kappa B subunits by TNF-alpha in mouse vascular endothelial cells. *Biochem Biophys Res Comm* 253:104-108.

34. Coffey RG, Yamamoto Y, Snella E and Pross S (1996) Tetrahydrocannabinol inhibition of macrophage nitric oxide production. *Biochem Pharmacol* 52:743-751.

35. Croxford JL and Miller SD (2003) Immunoregulation of a viral model of multiple sclerosis using the synthetic cannabinoid R (+) WIN55,212. *J Clin Invest* 111:1231-1240.

36. Curran NM, Griffin BD, O'Toole D, Brady KJ, Fitzgerald SN and Moynagh PN (2005) The synthetic cannabinoid R(+)WIN 55,212-2 inhibits the interleukin-1 signaling pathway in human astrocytes in a cannabinoid receptor-independent manner. *J Biol Chem* 280:35797-357806.

37. Demuth DG and Molleman A (2006) Cannabinoid signaling. *Life Sci* 78:549-563.

38. Derocq JM, Ségui M, Marchand J, Le Fur G and Casellas P (1995) Cannabinoids enhance human B-cell growth at low nanomolar concentrations. *FEBS Letter* 369:177-182.

39. Devane WA, Hanus L, Breuer A, Pertwee RG, Stevenson LA, Griffin G, Gibson D, Mandelbaum A, Etinger A and Mechoulam R (1992) Isolation and structure of a brain constituent that binds to the cannabinoid receptor. *Science* 258:1946-1949.

40. Dickson DW, Mattiace LA, Kure K, Hutchins K, Lyman WD and Brosnan, CF (1991) Microglia in human disease, with an emphasis on acquired immune deficiency syndrome. *Lab Invest* 64:135-156.

41. Di Marzo V, Brievogel CS, Tao Q, Bridgen DT, Razdan RK, Zimmer AM, Martin BR (2000) Levels, metabolism, and pharmacological activity of anandamide in CB(1) cannabinoid receptor knockout mice: evidence for non-CB(1), non-CB(2) receptor-mediated actions of anandamide in mouse brain. *J Neurochem* 75:2434-2444.

42. Ebert S, Gerber J, Bader S, Muhlhauser F, Brechtel K, Mitchell T J and Nau R (2005) Dose-dependent activation of microglia cells by Toll-like receptor agonists alone and in combination. *J Neuroimmunol* 159:87-96.

43. Eldridge JC and Landfield PW (1990) Cannabinoid interactions with glucocorticoid receptors in rat hippocampus. *Brain Res* 534:135-141.

44. Eldridge JC, Murphy LL and Landfield PW (1991) Cannabinoids and the hippocampal glucorticoid receptor: recent findings and possible significance. *Steroids* 56:226-231.

45. Eljaschewitsch E, Witting A, Mawrin C, Lee T, Schmidt PM, Wolf S, Hoertnagl H Raine CS, Schneider-Stock R, Nitsch R and Ullrich O (2006) The endocannabinoid anandamide protects neurons during CNS inflammation by induction of MKP-1 in microglia cells. *Neuron* 49:67-79.

46. Epinant J-C and Gilmore TD (1999) Diverse agents act at multiple levels to inhibit the Rel/NF-κB signal transduction pathway. *Oncogene* 18:6869-6909.

47. Facchinetti F, Del Gindice E, Furegato S, Passarotto M and Leon A (2003) Cannabinoids ablate release of TNF-α in rat microglial cells stimulated with LPS. *Glia* 41:161-168.

48. Fernandez-Ruiz J, Romero J, Velasco G, Tolon RM, Ramos JA and Guzman M (2007) Cannabinoid CB2 receptor: a new target for controlling neural cell survival? *Trends Pharmacol Sci* 28:39-45.

49. Fischer-Stenger K, Dove Pettit DA and Cabral GA (1993) Δ^9-Tetrahydrocannabinol inhibition of tumor necrosis factor-α: Suppression of post-translational events. *Amer Soc Pharm Exp Therap* 267:1558-1565.

50. Franciosi S, Choi HB, Kim SU and McLarnon JG (2005) IL-8 enhancement of amyloid beta-induced expression and production of pro-inflammatory cytokines and COX-2 in cultured human microglia. *J Neuroimmunol* 159:66-74.

51. Friedman H, Klein T and Specter S (1991) Immunosuppression by Marijuana and Components. In: Psychoneuroimmunology (Ader R, Felten DL & Cohen N eds), pp 931-953, Academic Press.

52. Galiegue S, Mary S, Marchand J, Dussossoy D, Carriere D, Carayon P, Bouaboula M, Shire D, Le Fur G and Casellas P (1995) Expression of central and peripheral cannabinoid receptors in human immune tissues and leukocyte subpopulations.*Eur J Biochem* 232:54-61.

53. Gallily R, Breuer A and Mechoulam R (2000) 2-Arachidonylglycerol, an endogenous cannabinoid inhibits tumor necrosis factor-alpha production in murine macrophages and in mice. *Eur J Pharmacol* 406:R5-R7.

54. Gerard CM, Mollereau C, Vassart G and Parmeatier M (1991) Molecular cloning of a human cannabinoid receptor which is also expressed in testis. *Biochem J* 279:129-134.

55. Ghosh S, May MJ and Kopp EB (1998) NFκB and Rel proteins: evolutionarily conserved mediators of immune responses. *Annu Rev Immunol* 16:225-260.

56. Ghosh S and Karin M (2002) Missing pieces in the NFκB puzzle. *Cell* 109:81-96.

57. Gill E W and Lawrence D K (1976) The physiochemical mode of action of tetrahydrocannabinol on cell membranes. In: The Pharmacology of Marijuana (MC Brande and S Szara eds), pp 147-155, Raven Press.

58. Gilmore TD (2006) Introduction to NF-κB: players, pathways and perspectives. *Oncogene* 25:6680-6684.

59. Giulian D and Baker TJ (1986) Characterization of ameboid microglia isolated from developing mammalian brain. *J Neurosci* 6:2163-2178.

60. Gonzalez-Scarano F and Baltuch G (1999) Microglia as mediators of inflammatory and degenerative diseases. *Ann Rev Neurosci* 22:219-240.

61. Griffin G, Tao Q and Abood ME (2000) Cloning and pharmacological characterization of the rat CB2 cannabinoid receptor. *J Pharmacol Exp Ther* 292:888-894.

62. Grisham MB, Palombella VJ, Elliott PJ, Conner EM, Brand S, Wong HL, Pien C, Mazzola LM, Destree A, Parent L and Adams J (1999) Inhibition of NF-kappa B activation in vitro and in vivo: role of 26S proteasome. *Methods Enzymol* 300:345-363.

63. Han IO, Kim KW, Ryu JH and Kim WK (2002) p38 mitogen-activated protein kinase mediates LPS not IFN-γ induced inducible nitric oxide synthase expression in mouse BV2 microglial cells. *Neurosci Letters* 325:9-12.

64. Herkenham M, Lynn AB, Little MD, Johnson MR, Melvin LS, de Costa BR and Rice KC (1990) Cannabinoid receptor localization in brain. *Proc Natl Acad Sci USA* 87:1932-1936.

65. Herring AC and Kaminski NE (1999) Cannabinol-mediated inhibition of nuclear factor κB, cAMP response element-binding protein, and IL-2 secretion by activated thymocytes. *J Pharmacol Exp Therap* 291:1156-1163.

66. Hoang T, Fenne IS, Cook C, Børud B, Bakker M, Lien EA and Mellgren G (2004) cAMP-dependent protein kinase regulates ubiquitin-proteasome-mediated degradation and subcellular localization of the nuclear receptor coactivator GRIP1. *J Biol Chem* 279:49120-49130.

67. Howlett AC and Fleming RM (1984) Cannabinoid inhibition of adenylate cyclase. *Mol Pharmacol* 26:532-538.

68. Howlett AC (1985) Cannabinoid inhibition of adenylate cyclase: biochemistry of the response in neuroblastoma cell membranes. *Mol Pharmacol* 27:429-436.

69. Howlett AC, Qualy JM and Khachatrian LL (1986) Involvement of Gi in the inhibition of adenylate cyclase by cannabimimetic drugs. *Mol Pharmacol* 29:307-313.

70. Howlett AC and Mukhopadhyay S (2000) Cellular signal transduction by anandamide and 2-arachidonoylglycerol. *Chem Phys Lipids* 108:53-70.

71. Howlett AC, Barth F, Bonner TI, Cabral G, Casellas P, Devane WA, Felder CC, Herkenham M, Mackie K, Martin BR, Mechoulam R, and Pertwee RG (2002) International Union of Pharmacology. XXVII. Classification of Cannabinoid Receptors. *Pharmacol Rev* 54:161-202.

72. Huang TT, Kudo N, Yoshida M and Miyamoto S (2000) A nuclear export signal in the N-terminal regulatory domain of IkappaBalpha controls cytoplasmic localization of inactive NF-kappaB/IkappaBalpha complexes. *Proc Natl Acad Sci USA* 97:1014-1019.

73. Hwang SY, Jung JS, Lim SJ, Kim JY, Kim TH, Cho KH and Han IO (2004) LY294002 inhibits IFN-gamma stimulated inducible nitric oxide synthase expression in BV2 microglial cells. *Biochem Biophys Res Comm* 318:691-697.

74. Hyers TM, Tricomi SM, Dettenmeier PA and Fowler AA (1991) Tumor necrosis factor levels in serum and bronchoalveolar lavage fluid of patients with the adult respiratory distress syndrome. *Am Rev Respir Dis* 144:268-271.

75. Jarai Z, Wagner JA, Varga K, Lake KD, Compton DR, Martin BR, Zimmer AM, Bonner TI, Buckley NE, Mezey E, Razdan RK, Zimmer A and Kunos G (1999) Cannabinoid-induced mesenteric vasodilation through an endothelial site distinct from CB1 or CB2 receptors. *Proc Natl Acad Sci USA* 96:14136-14141.

76. Jeon YJ, Yang KH, Pulaski JT and Kaminski NE (1996) Attenuation of inducible nitric oxide synthase gene expression by delta9-tetrahydrocannabinol is mediated

through the inhibition of nuclear factor-kB/Rel activation. *Mol Pharmacol*50:334-41.

77. Jobin C, Hellerbrand C, Licato LL, Brenner DA and Sartor RB (1998a) Mediation by NF-kappa B of cytokine induced expression of intercellular adhesion molecule 1 (ICAM-1) in an intestinal epithelial cell line, a process blocked by proteasome inhibitors.*Gut* 42:779-787.

78. Juel-Jensen BE (1972) Cannabis and recurrent herpes simplex. *Br Med J* 4:296.

79. Kagoshima M, Ito K, Cosio B and Adcock IM (2003) Glucocorticoid suppression of nuclear factor-kappa B: a role for histone modifications. *Biochem Soc Trans* 31:60-65.

80. Kaltschmidt C, Kaltschmidt B, Lannes-Vieira J, Kreutzberg GW, Wekerle H, Baeuerle P A and Gehrmann J (1994) Transcription factor NF-kappa B is activated in microglial during experimental autoimmune encephalomyelitis. *Prog Clin Biol Res* 388:367-381.

81. Kaminski NE, Koh WS, Yang KH, Lee M and Kessler FK (1994) Suppression of the humoral immune response by cannabinoids is partially mediated through inhibition of adenylate cyclase by a pertussis toxin-sensitive G-protein coupled mechanism. *Biochem Pharmacol* 48: 1899-1908.

82. Kaminski NE (1996) Immune regulation by cannabinoid compounds through the inhibition of the cyclic AMP signaling cascade and altered gene expression. *Biochem Pharmacol* 52:1133-1140.

83. Karin M (1998) New twists in gene regulation by glucocorticoid receptor: is DNA binding dispensable? *Cell* 93:487-490.

84. Karin M and Neriah B (2000) Phosphorylation meets ubiquitination: the control of NFκB. *Annu Rev Immunol* 18:621-663.

85. Kim OS, L CS, Kim HY, Joe E and Jou I (2005) Characterization of new microglia-like cells obtained from neonatal rat brain. *Biochem Biophys Res Commun* 328:281-287.

86. Kim WK, Jang PG, Woo MS, Han IO, Piao HZ, Lee K, Lee H, Joh TH and Kim HS (2004) A new anti-inflammatory agent KL-1037 represses proinflammatory cytokine and inducible nitric oxide synthase (iNOS) gene expression in activated microglia. *Neuropharmacol* 47:243-252.

87. Klegeris A, Bissonnette CJ and McGeer PL (2003) Reduction of human monocytic cell neurotoxicity and cytokine secretion by ligands of the cannabinoid-type CB2 receptor. *Br J Pharmacol* 139:775-786.

88. Klein TW and Friedman H (1990) Modulation of murine immune cell function by marijuana components. In: Drugs of Abuse and Immune Function (Watson R ed), pp 87-111, CRC Press.

89. Klein TW, KawakamiY, Newton C and Friedman H (1991) Marijuana components suppress induction and cytolytic function of murine cytotoxic T cells in vitro and in vivo. *J Toxicol Environ Health* 32:465-477.

90. Klein TW, Newton C and Friedman H (1998b) Cannabinoid receptors and immunity. *Immunol Today* 19:373-381.

91. Kremlev SG, Roberts RL and Palmer C (2004) Differential expression of chemokines and chemokine receptors during microglial activation and inhibition. *J Neuroimmunol* 149:1-9.

92. Kujtan PW, Carlen PL and Kapur BM (1983) Delta 9-tetrahydrocannabinol and cannabidiol: dose-dependent effects on evoked potentials in the hippocampal slice. *Can J Physiol Pharmacol* 61:420-426.

93. Lau FC, Bielinkski DF and Joseph JA (2007) Inhibitory effects of blueberry extract on the production of inflammatory mediators in lipopolysaccharide-activated BV2 microglia. *J Neurosci Res* 85:1010-1017.

94. Lawrence D K and Gill EW (1975) The effects of Δ^9-tetrahydrocannabinol and other cannabinoids on spin-labeled liposomes and their relationship to mechanisms of general anesthesia. *Mol Pharmacol* 11:595-602.

95. Lawrence T, Gilroy DW, Colville-Nash PR and Willoughby DA (2001) Possible new role for NFκB in the resolution of inflammation. *Nat Med* 7:1291-1297.

96. Li X and Stark GR (2002) NFκB-dependent signaling pathways. *Exp Hematology* 30: 285-296.

97. Ling EA and Wong WC (1993) The origin and nature of ramified and amoeboid microglial: a historical review and current concepts. *Glia*, 7:9-18.

98. Little PJ and Martin BR (1991) The effects of delta 9-tetrahydrocannabinol and other cannabinoids on cAMP accumulation in synaptosomes. *Life Sci* 48:1133-1141.

99. Makriyannis A, Yang D P, Griffin RG and Das Gupta S K (1990) The perturbation of model membranes by (-)-delta-9-tetrahydrocannibinol. Studies using solid-state 2H- and 13C-NMR. *Biochim Biophys Acta* 1028:31-42.

100. Marciano-Cabral F, Ferguson T, Bradley SG and Cabral G (2001) Delta-9-tetrahydrocannabinol (THC), the major psychoactive component of marijuana, exacerbates brain infection by Acanthamoeba. *J Euk Microbiol* (Suppl):4S-5S.

101. Martin BR (1996) Cellular effects of cannabinoids. *Pharmacol Rev* 38:45-74.

102. Massi P, Fuzio D, Viganò D, Sacerdote P and Parolaro D (2000) Relative involvement of cannabinoid CB(1) and CB(2) receptors in the Delta(9)-tetrahydrocannabinol-induced inhibition of natural killer activity. *Eur J Pharmacol* 387:343-347.

103. Matsuda LA, Lolait SJ, Brownstein MJ, Young AC and Bonner TI (1990) Structure of cannabinoid receptor and functional expression of the cloned cDNA. *Nature* 346:561-564.

104. McCoy KL, Gainey D and Cabral GA (1995) Δ^9-tetrahydrocannabinol modulates antigen processing by macrophages. *J Pharmacol Exp Therap* 273:1216-1223.

105. McCoy KL, Matveyeva M, Carlisle SJ and Cabral GA (1999) Cannabinoid inhibition of the processing of intact lysozyme by macrophages: evidence for CB2 receptor participation. *J Pharmacol Exp Ther* 289:1620-1625.

106. McGreer EG and McGreer PL (2003) Inflammatory processes in Alzheimer's disease. *Prog Neuropsychopharmacol Biol Psychiatry* 27:741-749.

107. Mechoulam R, Ben Shabat S, Hanus L, Ligumsky M, Kaminski NE, Schatz AR, Gopher A, Almog S, Martin BR, Compton DR, Pertwee RG, Griffin G, Bayewitch M, Barg J and Vogel Z (1995) Identification of an endogenous 2-monoglyceride present in canine gut, that binds to cannabinoid receptors. *Biochem Pharmacol* 50:83-90.

108. Miller EJ, Cohen AB, Nagao S, Griffith D, Maunder RJ, Martin TR, Weiner-Kronish J P, Sticherling M, Christopher E and Mathay MA (1992) Elevated levels of NAP-1/interleukin-8 are present in he airspaces of patients with the adult respiratory distress syndrome and are associated with increased mortality. *Am Rev Respir Dis* 146:427-432.

109. Molina-Holgado F, Molina-Holgado E, Guaza C and Rothwell NJ (2002) Role of CB1 and CB2 receptors in the inhibitory effects of cannabinoids on LPS-induced nitric oxide release in astrocyte cultures. *J Neurosci Res* 67:829-836.

110. Morahan PS, Klykken PC, Smith SH, Harris LS, Munson AE (1979) Effects on cannabinoids on host resistance to Listeria monocytogenes and herpes simplex virus. *Infect Immun* 23:670-674.

111. Munro S, Thomas KL and Abu-Shaar M (1993) Molecular characterization of a peripheral receptor for cannabinoids. *Nature* 365:61-65.

112. Newton CA, Klein T and Friedman H (1994) Secondary immunity to *Legionella pneumophila* and Th1 activity are suppressed by delta-9-tetrahydrocannabinol injection. *Infect Immun* 62:4015-4020.

113. Ng EW, Aung MM, Abood ME, Martin BR and Razdan RK (1999) Unique analogues of anandamide: arachidonyl ethers and carbamates and norarachidonyl carbamates and ureas. *J Med Chem* 42:1975-1981.

114. Nowell, KW, Pettit DA, Cabral WA, Zimmerman HW Jr, Abood ME and Cabral, GA (1998) High-level expression of the human CB2 cannabinoid receptor using a baculovirus system. *Biochem Pharmacol* 55:1893-1905.

115. Nunez E, Benito C, Pazos MR, Barbachano A, Fajardo O, Gonzalez S, Tolon RM and Romero J (2004) Cannabinoid CB2 receptors are expressed by perivascular microglial cells in the human brain: an immunohistochemical study. *Synapse* 53:208-213.

116. Orian A, Whiteside S, Israel A, Stancovski I, Schwartz AL and Ciechanover A (1995) Ubiquitin-mediated processing of NF-κB transcriptional activator precursor p105. *J Biol Chem* 270:21707-21714.

117. Palombella VJ, Rando AL, Goldberg AL and Maniatis T (1994) The ubiquitin-proteasome pathway is required for processing the NF-kappa B1 precursor protein and the activation of NF-kappa B. *Cell* 78:773-785.

118. Perry VH (2004) The influence of systemic inflammation on inflammation in the brain: implications for chronic neurodegenerative disease. *Brain Behav Immun* 18:407- 413.

119. Pertwee RG (2007) GPR55: a new member of the cannabinoid receptor clan? *Br J Pharmacol* 152:984-986.

120. Pomerantz JL and Baltimore D. (2002) Two pathways of NFκB. *Mol Cell* 10:693-701.

121. Puffenbarger RA, Boothe AC and Cabral GA (2000) Cannabinoids inhibit LPS-inducible cytokine mRNA expression in rat microglial cells. *Glia* 29:58-69.

122. Qin L, Li G, Qian X, Liu Y, Wu X, Liu B, Hong J-S and Block ML (2005) Interactive role of the toll-like receptor 4 and reactive oxygen species in LPS induced microglia activation. *Glia* 52:78-84.

123. Raborn ES, Marciano-Cabral F, Buckley NE, Martin BR and Cabral GA (2008) The cannabinoid delta-9-tetrahydrocannabinol mediates inhibition of macrophage chemotaxis to RANTES/CCL5: linkage to the CB(2) receptor. *J Neuroimmune Pharmacol* 3:117-129.

124. Ramirez BG, Blazquez C, Gomez DP, Guzman M and de Ceballos ML (2005a) Prevention of Alzheimer's disease pathology by cannabinoids: neuroprotection mediated by blockade of microglial activation. *J Neurosci* 25:1904-193.

125. Ray A and Prefontaine KE (1994) Physical association and functional antagonism between the p65 subunit of transcription factor NF-kappa B and the glucocorticoid receptor. *Proc Natl Acad Sci USA* 91:752-756.

126. Rock RB, Gekker G, Hu S, Sheng WS, Cheeran M, Lokensgard JR and Peterson PK (2004) Role of microglia in central nervous system infections. *Clin Microbiol Rev* 17:942-964.

127. Rodriguez MS, Thompson J, Hay RT and Dargemont C (1999) Nuclear retention of IκBα protects it from signal-induced degradation and inhibits nuclear factor κB transcriptional activation. *J Biol Chem* 274**:**9108-9115.

128. Ross RA, Brochie HC and Pertwee RG (2000) Inhibition of nitric oxide production in RAW264.7 macrophages by cannabinoids and palmitoylethanolamide. *Eur J Pharmacol* 401:121-130.

129. Ross RA (2003) Anandamide and vanilloid TRVP1 receptors. *Br J Pharmacol* 140:790-801.

130. Ryberg E, Larsson N, Sjögren S, Hjorth S, Hermansson NO, Leonova J, Elebring T, Nilsson K, Drmota T and Greasley PJ (2007) The orphan receptor GPR55 is a novel cannabinoid receptor. *Br J Pharmacol* 152:1092-1101.

131. Sacerdote P, Massi P, Panerai AE and Parolaro D (2000) In vivo and in vitro treatment with the synthetic cannabinoid CP55, 940 decrease the in vitro migration of macrophages in the rat: involvement of both CB1 and CB2 receptors. *J Neuroimmunol* 109:155-163.

132. Sachdev S, Bagchi S, Zhang DD, Mings AC and Hannink M (2000) Nuclear import of ikappaBalpha is accomplished by a ran-independent transport pathway. *Mol Cell Biol* 20:1571-1582.

133. Sakurai H, Chiba H, Miyoshi H, Sugita T and Toriumi W (1999) IkappaB kinases phosphorylate NF-kappaB p65 subunit on serine 536 in the transactivation domain. *J Biol Chem* 274:30353-30356.

134. Sakurai H, Suzuki S, Kawasaki N, Nakano H, Okazaki T, Chino A, Doi T and Saiki I (2003) Tumor necrosis factor-alpha-induced IKK phosphorylation of NF-kappaB p65 on serine 536 is mediated through the TRAF2, TRAF5, and TAK1 signaling pathway *J Biol Chem* 278:36916-36923.

135. Sancho R, Calzado MA, Di Marzo V, Appendino G and Munoz E (2003) Anandamide inhibits nuclear factor kappa B activation through a cannabinoid receptor-independent pathway. *Mol Pharmacol* 63:429-438.

136. Sasaki CY, Barberi TJ, Ghosh P and Longo DL (2005) Phosphorylation of RelA/p65 on Serine 536 Defines an IκBα-independent NF-κB pathway. *J Biol Chem* 280:34538-34547.

137. Sawzdargo M, Nguyen T, Lee DK, Lynch KR, Cheng R, Heng HH, George SR and O'Dowd BF (1999) Identification and cloning of three novel human G protein-coupled receptor genes GPR52, PsiGPR53 and GPR55: GPR55 is extensively expressed in human brain. *Brain Res Mol Brain Res* 64:193-198.

138. Schatz AR, Lee M, Condie RB, Pulaski JT and Kaminski NE (1997) Cannabinoid receptors CB1 and CB2: a characterization of expression and adenylate cyclase modulation within the immune system. *Toxicol Appl Pharmacol* 142:278-287.

139. Scheinman RI, Cogswell PC, Lofquist AK and Baldwin AS (1995) Role of transcriptional activation of I kappa B alpha in mediation of immunosuppression by glucocorticoids. *Science* 260:283-286.

140. Schmitz ML and Baeuerle BA (1991) The p65 subunit is responsible for the strong transcription activating potential of NF-κB. *EMBO J* 10:3805-3817.

141. Schreck R Albermann K and Baeuerle PA (1992b) Nuclear factor kappa B: an oxidative stress-responsive transcription factor of eukaryotic cells (a review). *Free Rad Res Comm* 17:221-237.

142. Sen R and Baltimore D (1986) Multiple nuclear factors interact with the immunoglobulin enhancer sequences. *Cell* 46:705-716.

143. Sizemore N, Lerner N, Dombrowski N, Sakurai H and Stark GR (2002) Distinct roles of the Ikappa B kinase alpha and beta subunits in liberating nuclear factor kappa B (NF-kappa B) from Ikappa B and in phosphorylating the p65 subunit of NF-kappa B. *J Biol Chem* 277:3863-3869.

144. Smart D, Gunthorpe MJ, Jerman JC, Nasir S, Gray J, Muir AI, Chambers JK, Randall AD and Davis JB (2000) The endogenous lipid anandamide is a full agonist at the human vanilloid receptor (hVR1). *Br J Pharmacol* 129:227-230.

145. Streit WJ, Graeber MB and Kreutzberg GW (1988) Functional plasticity of microglia: a review. *Glia* 1:301-307.

146. Tergaonkar V (2006) NFκB pathway: A good signaling paradigm and therapeutic target. *Int Biochem Cell Biol* 38:1647-1653.

147. Tzen CY, Cox RL and Scott RE (1994) Coordinate induction of IκB α and NFκB genes. *Exp Cell Res* 211:12-16.

148. Vermeulen L, DeWilde G, Notebaert S, Berghe WV and Haegeman G (2002) Regulation of the transcriptional activity of the nuclear factor κB p65 subunit. *Biochem Pharmacol* 64:963-970.

149. Vilhardt F (2005). Microglia: phagocyte and glia cell. *Int J Biochem Cell Biol* 37:17-21.

150. Vogel Z (1995) Identification of an endogenous 2-monoglyceride, present in canine gut, that binds to cannabinoid receptors. *Biochem Pharmacol* 50:83-90.

151. Waksman Y, Olson JM, Carlisle SJ, and Cabral GA (1999) The central cannabinoid receptor (CB1) mediates inhibition of nitric oxide production by rat microglial cells. *J Pharmacol Exp Ther* 288:1357-1366.

152. Walker WS (1994) Establishment of mononuclear phagocyte cell lines. *J Immunol Methods* 174:25-31.

153. Walker WS, Gatewood J, Olivas E, Askew D and Havenith CE (1995) Mouse microglia cell lines differing in constitutive and interferon-gamma-inducible antigen-presenting activities for naïve and memory CD4+ and CD8+ T cells. *J Neuroimmunol* 63:163-174.

154. Wang D and Baldwin AS (1998) Activation of nuclear factor-kappaB-dependent transcription by tumor necrosis factor-alpha is mediated through phosphorylation of RelA/p65 on serine 529. *J Biol Chem* 273:29411-29416.

155. Wang D, Westerheide SD, Hanson JL and Baldwin AS (2000) Tumor necrosis factor alpha-induced phosphorylation of RelA/p65 on Ser529 is controlled by casein kinase II. *J Biol Chem* 275:32592-32597.

156. Westlake TM, Howlett AC, Bonner TI, Matsuda LA and Herkenham M (1994) Cannabinoid receptor binding and messengerRNAexpression in human brain: an in vitro receptor autoradiography and in situ hybridization histochemistry study of normal aged and Alzheimer's brains. *Neurosci*, 63:637-652.

157. Wiley JL and Martin BD (2002) Cannabinoid pharmacology: implications for additional cannabinoid receptor subtypes. *Chem Phys Lipids* 121:57-63.

158. Wright SD, Ramos, RA, Tobias PS, Ulevitch RJ and Mathison JC (1990) CD14, a receptor for complexes of lipopolysaccharide (LPS) and LPS binding protein. *Science* 2491431-1433.

159. Yamamoto Y and Gaynor RB (2004) IκB kinases: key regulators of the NFκB pathway. Trends Biochem Sci 29:72-79.

160. Yang F, Tang E, Guan K and Wang CY (2003) IKK beta plays an essential role in the phosphorylation of RelA/p65 on serine 536 induced by lipopolysaccharide. *J Immunol* 170:5630-5635.

161. Ye S-M and Johnson RW (2001) Regulation of IL-6 expression in brain of aged mice by NFkB. *J Neuroimmunol* 117:87-96.

162. Zhang F, Hu Y, Huang P, Toleman CA, Paterson AJ and Kudlow JE (2007) Proteasome function is regulated by cyclic AMP-dependent protein kinase through phosphorylation of Rpt6. *J Biol Chem* 282:22460-22471.

Vita

LaToya Andrea Griffin-Thomas was born on August 16, 1976, in Baltimore, MD, and is an American citizen. She graduated from Western Senior High School, in Baltimore, MD in 1994. She received her Bachelor of Science in Biology from Hampton University, Hampton, VA in 1998. She returned to Hampton University in 2002, and received a Master of Science in Biology in 2002.

Education

Virginia Commonwealth University School of Medicine, Richmond, VA
Department of Microbiology and Immunology
Doctor of Philosophy, Microbiology and Immunology
Graduation Date: May 2009

Hampton University, Hampton, VA
Master of Science, Biology
Beta Kappa Chi Scientific Honor Society
Graduation Date: August 2002

Hampton University, Hampton, VA
Bachelor of Science, Biology
Beta Kappa Chi Scientific Honor Society
Graduation Date: December 1998

Western Senior High School, Baltimore, MD
Graduation Date: June 1994

Employment/ Skills

Virginia Commonwealth University School of Medicine, Richmond, VA
Department of Microbiology and Immunology
Graduate Student/Researcher, 2002-2009

Molecular Biology/Microbiology Techniques: DNA and RNA Extraction; Real-Time RT- PCR; Conventional PCR; Gram Staining; Restriction Enzyme Digestion; Bacterial Transformation and Mammalian Cell Transfection; Creation and Screening of a lambda phage DNA library; Plaque Lift Assays; Western immunoblotting; ELISA; Immunoprecipitation; Southern Blotting; Electrophoretic

Mobility Shift Analysis; Radiolabeling; Agarose and SDS-PAGE; Plasmid Isolation; Reporter Activity Assays; Protein Extraction.
Cell culture Techniques: Bacterial culture of *E. coli* and *Borrelia hermsii*; Mammalian cell tissue culture; Isolation of primary brain cells from rat pups.

Laboratory Management: documentation of all experimental protocols and results; data analyses; statistical analyses using Prism and SigmaStat; maintaining quality control and assurance by keeping record of lab inventory including receipt, proper storage and expiration, maintaining equipment upkeep and scheduling required maintenance repairs and/or certifications, and attending training demonstrations; designing and troubleshooting experiments; practicing standard laboratory safety protocols including chemical, radioisotope and animal handling safety; maintaining receipt and disposal records of radioactive materials; training of new laboratory employees.

Additional Skills: Light microscopy, Proficient written and oral communication skills and good organization skills.

Hampton University, Hampton, VA
Biological Sciences Department
Graduate Student/Researcher 2000-2002
General Biology Teacher, Summer 2002

Microbiology Techniques: Bacterial propagation and transformation.

Molecular Biology Techniques: Conventional PCR; Bacterial Cloning; Plasmid preparation; Restriction enzyme digestion, Plasmid ligation, PCR primer designing; Agarose gel electrophoresis; SDS-PAGE and Ni-NTA column protein purification

Biology Teacher, Preparation and instruction of class lectures; preparation and proctoring of examinations, demonstrated and supervised wet-laboratory experiments.

Awards Received

2003-2006 NIH Immunology Training Grant
2005 Graduate Research Award, oral presentation-ASM
2007 Graduate Research Award, oral presentation-ASM
2008, April, Travel Award-VCU Graduate School
2008, September, Carolina Cannabinoid Collaborative Award
2008, November, Graduate Research Award, oral presentation-ASM

Publications

Hovis KM, McDowell JV, **Griffin L**, Marconi RT. Identification and characterization of a linear plasmid encoded factor H-binding protein (FhbA) of the relapsing fever spirochete Borrelia hermsii. Journal of Bacteriology. 2004 May; 186(9): 2612-2618.

Cabral GA, Raborn ES, **Griffin L**, Dennis J, Marciano-Cabral F. CB2 receptors in the brain: role in central immune function. British Journal of Pharmacology. 2008 Jan; 153(2): 240-251.

Cabral GA and **Griffin-Thomas L**. Cannabinoids as Therapeutic Agents for Ablating Neuroinflammatory Disease. Endocrine, Metabolic & Immune Disorders – Drug Targets. 2008 Sep; 8(3):159-172.

Cabral GA and **Griffin-Thomas, L**. Emerging Role of the CB2 Cannabinoid Receptor in Immune Regulation and Therapeutic Prospects. Expert Reviews in Molecular Medicine. 2009 Jan; 11(3e).

Griffin-Thomas, L., Ferreira, G. A. and Cabral, G. A. Cannabinoids Inhibit NFkappaB Function in Microglia Cells: Dual Mode of Action. *Manuscript in preparation.*

Professional Memberships

American Society for Microbiology, National Branch
American Society for Microbiology, VA Branch
International Cannabinoid Research Society